Replisome components in sister chromatid cohesion establishment

Thesis submitted for degree of Doctor of Philosophy to
Imperial College London

Sudikchya Shrestha
Supervisor : Dr. Frank Uhlmann

The Francis Crick Institute,
London, UK
November 2022

Statement of originality

I, Sudikchya Shrestha, confirm that the thesis has been written by me based on four years of personally conducted experimentation and literature review. To the best of my knowledge, I have included citations whenever they are due.

Copyrights Declaration

One ring to load on DNA in G1, one ring acetylated in S phase

One ring to topologically entrap sister chromatids until it is cleaved in Anaphase

In the nucleus of S. cerevisiae whose cell cycle is well organized

Acknowledgements

From telomere to centromere
Frank, for his pure enthusiasm of science, for being kind, for his understated humor
Tony, for being so calm and kind
Martina, for her interesting stories
Luca, for being such a great friend, for sharing many fun puzzles and depressing books
Thomas, for providing humor in happiness and despair
Pei-Shang, for her kind laughter
Masa, for his dedication
Celine, our lab mom, for caring, for solving so many problems
Kim, our new PhD student who is already such a joy to have in lab
Karolina, for the laughs, optimism and colorfulness
Sam, for the many indulging conversations on TCM

May, for bringing 3NE together through bouldering and for her friendship
Previous lab members,
Tora, for his wisdom and inspiration
Lucy, for being always kind and inclusive
Deniz, for being such a force of bringing people together and fun ideas
Hon, for his memes and keeping things interesting
Sofia, for being so fun and optimistic
All present and past CSL members, for interesting discussions about science and life, and many many instances of help with experiments

Angel, from Rappsilber lab for help with CLMS
Allie, Jennifer and Chris, from Diffley lab, for sharing their expertise, and proteins for the replication part of the project
Fermentation STP and Media Prep, for their services that greatly assisted this project

Stephane Boissinot and Duncan Smith, my undergraduate professors who inspired me to pursue the research life

My parents and sister, for their unconditional love and support
Kristopher, who once told me *we are students for life*, and who is my ultimate source of joy and strength

Abstract

The chromosomal cohesin complex establishes sister chromatid cohesion during S phase, which forms the basis for the recognition of DNA replication products for their faithful segregation in mitosis. Here, I investigate the non-essential *S. cerevisiae* replication fork components Tof1, Csm3 and Mrc1, whose absence leads to defective sister chromatid cohesion. How these three proteins contribute to cohesion establishment is not yet known.

Tof1, Csm3 and Mrc1 serve known roles during DNA replication, including mediating replication checkpoint signalling, accelerating replication fork progression as well as the recruitment of topoisomerase I and FACT to the replisome. By modulating each of these replication functions independently of Tof1, Csm3 and Mrc1 and using separation of function mutants, I rule out a possible contribution of these functions to the establishment of sister chromatid cohesion. Instead, using purified recombinant components, I reveal direct protein interactions between Tof1/Csm3 and Mrc1 and the cohesin complex. Preliminary results from crosslinking mass spectrometry to identify interaction surfaces narrows down a small cluster of Tof1 and Mrc1 interaction sites in Smc1 and Smc3 subunits of cohesin. Tof1-Csm3 also directly interacts with the Chl1 helicase, another replisome component that contacts cohesin and contributes to cohesion establishment. My findings open the possibility that a series of direct physical interactions between replication fork components and the cohesin complex facilitate successful establishment of sister chromatid cohesion during DNA replication.

Table of Contents

List of Tables

List of Figures

Abbreviations

Å	Angstrom
Ab	Antibody
ACT	Acetyltransferase
ABC	ATP Binding Cassette
AND	Acidic Nucleoplasmic DNA-binding protein
ATP	Adenosine triphosphate
ADP	Adenosine diphosphate
BeF_3	Beryllium triFluoride
bp	base pairs
BrdU	5-bromo-2'-deoxyuridine
CAID	Chronic Atrial and Intestinal Dysrhythmia
cat	CATalytic domain
CBP	Calmoudulin Binding Protein
Cdc	Cell Division Cycle
CDK	Cyclin Dependent Kinase
CdLS	Cornelia de Lange Syndrome
ChIP	Chromatin immunoprecipitation
Chl	CHromosome Loss
Chr	Chromosome
CLMS	Crosslinking Mass Spectrometry
CMG	Cdc45-MCM-GINS
co-IP	Co-immunoprecipitation
Csm	Chromosome Segregation in Meiosis
CTD	C-Terminal Domain
Ctf	Chromosome Transmission Fidelity
DDX11	DEAD/H-Box Helicase - 11
DNA	DeoxyriboNucleic Acid
DNAse	Deoxyribonuclease
Dna	DNA synthesis defective
dNTP	Deoxynucleotide triphosphate
dsDNA	Double stranded DNA
DTT	Dithiothreitol
ECL	Enhanced chemiluminescence
Eco	Establishment of COhesion

EDTA	Ethylene diamine tetraacetic acid
FACS	Fluorescence activated cell sorting
FACT	FAcilitates Chromatin Transactions
Fen	Flap Endonuclease
g	gram
G1	Gap Phase 1/ Growth Phase 1
G2	Gap Phase 2/ Growth Phase 2
GAL	GALactose
GFP	Green Fluorescent Protein
GINS	Go, Ichi, Nii, San
GNAT	Gcn5-related N-AcetylTransferase
h	hours
HA	hemagglutinin
HCl	HydroChloric Acid
HEAT	(Huntingtin, elongation factor 3 (EF3) protein phosphatase 2A (PP2A), and the yeast kinase TOR1)
HeLa	derived from Henrietta Lacks
HEPES	4-(2-hydroxyethyl)-1-piperazineethansulfonic acid
Hi-C	High-throughput Chromosome conformation capture
HRP	Horseradish peroxidase
HU	Hydroxyurea
IP	Immunoprecipitation
kB	kiloBase
kDa	KiloDalton
KOH	Potassium Hydroxide
K-Glut	Potassium Glutamate
l	litre
M	Molar
mA	milliAmpere
MAT	MAting Type
MCM	Mini-Chromosome Maintenance
min	minute
ml	millilitre
mm	millimetre
mM	millimolar
Mec	Mitosis Entry Checkpoint
$MgCl_2$	Magnesium Chloride II

Mps	MonoPolar Spindle
Mrc	Mediator of the Replication Checkpoint
MS	Mass Spectrometry
NaCl	Sodium Chloride
NaOAc	Sodium Acetate
NHS-ester	N-Hydroxysuccinimide ester
NIPBL	NIpped-B-Like protein
nm	nanometre
Noc	Nocodazole
NP-40	Nonyl Phenoxypolyethoxylethanol
NTD	N-Terminal Domain
OD	Optical Density
ori	Origin of replication
ORC	Origin Recognition Complex
PAGE	PolyAcrylamide Gel Electrophoresis
PBS	Phosphate-buffered saline
PBSA	Phosphate Buffered saline Albumin
PCNA	Proliferating Cell Nuclear Antigen
PCR	Polymerase Chain Reaction
Pds	Precocious Dissociation of Sisters
pH	potential of Hydrogen
PI	Propidium Iodide
PI	Protease Inhibitors
PIP	PCNA interacting protein
Pol	POLymerase
Rad	Radiation
Rfa	Replication Factor A
RFB	Replication Fork Barriers
RFC	Replication Factor C
RNA	RiboNucleic Acid
RNAse	Ribonuclease
RPA	Replication Protein A
RT	Room temperature
rpm	revolutions per minute
s	seconds
S phase	Synthesis phase
Scc	Sister Chromatid Cohesion

SDS	Sodium dodecyl sulphate
SGO	Shughosin
SMC	Structural Maintenance of Chromosome
Smc3Ac	Smc3 Acetylation
ssDNA	Single stranded DNA
ssSeq	Strand-specific sequencing
STAG	STromal AntiGen
Sulfo-SDA	sulfo-NHS-Diazirine
TAE	Tris Acetate EDTA
TCA	Trichloroacetic acid
TCEP	Tris (2-CarboxyEthyl) Phosphine
TCM	Tof1-Csm3-Mrc1
tetO	tetracycline Operator
tetR	tetracycline Repressor
Tim	TIMeless
Tof	TOpoisomerase I-interacting Factor
Top	Topoisomerase
Tris	2-amino-2-(hydroxymethyl)-1,3-propanediol
ts	Temperature sensitive
U	units
UV-A	Ultraviolet A
v/v	volume per volume
w/v	weight per volume
WBS	Warsaw Breakage Syndrome
Wpl	Wings A Part-Like
WT	Wild Type
YP	Yeast Peptone
YPD	Yeast Peptone Dextrose
ZnF	Zinc Finger
µg	microgram
µl	microlitre

Chapter 1. Introduction

1.1 Distributing the genome during cell division

Cell division is a fundamental process that allows continuity of life, as well as growth and regeneration in multicellular organisms. As a result of cell division, one cell divides to give rise to two progeny cells. Each progeny cell should have a full copy of the genome – the information template made of DNA.

DNA replication is a key molecular process prior to cell division which ensures that there are two copies of the genome, one for each progeny cell. Chromosome segregation is another key molecular process in cell division that ensures that each daughter cell receives a full copy of the genome. Without chromosome segregation, the monumental task of replicating DNA is rendered obsolete.

In fact, the primary goal of cell division can be viewed as a means to equally distribute the duplicate copies of the replicated genome. Virtually all life, other than viruses, fulfils this goal. There are important differences in cell division between prokaryotes and eukaryotes which already differ in their relative genome sizes and circular/linear nature of their chromosomes. In prokaryotes which are more likely to possess smaller genomes in circular forms, chromosome segregation occurs concomitantly with DNA replication (Lin and Grossman 1998). Eukaryotes, which mostly possess multiple linear chromosomes, have evolved the cell cycle in which DNA replication and chromosome segregation are temporally separated. DNA replication occurs during S phase. Meanwhile, chromosome segregation only occurs when cells progress to Anaphase during mitosis, and sister chromatids are pulled to opposite directions by bipolar spindles. This allows large eukaryotic genomes to be condensed prior to chromosome segregation, preventing replicated DNA from entangling with each other. It has been argued that evolution of the cell cycle allowed eukaryotes to develop large genomes (Nasmyth, Peters et al. 2000).

Each progeny cell must receive exactly one copy of the genome. Faithful chromosome segregation is ensured in eukaryotes by keeping replicated chromosomes together in a process now described as sister chromatid cohesion until they can be separated in a coordinated manner.

Several interesting theories were originally proposed for how sister chromatid cohesion is accomplished in cells (Nasmyth, Peters et al. 2000). One hypothesis implicated topoisomerases suggesting that the inter-catenation between sister chromatids may only be resolved by action of topoisomerases in mitosis. As cells progress to Anaphase, an increase in expression of topoisomerases was thought to fully resolve the entanglement allowing the sisters to separate. A second hypothesis proposed that the centromeric region, which had been observed via chromosome staining to continue to link sister chromatids, is not replicated until Anaphase. Late replication of these regions in Anaphase was thought to finally initiate chromosome segregation. The earliest speculations even vaguely considered that “positive attraction” along the main axis of sister chromatids was sufficient to hold sister chromatids together and this attraction converted to “repulsion” to initiate chromosome segregation. As we are well aware today, none of these models were exactly correct.

Genetic studies eventually determined that replicated DNA products are held together by a dedicated protein complex appropriately named cohesin. Cohesin core and accessory subunits were identified for their sister chromatid cohesion function through genetic screens looking for mutants leading to precocious separation of sister chromatids (Guacci, Hogan et al. 1994, Michaelis, Ciosk et al. 1997). Cohesin and associated proteins are well conserved across eukaryotes and concerted efforts have rapidly increased our knowledge of sister chromatid cohesion.

In the next section, I have attempted to provide a brief outline of our current understanding of Cohesin and Sister Chromatid Cohesion, while also sharing the gaps in our knowledge.

1.2 Cohesin; Structure and Function

Introducing Cohesin

The protein tether during sister chromatid cohesion is the tetrameric cohesin complex (Nasmyth and Haering 2009, Uhlmann 2016). Across the chromosome axis, many cohesin molecules physically hold replicated products together and are capable of resisting mechanical tension exerted by the bipolar spindles (Nicklas 1983). Only enzymatic cleavage of cohesin in Anaphase eventually allows the chromosomes to move to two different progeny cells (Uhlmann, Lottspeich et al. 1999).

Cohesin is a large multimeric ring-shaped complex made up of four core essential subunits. A cartoon schematic of cohesin can be seen in figure 1.1A. The main circumference for the canonical ring first seen in electron micrographs (Anderson, Losada et al. 2002, Haering, Löwe et al. 2002) is formed by two proteins Smc1 and Smc3 of the SMC (Structural Maintenance of Chromosomes) family. The SMC family of proteins is really well conserved across prokaryotes and eukaryotes (Losada and Hirano 2005, Yoshinaga and Inagaki 2021). Each SMC protein consists of alpha helical coils with a globular domain on N and C terminus as well as in the middle. The middle globular region forms the hinge domain where the coils also fold to then connect the N and C terminus globular domains forming the head region. The coils to either side of the hinge thus run antiparallel to each other and form intramolecular coiled coils (Haering, Löwe et al. 2002).

SMC proteins always occur in dimer form. While mostly homodimeric in bacteria (Melby, Ciampaglio et al. 1998), it is heterodimeric in eukaryotes. In cohesin, the hinge regions of Smc1 and Smc3 interact through hydrophobic interactions to form a stable hinge interface. The heads of Smc1 and Smc3 combine to form two ABC (ATP Binding Cassette) type ATPases. Since the heads are always engaging and disengaging upon ATP binding and hydrolysis (Lammens, Schele et al. 2004), Smc1 and Smc3 would not be sufficient of forming a stabilized closed ring in the cellular environment replete with ATPs. A kleisin protein Scc1, connects with Smc3 head at the N terminal domain (NTD) and Smc1 at the C terminal domain (CTD), and through this arrangement is capable of closing the ring (Schleiffer, Kaitna et al. 2003). Scc1 can also be enzymatically cleaved leading to disruption of the ring structure.

Since three subunits are technically capable of forming a closed ring, some labs prefer to refer to just a complex of Smc1, Smc3 and Scc1 as the cohesin complex. In this tripartite ring, altogether there are three different gates (Smc1-Smc3 hinge, Smc1 head-Scc1 (CTD) and Smc3 head-Scc1(NTD)) through which DNA can enter and exit. Various means of probing this question has led to different conclusions (Gruber, Arumugam et al. 2006, Murayama and Uhlmann 2015, Beckouët, Srinivasan et al. 2016, Collier and Nasmyth 2022).

While investigation is still ongoing to conclusively determine which gates are utilized for DNA entry and exit, the experimental evidence is unanimous on the capability of the ring complex to topologically embrace DNA. Topological DNA loading by cohesin has been observed in biochemistry experiments (Ivanov and Nasmyth 2005, Murayama and Uhlmann 2014, Minamino, Higashi et al. 2018). In the same manner that topological DNA loading of PCNA was demonstrated (Yao, Turner et al. 1996), cohesin topologically loaded on DNA is only

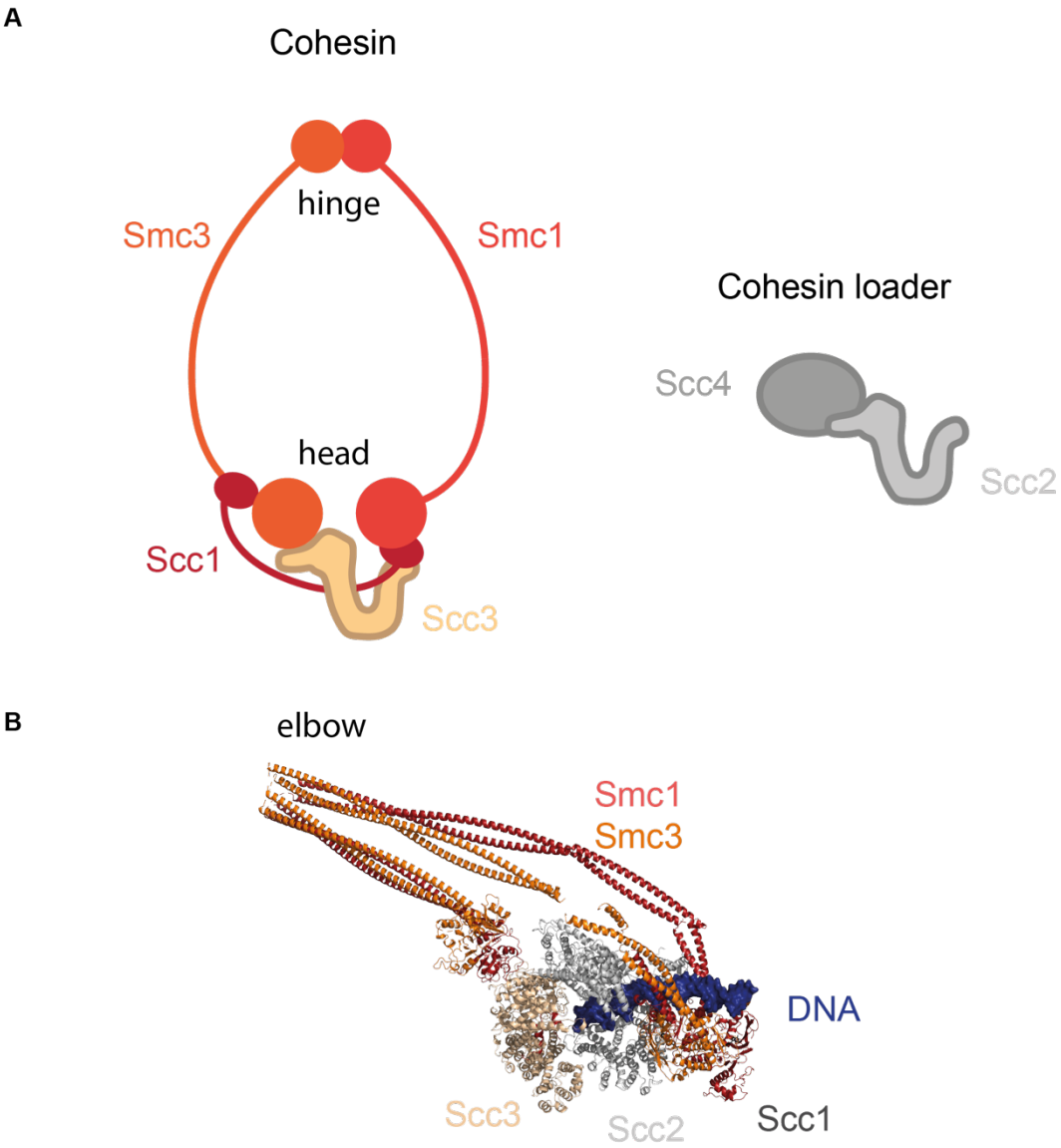

Figure 1.1 Cohesin structure (model and prediction)

A. Schematic representation of cohesin with its four subunits Smc1, Smc3, Scc1 and Scc3, along with cohesin loader complex consisting of subunits Scc2 and Scc4

B. Modelled prediction of *Schizosaccharomyces pombe* Cohesin structure in the process of DNA loading as described in Higashi et al. 2018.

released when DNA or Scc1 subunit of cohesin is enzymatically cut. Covalently closing all three gates of cohesin has also confirmed in parallel that cohesin can trap DNA inside its tripartite ring structure (Srinivasan, Scheinost et al. 2018).

The fourth core subunit Scc3 has been found to be crucial for both DNA loading and unloading (Murayama and Uhlmann 2014, Murayama and Uhlmann 2015, Li, Muir et al. 2018, Collier, Lee et al. 2020). Consistent with this, Scc3 appears to always colocalize in chromosome spreads with Smc1, Smc3 and Scc1 (Tóth, Ciosk et al. 1999). Scc3 is made up of multiple HEAT (Huntingtin, elongation factor 3 (EF3) protein phosphatase 2A (PP2A), and the yeast kinase TOR1) repeats, forms a shape that is sometimes referred to as a dragon (Hara, Zheng et al. 2014) or a hook. To form tetrameric cohesin, Scc3 interacts with the flexible middle region of Scc1.

A complete structure of the full tetrameric cohesin loaded on DNA has not been resolved owing largely due to the many flexible domains within its subunits. The coiled coils of Smc1 and Smc3 are very flexible, and so is the middle region of Scc1. Recently, three labs independently labs published corroborating structures of cohesin expected to be in process of loading onto DNA (Collier, Lee et al. 2020, Higashi, Eickhoff et al. 2020, Shi, Gao et al. 2020). In these structures, the Smc1 and Smc3 heads are engaged through binding of ATP in non-hydrolysable conditions. Meanwhile, DNA is clamped between the heads and the Scc2 subunit of cohesin loader (introduced in the next section). Using this structure as template, a near complete structure of *Schizosaccharomyces pombe* cohesin including the rest of the Smc1 and Smc3 coiled coils has been modelled through incorporating structures of subunit domains from *Saccharomyces cerevisiae* and *Chaetomium thermophilum* (figure 1.1B) (Higashi, Eickhoff et al. 2020). In this model is also visible the characteristic1 elbow where Smc1 and Smc3 coiled coils bend, resulting in hinge folding back into the structure.

Cohesin accessory subunits

Cohesin loading onto DNA is made highly efficient by the aptly named cohesin loader composed of Scc2 and Scc4 (cartoon model in figure 1.1A) (Ciosk, Shirayama et al. 2000). Unlike Scc3, Scc2-Scc4 do not always colocalize with cohesin. Scc2 is structurally similar to Scc3 also composed of HEAT repeats and a dragon-like shape (see figure 1.1B) (Kikuchi, Borek et al. 2016, Chao, Murayama et al. 2017). Similar to Scc3, Scc2 also interacts with the flexible Scc1 kleisin however at a different upstream non-overlapping motif. Biochemical studies have shown that Scc2 C terminal region containing the HEAT repeats is sufficient for

stimulating the ATPase activity of cohesin for loading on DNA (Murayama and Uhlmann 2014, Petela, Gligoris et al. 2018). The N terminus of Scc2 is important for its association with Scc4 and Scc4 in turn interacts with nucleosome remodelling factors, which then recruit cohesin to nucleosome free regions of the genome for loading (Muñoz, Minamino et al. 2019).

The two other accessory subunits Pds5 and Wpl1 form a complex and together can facilitate cohesin unloading (Sutani, Kawaguchi et al. 2009, Murayama and Uhlmann 2015). Pds5 is also another dragon-like protein similar to Scc3 and Scc2 in structure, and binds to Scc1 at the same region as Scc2. This means that Pds5 and Scc2 cannot bind to cohesin complex at the same time. Indeed it is thought that once loading by Scc2-Scc4 is complete, Pds5 replaces Scc2 in cohesin complex (Murayama and Uhlmann 2015, Petela, Gligoris et al. 2018) wherein it has dual stabilizing and distabilizing roles towards cohesin on DNA that are not entirely clear.

Mechanisms of cohesin function

The ring architecture of cohesin supplements its function in sister chromatid cohesion. Given that cohesin can topologically load onto DNA, two models among others have been considered as to how this may assist in sister chromatid cohesion. The handcuff model suggested that dimerization of individual cohesins on each sister DNA interact to keep the sisters associated (figure 1.2A) (Zhang, Kuznetsov et al. 2008). Another model predicted that the same cohesin is able to topologically entrap both replicated sisters (figure 1.2B). *In vitro* it has been shown that a single purified cohesin is capable of sequentially capturing a dsDNA followed by a ssDNA (Murayama, Samora et al. 2018) a situation that may be possible at the replication fork with dsDNA in the leading strand and ssDNA in the lagging strand. When the ssDNA is converted to dsDNA *in vitro*, cohesin continues to topologically entrap two dsDNA. Like topological loading, second ssDNA capture by cohesin is dependent on cohesin loader and ATP. Parallel experiments with a covalently closed cohesin ring has similarly shown that 2 mini-chromosomes can be captured inside one cohesin ring *in vivo* (Srinivasan, Scheinost et al. 2018).

Other closely related paralogs of SMC proteins, kleisins and HEAT repeats also form multisubunit complexes very reminiscent of cohesin. In eukaryotes, these are Condensin and Smc5/6 which perform chromosome condensation and DNA repair respectively. (Uhlmann 2016). Alongside these specialized protein complexes, cohesins as well contribute

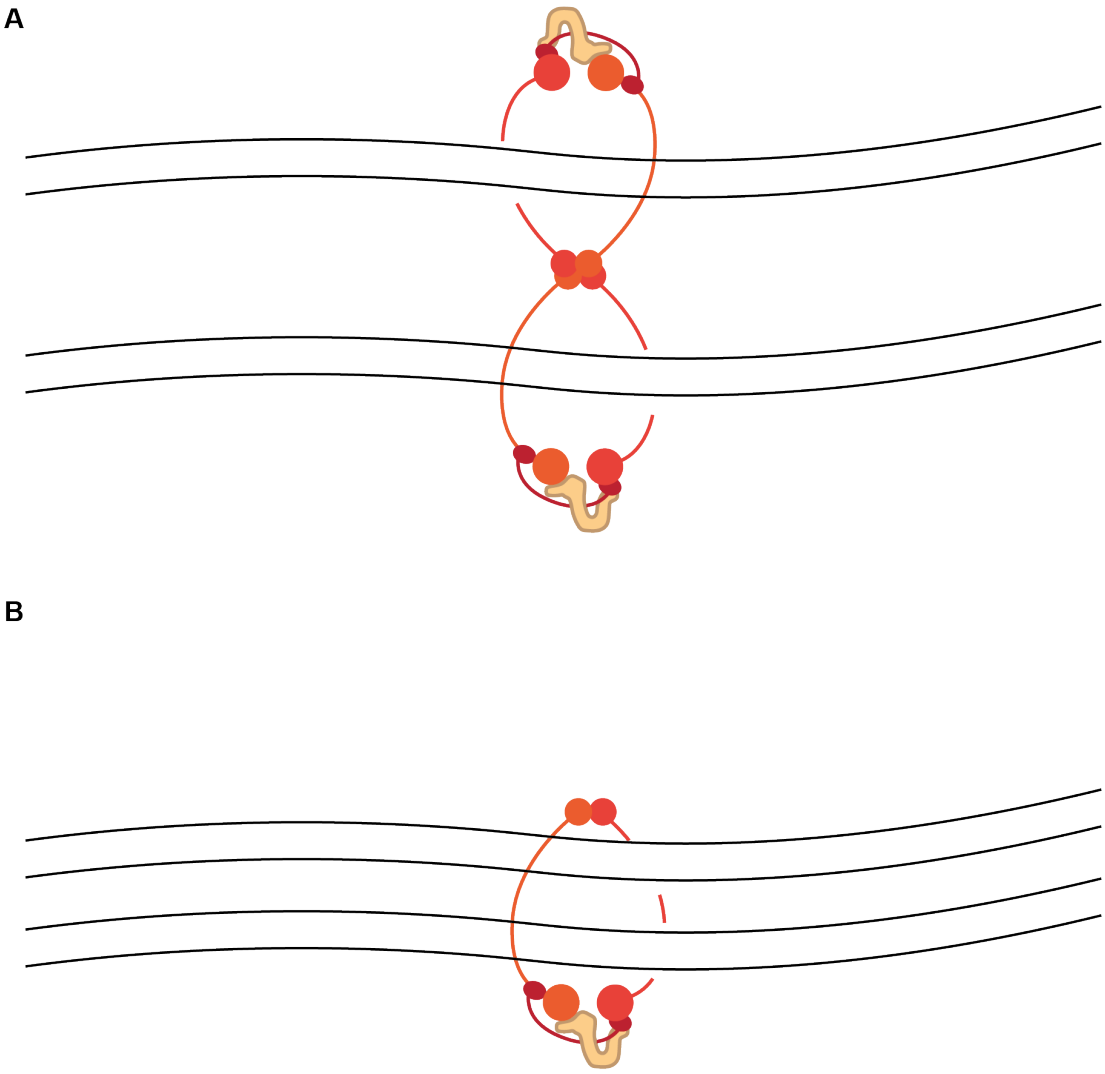

Figure 1.2 Schematic for proposed models of sister chromatid cohesion

A. Handcuff model through dimerization of cohesins individually loaded on sister DNAs
B. Cohesin topologically embraces two dsDNA

to chromosome condensation and DNA repair. Like condensin, cohesin can bring together distant sections of DNA to organize the genome. HiC maps that interrogate physical contacts within the genome have shown a reduction in cis-chromosomal contacts in absence of cohesin (Rao, Huang et al. 2017). Through genome organization, cohesin can also influence the transcriptional landscape of the cell. The mechanism through which cohesins may be performing genome organization is also under scrutiny. One possibility is that similar to its function in sister chromatid cohesion, cohesin may be sequentially entrapping two DNA to bring them together. The second ssDNA capture may be from R-loops at highly transcribed regions. Alternatively, loop extrusion has been proposed as a model for chromosome condensation based on single molecule experiments of purified cohesin complexes extruding loops (Davidson, Bauer et al. 2019). The relative contributions of these two mechanisms in cells for genome organization by cohesin is currently unclear.

Secondly, cohesins are also recruited to sites of replication fork stalling and DNA damage in S phase and G2 where it performs damage induced cohesion facilitating DNA resection and repair (Heidinger-Pauli, Ünal et al. 2008, Delamarre, Barthe et al. 2020). Evidence for the role of cohesin in various cellular processes like sister chromatid cohesion, chromosome organisation, transcription regulation and DNA repair are strong. Meanwhile, the mechanisms through which cohesins contribute to these functions remain a subject of intense debate.

Cohesin regulation during the cell cycle

The association of cohesin with DNA changes throughout the cell cycle and this is closely tied to its function in sister chromatid cohesion. Figure 1.3 presents a simple schematic showing the status of cohesin dynamics on DNA and includes other accessory regulatory proteins that contribute to it.

Soon after ample expression of Scc1 in late G1, cohesin molecules are loaded onto DNA by the cohesin loader complex Scc2-Scc4 (Ciosk, Shirayama et al. 2000). The turnover of cohesin on DNA at this point is quite high, as at the same time it is prone to being dissociated from DNA by unloading action of Pds5-Wpl1 (Gerlich, Koch et al. 2006, Lopez-Serra, Lengronne et al. 2013). Cohesin on DNA inevitably encounters the replication fork in S phase. Several proteins associated with the replisome have been identified as cohesion establishment factors for their role in establishing sister chromatid cohesion. Cohesins are now established and cohesive as they entrap equivalent sections of sister chromatids

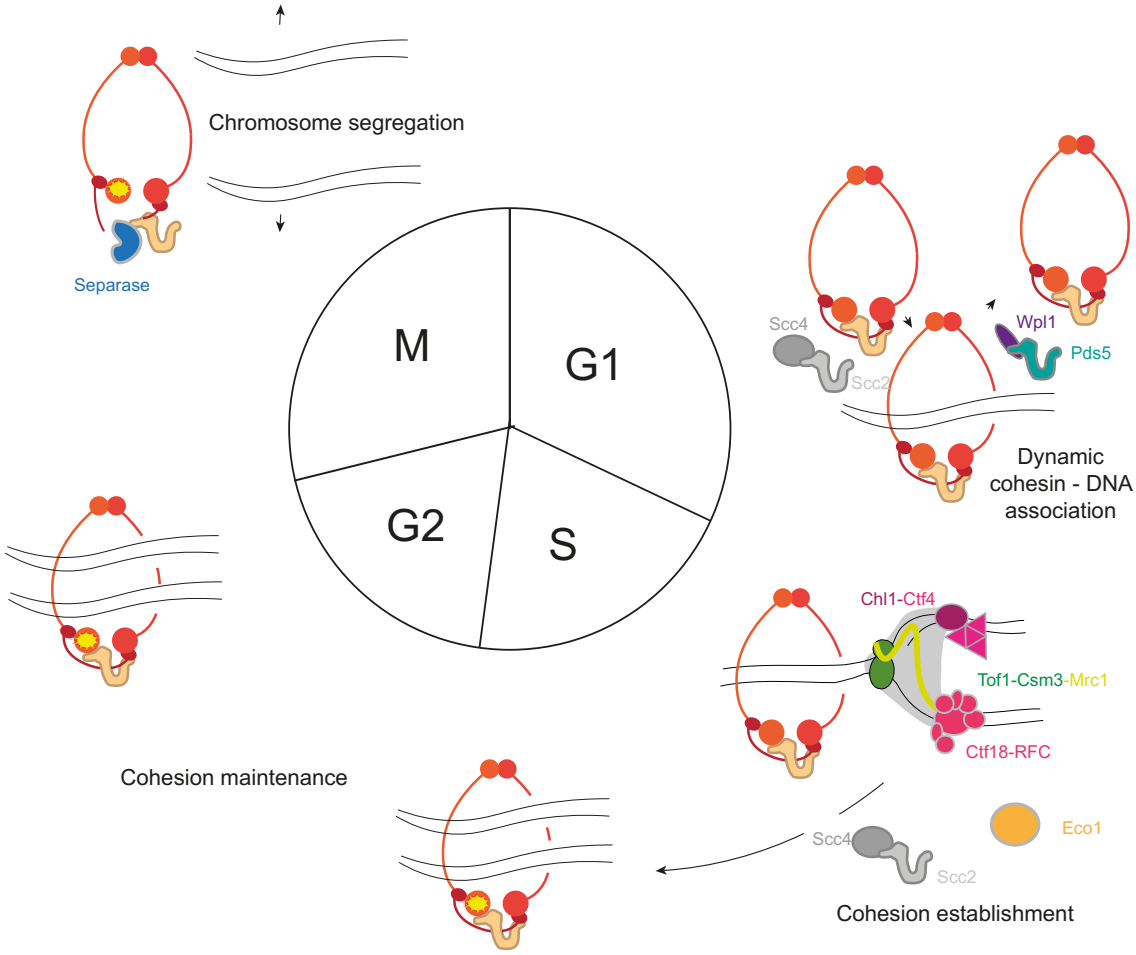

Figure 1.3 Schematic depicting cohesin association with DNA during the cell cycle

together. During the process of cohesion establishment, Eco1 protein also acetylates cohesin due to which cohesin becomes more stable in its association with DNA such that sister chromatid cohesion is maintained for the remainder of S phase, G2 all the way to Anaphase of Mitosis. Chromosome segregation occurs during cell division in Anaphase when the kleisin Scc1 subunit is proteolytically cleaved by an enzyme called separase allowing sister chromatids to move to two progeny cells (Uhlmann, Wernic et al. 2000). In higher eukaryotes, prior to this cleavage, cohesin is also successively removed from the arms except at the centromeres leading to the characteristic X shape of the sister chromatids during early mitosis. However, in budding yeast, my model organism of study, cohesin is maintained across the arms of the chromosome until cleavage in anaphase. Upon cleavage, Scc1 is also degraded and cohesin association with chromosomes is only replenished in the next cell cycle upon re-expression of all necessary subunits including Scc1 in late G1.

1.3 Sister chromatid cohesion establishment

Cohesion establishment occurs during S phase

Establishment of sister chromatid cohesion is a fundamental process through which sister chromatids are held together post replication and throughout G2 until their timely separation during Anaphase of mitosis. During cohesin establishment, cohesin molecules achieve the cohesive state wherein they are holding together two identical sections of sister chromatids in a stable manner.

Cohesion establishment occurs in S phase. We know this because when the expression of Scc1 subunit of cohesin is controlled such that it is only expressed after completion of DNA replication, sister chromatid cohesion is not established (Uhlmann and Nasmyth 1998).

It is also energetically efficient for sister chromatid cohesion to be established during replication. During replication, newly replicated sections of DNA are in spatial proximity to each other, and this time-sensitive advantage can be utilized for co-entrapment of identical sections of DNA by cohesin. If, however, sister chromatid cohesion was to be established in G2, equivalent sections of sister chromatids will have diffused away from each other and a mechanism would need to be available to recognize identical sections of DNA. In diploid eukaryotes, it would be a mess trying to differentiate sister chromosomes from homologous

chromosomes. Therefore, the ideal time for cohesion establishment is either exactly during replication or immediately following replication. In the cell, identical sections of DNA are found to remain in close proximity to each other for the entire duration post replication and during G2 (Selig, Okumura et al. 1992, Guacci, Hogan et al. 1994) until their timely separation in Anaphase of mitosis.

However, it is not just spatial proximity of equivalent section of sister chromatids that is necessary for Cohesin to co-entrap them. Cells that go through S phase without Scc1 subunit of Cohesin and with a defective topoisomerase II, such that they have no sister chromatid cohesion but their sister chromatids are intercatenated, become unviable even with expression of Scc1 in G2 (Uhlmann and Nasmyth 1998). This study further clarified that a complete tetrameric cohesin complex is capable of binding to DNA in G2 but unable to establish cohesion even when sister chromatids are in proximity. This suggests that cohesin establishment specifically requires other aspects of DNA replication.

Indeed, several components of the DNA replication machinery have been implicated in sister chromatid cohesion. They are not essential for cohesin loading onto DNA but they are necessary for conversion of cohesin into a cohesive state. In absence of these replisome components, sister chromatid cohesion is defective. Together, these replisome associated proteins are called cohesion establishment factors.

Further circumstantial evidence also suggests that cohesion establishment occurs during DNA replication. Cohesin molecules associate with DNA during late G1 phase of the cell cycle soon after protein expression of all 4 subunits of the cohesin tetramer (Michaelis, Ciosk et al. 1997). This makes it inevitable that during DNA replication, the replisome will encounter cohesin on DNA. This encounter has been the subject of much speculation and several models have been proposed for how an encounter between replisome and cohesin may lead to cohesion establishment which I will discuss in the next section.

The cohesin complexes in late G1 are very dynamic in their association with DNA (Gerlich, Koch et al. 2006, Chan, Roig et al. 2012, Lopez-Serra, Lengronne et al. 2013). About one-third of expressed cohesin is associated with DNA and two-third remain free in late G1. This equilibrium is maintained by cohesin loader complex Scc2-Scc4 loading cohesin on DNA (Ciosk, Shirayama et al. 2000) and cohesin unloader Wpl1 knocking cohesin off DNA (Sutani, Kawaguchi et al. 2009). During the process of cohesion establishment, the Smc3 subunit of cohesin is acetylated at two lysine residues. This acetylation event occurs during replication and is otherwise highly inefficient in G1, G2 or early mitosis (Ünal, Heidinger-

Pauli et al. 2008). Smc3 acetylation leads to a more stable association of cohesin with DNA, making action of Wpl1 on DNA-associated cohesin futile.

Therefore, two main events need to occur during cohesion establishment. Cohesin becomes cohesive and holds together equivalent sections of sister chromatids. At the same time, Smc3 subunit of cohesin is acetylated, making it more stable in its association with DNA such that the tethering of sister DNAs is secure and is not easily dislodged by unloading action of Wpl1.

Models for cohesion establishment

The encounter of active replisome with cohesin on DNA is a big black box. How is cohesin that is loaded on a single copy of dsDNA tethering two sister dsDNA by the end of replication? At least four distinct models have been imagined so far (figure 1.4). Currently, there is not enough evidence to determine which of these models are correct. Nor is there enough evidence to exclude any of these models.

These models are not necessarily mutually exclusive of each other as genetic experiments suggest at least two cohesion establishment pathways occur in cells (Xu, Boone et al. 2007, Srinivasan, Fumasoni et al. 2020). Below, I have provided a description of each model and commented on various experimental evidence available that can support the likelihood of it occurring in the cells.

Replisome passage through cohesin ring

The first model suggests that when the replisome encounters cohesin, it is able to pass through the ring (figure 1.4A). For this to be plausible, the size of the replisome should be small enough to fit through the internal diameter of cohesin.

Electron micrographs of human cohesin complexes show cohesin Smc1 and Smc3 dimer adopting a ring like conformation (Anderson, Losada et al. 2002) which have informed the cartoon images of cohesin that have since been adopted showing the Smc1 and Smc3 coiled coil subunits forming the main structure of the ring. When Smc1 and Smc3 are fully extended, the diameter of cohesin is expected to be around 40nm (Haering, Löwe et al. 2002). Meanwhile, the most complete structure of the replisome that is currently available

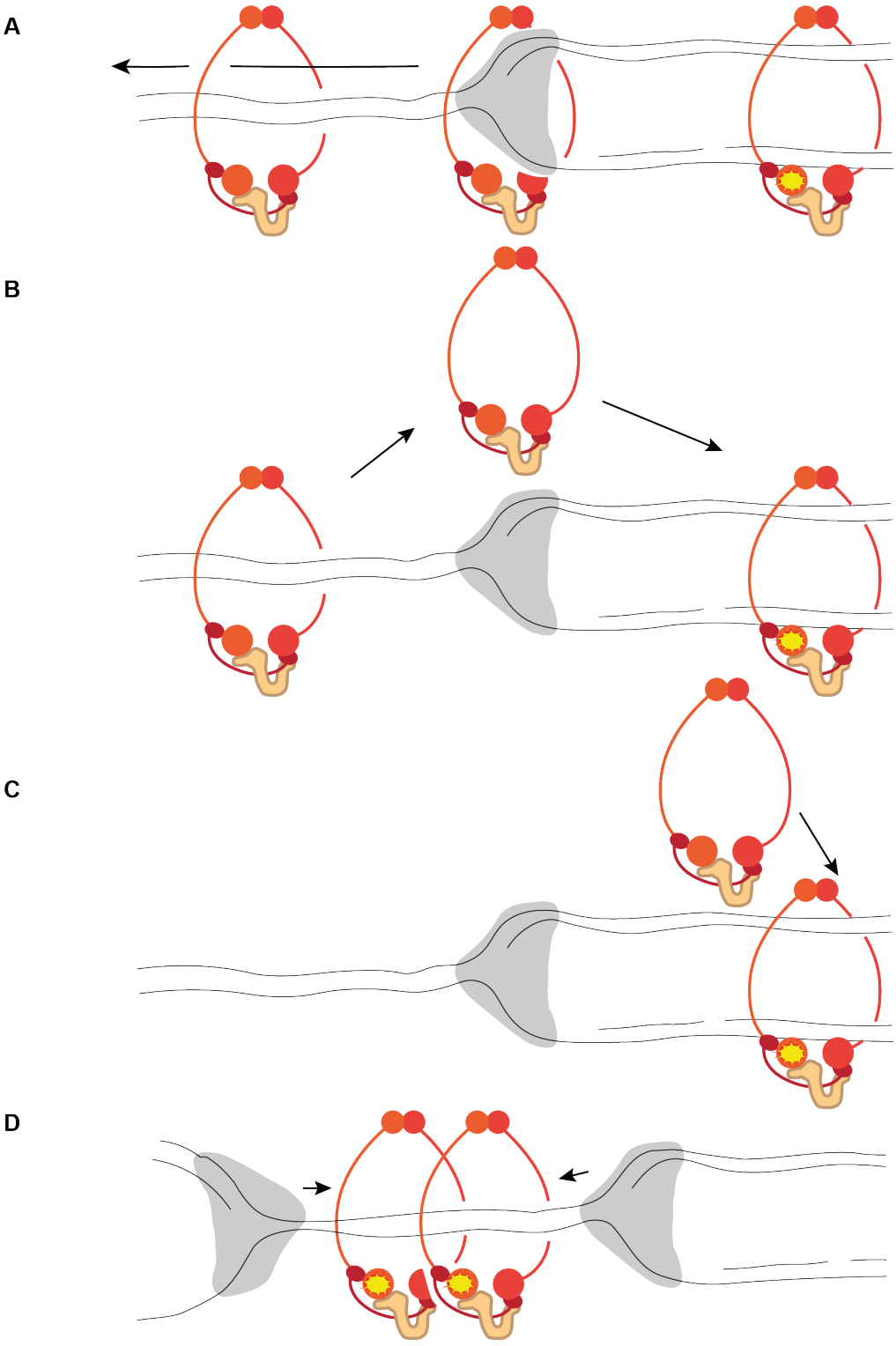

Figure 1.4 Schematic for proposed models of encounter between replisome and cohesin that lead to cohesion establishment

A. Replisome passage through cohesin ring
B. Transient cohesin unloading and reloading behind the replication fork
C. *De novo* loading of cohesin behind the replication fork
D. Replisome pushing of cohesin for establishment at replication termination sites

includes the CMG helicase and associating proteins Tof1, Csm3 and Ctf4 which together form a diameter of approximately 21.2 nm (Baretić, Jenkyn-Bedford et al. 2020). While we still do not know the size of a fully assembled replisome, and the size would subsequently increase when more proteins (eg. polymerase epsilon, polymerase alpha, Mrc1) are included, so far nothing is known in the replisome that would not be able to fit through the cohesin ring.

Single molecule studies have shown that cohesin translocating on DNA is able to bypass small protein complexes like histones (Stigler, Çamdere et al. 2016). On the other hand, a separate study observed that MCM hexamer, which is part of the CMG helicase poses a barrier for cohesin translocating on DNA (Dequeker, Scherr et al. 2022). Meanwhile, single molecule studies using *Xenopus leavis* egg extract have shown significant instances (32.4%) where replication is able to proceed past the cohesin ring (Kanke, Tahara et al. 2016). However, this study cannot differentiate between mechanisms of this model or model B which I will describe shortly.

A separate single molecule study that observed loop extruding cohesin instead of cohesin simply translocating on DNA, found cohesin bypass of large 200 nm nanoparticles (Pradhan, Barth et al. 2022). At least this observation of cohesin bypass cannot be explained by passage through cohesin ring as it would be physically impossible to fit a 200 nm particle inside the fully extended cohesin ring.

Something to also consider is that structural studies of cohesin gripping DNA, which is considered to be an intermediatory step in topological loading of cohesin on DNA shows cohesin not in a ring-like conformation but rather a closed conformation where parallel positions in the Smc1 and Smc3 dimer contact each other and fold at the elbow (figure 1.1B), (Higashi, Eickhoff et al. 2020). The structural conformation of cohesin once it is topologically loaded is unknown, but if it remains in closed conformation, a switch to a ring like conformation would need to be possible for replisome passage through cohesin.

It is also possible that the replisome alters its conformation upon encounter with cohesin, thereby facilitating the compaction of replisome during passage. Alternatively, components of the replisome could dissociate and reassociate after passage through cohesin ring. Mrc1, a replisome protein and a cohesion establishment factor has been shown to have dynamic association with the replisome (Lewis, Spenkelink et al. 2017)

Transient cohesin unloading and reloading behind the fork

The second model proposes that when replisome reaches cohesin on DNA, cohesin is unloaded and subsequently reloaded behind the replication fork (figure 1.4B). This model has similarities with the first model because in both cases, cohesin that is on DNA in front of the replication fork is converted into cohesive cohesin behind the replication fork. However, instead of replisome passing through cohesin ring, this model proposes the mechanism to be transient dissociation from DNA.

Encounter with replisome could lead to cohesin getting knocked off DNA. In single molecule experiments, instances (29.4%) of the replisome knocking cohesin off DNA upon encounter have been observed (Kanke, Tahara et al. 2016). This could represent cohesin that was dissociated but not successfully established behind the replication fork. Similarly, an *in vivo* assay for checking the capability of preloaded cohesin to tether newly replicated minichromomes found that in absence of some cohesion establishment factors, not only cohesin cannot become cohesive but cohesin association with even single dsDNA is almost completely lost (Srinivasan, Fumasoni et al. 2020). A separate study found *in vivo* that in absence of some cohesin establishment factors such as Tof1 and Chl1, there is an overall decrease in cohesin associated with DNA after replication suggesting that inefficient cohesion establishment during a Tof1-Chl1 dependent pathway leads to cohesin removal from DNA (Leman, Noguchi et al. 2010). In instances of successful cohesion establishment, removal of cohesin could be immediately compensated by establishment of cohesin immediately behind the replication fork.

In this model, components of the replisome could transiently tether DNA as it is relocated behind the replication fork. Chl1, which is also a replisome component, can form interactions with cohesin complex (Samora, Saksouk et al. 2016).

This model also predicts cohesin reloading behind the fork. Biochemical experiments suggest that cohesin captures two DNA in a sequential manner, and that *in* vitro, this is most efficient when it first topologically loads onto dsDNA and then captures ssDNA (Murayama, Samora et al. 2018). Based on this, a possible scenario is that cohesin is loaded behind the replication fork at the leading strand and then captures ssDNA from the incomplete lagging strand.

De novo loading of cohesin behind the replication fork

This model suggests that cohesin from the unbound fraction in the nucleus is loaded *de novo* behind the replication fork (figure 1.4C). The only difference of this model to the previous model is that cohesin is not recycled from ahead of the fork in this case. Both models require cohesin loading action during S phase likely with the help of the cohesin loader complex Scc2 and Scc4. Consistent with this, absence of loader in S phase leads to cohesion defects (Murayama, Samora et al. 2018). At the same time, cells are still viable if cohesin loader is inactive during S phase suggesting that at least one of the cohesion establishment pathways is loader independent (Lengronne, McIntyre et al. 2006).

Although this model does not strictly require encounter between replisome and cohesin, any *de novo* loading of cohesin on DNA that is too far away behind the replication fork is unlikely to favor capture of sister chromatids. As I previously described, the ideal time window for cohesion establishment is expected to be during or immediately after DNA replication when identical replication products are close together. When speculating on the mechanism of this model, it is possible that replisome components may be interacting with cohesin loader and/or cohesin complex to ensure that the *de novo* loading of cohesin occurs directly behind the replication fork.

Replisome pushing of cohesin at replication termination sites

The final model predicts that when replisome encounters cohesin, it pushes cohesin to replication termination sites where cohesin are finally established when two replication forks converge (figure 1.4D).

Single molecule studies have also observed pushing of cohesin by the replisome (Kanke, Tahara et al. 2016, Cameron, Gruszka et al. 2022). An immediate prediction of this model would be that in this case cohesins would localize at replication termination sites. However, even this is difficult to check *in vivo*. Cohesins are initially loaded in G1 at nucleosome free regions (Lopez-Serra, Kelly et al. 2014, Muñoz, Minamino et al. 2019) by cohesin loader at cohesin loader DNA binding sites. They are then almost immediately pushed by transcription machinery and thereby repositioned at transcription termination sites (Lengronne, Katou et al. 2004). Given this strong effect of transcription on cohesin, any effect of replisome on cohesin would be masked and therefore has not been hitherto observed. It would require cohesin ChIP at short time intervals during replication in the absence of transcription to resolve this question *in vivo*.

In yeast, an average replisome moves through 20 kB of DNA before merging with a converging fork (Pasero, Bensimon et al. 2002). While cohesin pushing has been observed in tethered DNA in single molecule experiments in *Xenopus leavis* extracts using a tethered DNA template with sparse nucleosome occupancy, the context of chromatin in the nucleus is more crowded and complex. It would be of great interest to directly observe if replisome are able to push cohesin for a distance of 20 kB in the context of nucleosomes, other DNA binding proteins, transcription etc.

All of the above described of models are proposed speculations and they are by no means exhaustive or exclusive of each other. Despite at least two decades of research, cohesin establishment is an ongoing mystery that remains to be resolved. It is indeed non-trivial to investigate which of these models are able to correctly describe cohesion establishment. A huge arsenal of techniques, ranging from *in vivo* genetics, IP of covalently closed cohesin rings, *in vitro* biochemical reconstitution of cohesin loading and single molecule experiments, have been dedicated to uncovering the mystery of cohesion establishment.

1.4 Cohesion establishment factors

Smc3 acetylation by Eco1

In G1 phase, cohesin association with DNA is dynamic (Gerlich, Koch et al. 2006, Chan, Roig et al. 2012, Lopez-Serra, Lengronne et al. 2013). Acetylation of the Smc3 subunit of cohesin that occurs during cohesion establishment converts a subset of DNA bound cohesin into a more stably associated state ensuring that sister chromatid cohesion persists into G2 and early mitosis (Bernard, Schmidt et al. 2008).

Smc3 acetylation is carried out by an acetyl transferase called Eco1 which stands for Establishment of cohesion 1 (Skibbens, Corson et al. 1999, Tóth, Ciosk et al. 1999, Ivanov, Schleiffer et al. 2002). It is a small protein of 31kDa whose expression is restricted to S phase. Originally Eco1 used to be called Ctf7 because it was identified in a large genetic screen for genes necessary for chromosome transmission fidelity (Spencer, Gerring et al. 1990). Ctf7 was renamed to Eco1 to better describe its role in establishing sister chromatid cohesion (Tóth, Ciosk et al. 1999). Mutations in Eco1 leads to precocious separation of sister chromatids however, Eco1 is not a subunit of cohesin and unlike cohesin loader and

Pds5-Wpl1, is not involved in cohesin association and dissociation from DNA. Also unlike core cohesin subunits, Eco1 is only essential in S phase for cohesion establishment and is dispensible post-replication for cohesin maintenance (Skibbens, Corson et al. 1999, Tóth, Ciosk et al. 1999).

Homology studies predicted that Eco1 is a member of the Gcn5-related-N-acetyltransferase (GNAT) family. Purified Eco1 confirmed that Eco1 has acetyltransferase (ACT) activity (Ivanov, Schleiffer et al. 2002). Further investigation by three laboratories independently identified that Eco1 acetylates Smc3 subunit of cohesin at lysines K112 and K113 (Ben-Shahar, Heeger et al. 2008, Ünal, Heidinger-Pauli et al. 2008, Zhang, Shi et al. 2008, Skibbens 2009). In each case, acetylation at K112 and K113 was identified through mass spectrometry and was followed up with validation studies involving mutations of those residues. Cells become unviable when K112 and K113 are mutated to a similarly charged arginine which unlike lysine cannot be acetylated. On the other hand, viability of cells without a functional Eco1 can be rescued if those lysine are converted to acetyl mimicking glutamine (Q) (Ünal, Heidinger-Pauli et al. 2008) or aspargine (N) which is biophysically similar to an acetylated lysine (Ben-Shahar, Heeger et al. 2008). For the above reason, the essential function of Eco1 is attributed to be Smc3 acetylation which occurs sequentially at the tandem lysine residues, first at K112 and then K113 (Chao, Wade et al. 2017) even though K113 has been found to be the more biologically important one out of the two residues (Ben-Shahar, Heeger et al. 2008, Ünal, Heidinger-Pauli et al. 2008, Zhang, Shi et al. 2008).

However, in fission yeast cells, Eso1 (homolog of Eco1) remains essential even with acetylation mimicking mutant of Psm3 (Smc3 homolog), suggesting that across species, Eco1 acetylation of Smc3 may not be the only molecular event through which cohesin association is stabilized in post replicative chromosomes (Feytout, Vaur et al. 2011).

In terms of other possible functions of Eco1, Eco1 can also auto-acetylate and other targets of Eco1 have been identified which include Scc1, Scc3, Pds5 (Ivanov, Schleiffer et al. 2002) and also interestingly Mps3 which is involved in spindle pole body function (Ghosh, Gardner et al. 2012). However, it remains to be directly explored whether these acetylation events really occur in cells and if so, what the biological relevance of these events might be.

In contrast, the functional relevance of Smc3Ac has been thoroughly investigated. K112 and K113 are located at the head region of Smc3. Structural studies show that the lysine residues are part of a loop rich in positively charged amino acids and they engage in interaction with both DNA and Scc2 subunit of cohesin loader (Collier, Lee et al. 2020, Higashi, Eickhoff et al. 2020, Shi, Gao et al. 2020). Changing the conserved lysine residues

to acetyl mimicking glutamine interrupts formation of cohesin gripping state, which is a reaction intermediate for topological loading of cohesin (Higashi, Eickhoff et al. 2020). Consistent with this Smc3 K112Q K113Q also leads to reduced cohesin loading *in vivo* and *in vitro* (Hu, Petela et al. 2015, Collier, Lee et al. 2020). Acetylation neutralizes the positively charged lysine which is expected to disrupt interaction with DNA and acidic residues in Scc2 that it contacts with.

The main cellular phenotype upon Eco1 acetylation of Smc3Ac in a normal cell cycle is stabilized association of cohesin on DNA. However, the above described observations are mostly concerned with a reduced loading of cohesin on DNA upon acetylation mimicking states. The above observations make sense if cohesin unloading and loading occur through similar pathways. Pds5 resembles Scc2 in structure (Lee, Roig et al. 2016) and if K112 and K113 make similar contact with Pds5 and DNA, acetylation of those residues could abrogate unloading the same way it abrogates loading. Cohesin unloading assays are consistent with this wherein mimic of Smc3Ac abrogates the DNA stimulation of cohesin ATPase and prevents unloading of cohesin form DNA (Murayama and Uhlmann 2015).

An important early discovery is also that disrupting Wpl1 or Pds5 function can also overcomes lethality of *eco1Δ* or *eco1-1* (Ben-Shahar, Heeger et al. 2008, Sutani, Kawaguchi et al. 2009). Wpl1 forms a stable complex with Pds5 and Pds5 stimulates interaction of Wpl1 with cohesin tetramer (Sutani, Kawaguchi et al. 2009, Murayama and Uhlmann 2015). Together, Pds5 and Wpl1 stimulate cohesin unloading from DNA. *In vitro*, Wpl1 can both load and unload cohesin on DNA, through ATPase activity at Smc1 and Smc3 head interface. Although the mechanistic details are still a work in progress, Eco1 acetylation of K112 and K113 seems to function as a lock on cohesin that prevents unloading of cohesin through disrupting contact with DNA and possibly Pds5 for unloading reaction. A structural study directly investigating whether Smc3 K112 and K113 are directly involved in interaction with Pds5 would be of great interest.

Eco1 must acetylate Smc3 in a timely manner to promote stabilized sister chromatid cohesion because if acetylation occurs prior to cohesin association with DNA, it can prevent cohesin loading. Without acetylation, cohesin dynamically turns over on DNA such that if acetylates occurs too late, it is unable to keep sister chromatids together. Eco1 expression is cell cycle regulated to peak at S phase and Smc3ac has been shown to increase with S phase progression (Ünal, Heidinger-Pauli et al. 2008). Overexpression of Eco1 in other stages of the cell cycle is unable to perform Smc3 acetylation (Borges, Lehane et al. 2010). However, Eco1 stabilization of cohesin association with DNA can still be functionally

uncoupled from DNA replication given that *wpl1Δ* or SMC3K113N can restore viability of *eco1* cells. So, what is it during a normal cell cycle that ties Eco1 activity to DNA replication?

Early studies already associated Eco1 with the replication fork based on genetic interactions of Eco1 with PCNA (Skibbens, Corson et al. 1999), which were further confirmed by the discovery of a loosely conserved PCNA interacting motif (PIP Box) in the N terminal region. Although Eco1 PIP Box Qxx(L/I) is missing the end FF residues of the canonical PIP Box Qxx(L/I)xxFF, Eco1 has been shown to interact with PCNA (Moldovan, Pfander et al. 2006). The PIP box in Eco1 is essential for cell viability but this can be rescued if Eco1 is tethered to two proteins at the lagging strand, Fen1 and to a much lesser extent Cdc9, suggesting that PCNA recruits Eco1 to lagging strand maturation sites (Liu, Bouchoux et al. 2020). Interaction of Eco1 with another integral component of the replication fork, the MCM complex has also been identified (Yoshimura, Sutani et al. 2021). Eco1 also contains a Zinc finger (ZnF) domain which may be important for association with DNA. A study by Masashi Minamino in our lab which is currently under review for publication shows that Eco1 activity is stimulated by a nick or flap on DNA, such as may be found at lagging strand maturation sites behind the replication fork. The full details of Eco1 activity at the replication fork is still ongoing.

Meanwhile, during the cell cycle Smc3 is also deacetylated by Hos1 which was identified in a screen for known deacetylases without which Smc3 maintained acetylation status in G1 (Borges, Lehane et al. 2010). It is not the deacetylation reaction that eventually disrupts sister chromatid cohesion but instead cohesin cleavage by Separase in Anaphase. Deacetylation occurs after this cleavage such that in the next G1, non-acetylated Smc3 with higher loading efficiency is loaded onto DNA.

Eco1 is a highly conserved protein and it has two paralogs in humans, Esco1 and Esco2 in which the ACT domain and ZnF domain are conserved with their yeast counterparts. Both are essential in human cells and so are thought to specialize in their functions (Hou and Zou 2005). Esco2 has the PIP box Qxx(L/I) and is only expressed during S phase suggesting that it is important for replication coupled acetylation and more similar to yeast Eco1 (Minamino, Negishi et al. 2018).

Along with sister chromatid cohesion, cohesin also functions in chromosome condensation and DNA damage response in G2. Eco1 activity has also been linked to these cohesin functions (Ström, Lindroos et al. 2004, Barton, Massari et al. 2022). How Eco1 activity is regulated for these functions remains an open question.

Eco1's expected association with PCNA was the first link that tied cohesion establishment to the replisome machinery. This spearheaded the discovery of several other non-essential replisome components that were subsequently identified as cohesion establishment factors which will be discussed at length in the next section.

Cohesion establishment factors

After discovery of Eco1, several non-essential members of the replisome were also identified to have a role in sister chromatid cohesion. They have been collectively called cohesion establishment factors because while they are not necessary for the initial association of cohesin with DNA in G1, they are necessary for intact sister chromatid cohesion. The main cohesion establishment factors are Chl1, Ctf4, Tof1, Csm3, Mrc1 and Ctf18 (see figure 2.1A for their depiction at the replication fork).

First, Ctf18-RFC complex and Ctf4 were identified to have cohesion defects (Hanna, Kroll et al. 2001, Mayer, Gygi et al. 2001). In their study and in future studies including this PhD thesis, sister chromatid cohesion was assayed using GFP dot assay for GFP visualization of cohesion at a specific locus of the genome (Straight, Belmont et al. 1996). Subsequently, a large genetic screen was conducted to identify genes that demonstrated synthetic growth defects if deleted alongside Ctf8 which is a component of the Ctf18-RFC complex (Mayer, Pot et al. 2004). The synthetic genetic interaction screen identified 55 candidates that were narrowed down to Chl1, Tof1, Csm3, Ctf4 based on the GFP dot assay. Three proteins related to microtubule function were also identified but not pursued further as cohesion defects in their case would be related to assembly of mitotic spindle. Finally, Mrc1 was identified in a comparable synthetic lethality screen with Ctf4 (Warren, Eckley et al. 2004, Xu, Boone et al. 2004).

Alongside the above discoveries in budding yeast, the role of Chl1, Ctf4, Tof1, Csm3, Mrc1 and Ctf18 in cohesion establishment is also conserved in larger eukaryotes (Errico, Cosentino et al. 2009, Leman, Noguchi et al. 2010, van der Lelij, Chrzanowska et al. 2010).

Ctf4-Chl1

Ctf4 forms a homotrimer complex that serves as a major interaction hub at the replisome as it has three docking sites through it can interact with CMG, polymerase alpha and its several other interaction partners (Simon, Zhou et al. 2014, Villa, Simon et al. 2016). A recent study

has shown that Ctf4 contribution to cohesion establishment is primarily through recruitment of Chl1 helicase to the replication fork (Samora, Saksouk et al. 2016). Chl1 is an accessory DNA helicase that unwinds in 5'-3' direction but this helicase activity is not strictly required for cohesion establishment (Samora, Saksouk et al. 2016, Cortone, Zheng et al. 2018). Chl1 can also interact with cohesin *in vivo* (Samora, Saksouk et al. 2016) and this interaction is expected to be key to its cohesion establishment role.

Ctf18-RFC

Ctf18-RFC complex is a part of a family of RFC complexes that participate in PCNA loading and unloading. As such, it contains the core Rfc2-5 subunits, as well as a unique Ctf18 protein and accessory subunits Ctf8 and Dcc1 (Kupiec 2016). Ctf18 has been recently shown to preferentially load PCNAs to the leading strand and cohesion defect in *ctf18* can be rescued by restoring PCNA levels at the replication fork (Liu, Bouchoux et al. 2020). However, PCNA is the recruitment platform for Eco1 at the lagging strand suggesting that the effect of PCNA loading dynamics in cohesion establishment is a complex problem. Ctf18 also participates in the intra S checkpoint and it interacts with polymerase epsilon, however neither of these roles are necessary for sister chromatid cohesion (Liu, Bouchoux et al. 2020).

Tof1-Csm3-Mrc1

Tof1, Csm3 and Mrc1, which form a heterotrimeric complex at the helicase perform several roles during DNA replication. They have so far been sparsely explored for their role in cohesion establishment. Most notable is a study in HeLa cells that found that interaction of Tof1 and Chl1 orthologs, Timeless and DDX11, is important for cohesion establishment (Cortone, Zheng et al. 2018). The study speculated based on lack of conservation of interaction motifs that Tof1 interaction with Chl1 is unlikely to be conserved in *S. cerevisiae*. Uncovering the role of Tof1, Csm3 and Mrc1 in cohesion establishment has been the main aim of my PhD project.

Epistasis between cohesion establishment factors

Cohesion establishment factors do not reach the drastic mis-segregation that can be observed in temperature sensitive mutants of cohesin or cohesin loader complex. Studies probing epistasis between cohesion establishment factors has since clarified that at least two separate pathways contribute to cohesion establishment and disrupting one pathway leads to compromised cohesion but cohesion is not entirely abrogated. The epistasis

interactions have separated them into two different groups - Tof1, Csm3, Chl1 and Ctf4 belong to one group and Ctf18 and Mrc1 belong to another (Xu, Boone et al. 2007, Srinivasan, Fumasoni et al. 2020). Deleting or introducing conditional mutants on two proteins of the same group results in the same level of cohesion defects as single deletions whereas double deletions between groups create additive defects. The double deletions create very sick cells however, some of them are still viable. The two groups were also corroborated in a recent study that further suggested that Tof1, Csm3, Chl1 and Ctf4 promote conversion of pre-loaded cohesin into a cohesive state (Srinivasan, Fumasoni et al. 2020). Meanwhile, Mrc1 and Ctf18 have been linked to require activity of cohesin loader in S phase.

In terms of considering whether cohesion establishment factors operate upstream or downstream of Eco1 acetylation during cohesion establishment, what we know is that in each case, deletion of the establishment factor leads to reduced Smc3 acetylation (Borges, Smith et al. 2013). As mentioned previously, *wpl1Δ* can rescue *eco1Δ* by stabilizing cohesin on DNA. Deletion of Wpl1 is also able to rescue cohesion defects in *tof1Δ*, *csm3Δ*, *mrc1Δ*, *ctf18Δ* but not in *chl1Δ* and *ctf4Δ*. Interestingly, this grouping of cohesion establishment factors is different from the other epistasis investigations. At the very least, we also know that downstream contribution to Eco1 acetylation by cohesion establishment factors is not through direct control of Eco1 protein expression levels.

For the large part the mechanistic contributions of cohesion establishment factors still remain enigmatic. While an assay exists to identify their involvement in cohesion establishment using genetics, it is non-trivial to investigate the molecular mechanism through which they are establishing cohesion.

Other replisome components in cohesion establishment

The list of cohesion establishment factors has also continued to expand with inclusion of other replisome associated components like nucleosome remodelling factors (Zhang, Shi et al. 2017). This opens the possibility of crosstalk between nucleosome assembly and cohesion establishment.

An earlier hypothesis tested whether cohesion establishment might be dependent on okazaki fragment processing (Borges, Smith et al. 2013). In the trombone model of replication, the lagging strand loop can pose as an obstacle for passage through cohesin

(Hamdan and Richardson 2009, Uhlmann 2009). While Chl1 and Ctf4 show synthetic lethality with Okazaki fragment processing factors Fen1 and Dna2 for reasons as yet enigmatic, Okazaki fragment processing does not seem to be involved in cohesion establishment. Neither deleting Fen1/Dna2 nor increasing Okazaki fragment length by deleting CAF-1 subunits leads to cohesion defects.

All identified cohesion establishment factors other than Eco1 are nonessential components of the replisome. As I have detailed through the original discoveries of cohesion establishment factors, it is clear that the genetic screens were conducted to identify non-essential proteins. Meanwhile, other essential replisome components have largely remained unexplored.

In early 2000s, cohesion defects was observed in a very small C terminal truncation of polymerase epsilon (Edwards, Li et al. 2003). However, this has not been followed up. Whether leading strand or lagging strand synthesis directly contribution to sister chromatid cohesion remains unknown.

At the same time, addressing essential components of the replisome is not straightforward because mutating or deleting essential replisome components will abrogate replication without which cohesion establishment cannot be studied. Understanding their role in cohesion establishment would require studying separation of function mutants. Alternatively, they can be studied in an in vitro or single molecule set up for closer observation of contribution of individual components. Such endeavours are currently ongoing in our lab.

1.5 Cohesinopathies and other cohesin-associated diseases

Cohesinopathies are genetic diseases where the primary factor causing disease is mutations in cohesin subunits or associated proteins. A prime example of this is Cornelia de Lange Syndrome (CdLS) where phenotypes can be observed from birth affecting physical growth (facial abnormalities and upper limb growth defects), behaviour and neurodevelopment (Kline, Moss et al. 2018). CdLS is diagnosed in 1 in 30,000 live births across the world (Kline, Krantz et al. 2007). 70% of the cases can be attributed to mutations in NIPBL (human ortholog of SCC2), 5% can be attributes to SMC1A (human ortholog of SMC1) and another

5%-10% can be explained by mutations in SMC3 and other related genes involved in genome organisation. Interestingly, sister chromatid cohesion defects are not observed in cell lines derived from patients of CdLS but frequently, significant irregularities in the transcription landscape of the cells have been observed (Parenti and Kaiser 2021). Similarly, irregular transcription of development genes has been identified in another genetic disease Roberts Syndrome attributed exclusively to mutations in ESCO2 (one of the two human orthologs or Eco1) (Mfarej and Skibbens 2020). Patients of Roberts Syndrome also exhibit facial abnormalities and neurodevelopment disorders, similar to CdLS. It is indeed the chromosome organization and gene regulation function of cohesin that are more frequently linked to cohesinopathies rather than cohesin function in sister chromatid cohesion. This is also true in Chronic Atrial and Intestinal Dysrhythmia (CAID), a more recently identified cohesinopathy caused by mutations in SGO1 (Chetaille, Preuss et al. 2014). SGO1 encodes for Shugoshin that is important for protection of cohesin from separase activity at the centromeres. CAID is thought to result from disruption of transcriptional patterns during development of heart and intestines. The exact knock-on effects of the mutations in a multicellular network that leads to transcriptional dysregulation and disease need a further investigation.

Meanwhile, mutations in DDX11 (human ortholog of Chl1) can cause Warsaw Breakage Syndrome (WBS) wherein patients exhibit microcephaly. In contrast to CdLS and CAID, precocious sister chromatid cohesion can be observed in patient derived cell lines of WBS (Pisani 2019). Cohesin core and associated genes have also been attractive candidates for mutations leading to tumorigenesis since a hallmark of cancer is aneuploidy. Mutations of SMC1A, SMC3 and NIPBL have been found in colorectal cancers (Barber, McManus et al. 2008), mutations of RAD21 gave been found in leukaemia (Rocquain, Gelsi-Boyer et al. 2010) and loss of STAG2 protein expression was identified in a large diversity of human tumors (Solomon, Kim et al. 2014).

Perhaps the most important function of cohesin in sister chromatid cohesion occurs in oocytes. Usually, sister chromatid cohesion is established in S phase and maintained throughout G2, Prophase and Metaphase until sister chromatids separate in Anaphase. In dividing human cells, sister chromatid cohesion is maintained for less than a day. In human oocytes, sister chromatid cohesion can need maintaining for over 40 years. Unsurprisingly, mutations in STAG3 (meiotic human ortholog of Scc3) have been linked to premature ovarian failure (Caburet, Arboleda et al. 2014).

Chapter 2: The Replisome

2.1 DNA replication

DNA replication is a very fundamental process that occurs once per cell cycle to allow for the faithful duplication of the entire genome, resulting in two identical copies of the genome. The discovery of the double helical structure of DNA immediately anticipated the semiconservative pathway through which parental strands are used as a template upon which new DNA are synthesized. While the concept is simple, it requires a vast molecular machinery to perform its job.

The replisome is the main molecular machine that performs DNA replication during S phase. The eukaryotic replisome constitutes of the CMG (Cdc45-MCM-GINS) helicase that unwinds the DNA, the DNA polymerases that add new dNTPs to synthesize new DNA, topoisomerases that overcome supercoiling ahead of the fork, histone chaperones that recycle as well as deposit new histones in the newly replicated DNA among others.

DNA replication can be divided into three key stages – initiation, elongation and termination. Initiation already starts in G1 when MCM double hexamers are recruited to sites of replication origin in an intricate sequence of events. These MCMs are loaded on DNA in a way such that dsDNA is incorporated into the channel in their ring-like architecture (Remus and Diffley 2009). When CDK activity rises in S phase, further factors are recruited to the replisome in a kinase dependent manner and replisomes are said to fire as an active CMG helicase unwinds the dsDNA and DNA polymerases add new dNTPs behind CMG in a strand specific manner. After primer synthesis, DNA polymerase epsilon synthesizes majority of the leading strand and DNA polymerase delta synthesizes the lagging strand (Yurieva and O'Donnell 2016). Termination of DNA replication occurs when two replication forks meet at converging sites. Upon termination, the replisomes are disassembled from the DNA (Moreno and Gambus 2020).

DNA replication has been reconstituted in vitro with purified replisome components and in this biochemical assay, a fully functioning active replisome consists of over at least 14 protein complexes, many of which consist of multiple subunits (Yeeles, Deegan et al. 2015, Yeeles, Janska et al. 2017). Of these, Tof1, Csm3 and Mrc1 are three non-essential components of the replisome.

2.2 Replication proteins Tof1 Csm3 and Mrc1

Tof1, Csm3 and Mrc1 associate with the CMG helicase

Tof1, Csm3 and Mrc1 (TCM) are non-essential members of the replisome that can form a heterotrimeric complex. All three proteins physically associate with the helicase after CMG activation, after which they travel with the replisome (Nedelcheva, Roguev et al. 2005, Gambus, Jones et al. 2006, Bando, Katou et al. 2009).

Tof1 and Csm3 of sizes 141kDa and 50kDa respectively form a very tight complex before they engage with the CMG helicase. If either Tof1 or Csm3 is deleted from the cell, the other protein cannot associate with the replisome (Bando, Katou et al. 2009) making their deletion phenotypes virtually indistinguishable *in vivo*. In fact, Csm3 stability depends on interaction with Tof1 because Csm3 is degraded in *tof1Δ* cells. Phosphorylation of Tof1 by yet unknown kinase(s) is necessary for its association with the replisome (Bastia, Srivastava et al. 2016). Tof1-Csm3 complex also contribute to the efficient association of the highly flexible and negatively charged 120kDa Mrc1 with the replisome, as Mrc1 levels at the replication fork are reduced but not completely abrogated. This frequently shows up as a confounding factor for whether some replication phenotypes of *tof1Δ/ csm3Δ* are due to reduced Mrc1 recruitment to the replication fork. In contrast, absence of Mrc1 does not reduce Tof1-Csm3 association with the replisome.

A structure of *Saccharomyces cerevisiae* Tof1 and Csm3 with the CMG helicase and Ctf4 was resolved using cryo electron microscopy recently (figure 2.1B) (Baretić, Jenkyn-Bedford et al. 2020). In this structure, both Tof1 and Csm3 are shown to be primarily composed of alpha helices that combine to form a bean like architecture that mimics the curvature of the N terminal face of the MCMs. The study also describes an “MCM-plugin” in Tof1, a structure that reaches deep into Mcm6, Mcm4, Mcm7 and also contact dsDNA. The Tof1-Csm3 complex are effectively placed at the “head of the replisome” and they also “grip” dsDNA before the DNA strands are separated after entry into the MCM hexamer channel. The C terminal end of Tof1 (amino acids 782 - 1238) could not be resolved and is therefore predicted to be a “flexible tether” which would then have more range and access for interactions with proteins that are not directly members of the core replisome. Consistent with this, C terminal region of Tof1 has indeed been shown to interact with Topoisomerase 1 and FACT.

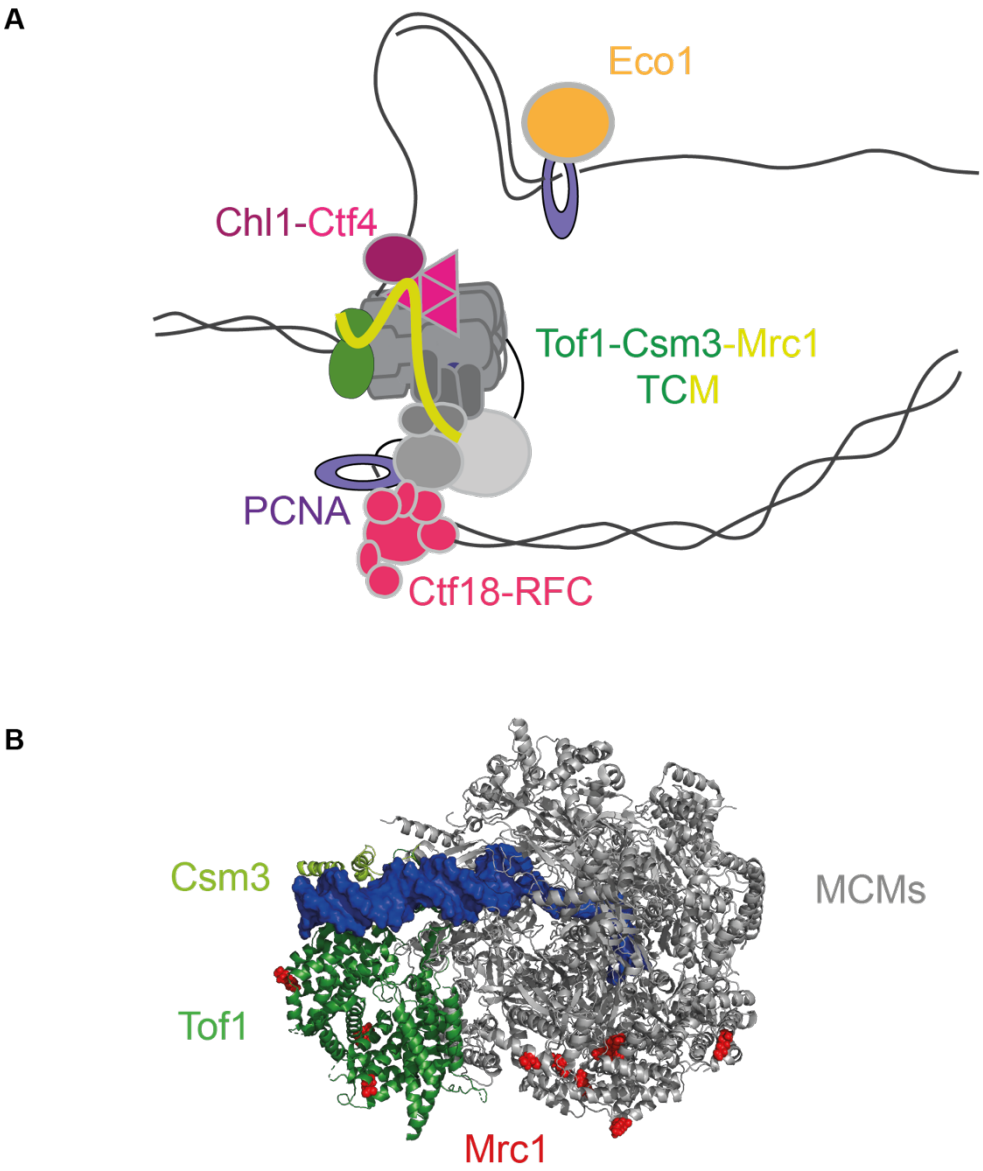

Figure 2.1 Cohesion establishment factors at the replication fork

A. Schematic showing the main cohesion establishment factors at the replication fork
B. Strcuture of Tof1 and Csm3 associated with the MCM subunits of the CMG helicase. Highlighted in red, expected localization of Mrc1 based on amino acids in Tof1 and MCMs that was shown to crosslink with Mrc1 (PDB: 6SKL and Baretić, Jenkyn-Bedford et al. 2020)

The same study also attempted to resolve the structure of Mrc1 but had less success. Instead, using protein crosslinking mass spec, they identified Mrc1 contacts that thread throughout the replisome (figure 2.1B). The N terminal of Mrc1 contacts Tof1, the central region of Mrc1 contacts Mcm6/Mcm2 and C terminal contacts Cdc45 and Ctf4. Indeed, interaction assays have shown that Mrc1 contacts at the replisome reach all the way to the tail (Lou, Komata et al. 2008). More recently, these structural observations of TCM at the replisome have also been corroborated using human proteins (Jones, Baris et al. 2021).

Replication roles of Tof1, Csm3 and Mrc1

Although all three are non-essential proteins, they perform numerous roles at the replication fork and these have been extensively studied. The full form of Mrc1 is Mediator of replication checkpoint 1 as it was discovered for its role in mediating intra S checkpoint signalling (Tanaka and Russell 2001). Mrc1 mediates signalling between the main sensor kinase Mec1 and main effector kinase Rad53 which leads to activation of the intra S phase checkpoint (Alcasabas, Osborn et al. 2001, Tanaka and Russell 2001). There are two routes to intra S checkpoint activation and Mrc1 mediates signalling for the DNA Replication checkpoint pathway when replication fork progression is impeded whereas another mediator Rad9 mediates signalling for the DNA damage checkpoint pathway (Gottifredi and Prives 2005, Pardo, Crabbé et al. 2017). Similar to Mrc1, some studies have also identified Tof1 involvement in intra S phase checkpoint signalling (Foss 2001, Chou and Elledge 2006). However, this role of Tof1 has never been delineated from its role in stabilizing Mrc1 at the replisome.

The activation of intra S checkpoint leads to Rad53 phosphorylation of multiple downstream proteins targeting pathways leading to cell cycle arrest, repression of late firing origins, upregulation of dNTP pools, preservation of replication fork function. TCM also get phosphorylated by Rad53 (McClure and Diffley 2021). TCM roles in mediation and response to intra S checkpoint is suitable given their advantageous position at the CMG helicase. Rad53 phosphorylation of Mrc1 has been shown to directly slow down CMG helicase (McClure and Diffley 2021) possibly related to their role in preventing helicase-polymerase decoupling (Katou, Kanoh et al. 2003). For this role in coupling helicase and polymerase activities under replication stress conditions, TCM are also referred to as the fork protection complex.

Alternatively, TCM is sometimes also called the replication progression complex for their role in modulating maximal replisome speed, this has been investigated at length both *in vivo*

and *in vitro* across various eukaryotes (Szyjka, Viggiani et al. 2005, Tourrière, Versini et al. 2005, Hodgson, Calzada et al. 2007, Petermann, Helleday et al. 2008, Yeeles, Janska et al. 2017, Baris, Taylor et al. 2022). Most updated estimates by highly sensitive nanopore sequencing of BrdU pulse labelled DNA determine a WT DNA replication speed of 2.4 kbp/min that is reduced to 1.6 kbp/min in *tof1Δ* or *csm3Δ* and 1.2 kbp/min in *mrc1Δ* (Theulot, Lacroix et al. 2022). Similarly, in the reconstituted replisome, omission of Mrc1 leads to a more significant decrease of replication speed compared to omission of Tof1/Csm3. The replication speed when Tof1/Csm3 is omitted could be partially rescued by adding increasing concentrations of Mrc1 suggesting that Mrc1 might be the main modulator of replication speed and Tof1/Csm3 contribution is through stabilization of Mrc1 at the fork, although they could not fully rule out an independent contribution of Tof1/Csm3 in replication speed (Yeeles, Janska et al. 2017). Meanwhile, Mrc1 has been shown to directly stimulate CMG helicase unwinding rate (McClure and Diffley 2021), yet the mechanistic details of this stimulation remains unknown.

While the above replication roles are overlapping for all three proteins and it is not yet resolved whether Tof1/Csm3 contribution to them is simply through Mrc1, some replication roles of Tof1 are independent of Mrc1. Tof1 stands for Topoisomerase I associated factor 1 because it was originally discovered as a protein that interacts with Topoisomerase I (Park and Sternglanz 1999). Topoisomerase I and topoisomerase II are swivelases that overcome supercoiling at the replication fork by nicking and cutting DNA respectively (Bermejo, Doksani et al. 2007). Recently, it was found that the flexible C terminal tail of Tof1 is directly responsible for Topoisomerase I recruitment to the replisome (Shyian, Albert et al. 2020, Westhorpe, Keszthelyi et al. 2020).

The flexible C terminal region of Tof1 also further interacts with FACT nucleosome chaperone and enhances its nucleosome disassembly activity by locally recruiting it at the head of the replisome (Safaric, Chacin et al. 2022). The specific peptide sequences in the C terminal of Tof1 that engage in interactions with FACT and Topoisomerase 1 are very close in tandem but do not overlap.

Tof1/Csm3 also promote replication fork pausing at replication fork barriers (RFBs) usually at locations of unusual DNA structures like rDNA repeats and/or high likelihood of replisome-transcription collisions (Mohanty, Bairwa et al. 2006, Hodgson, Calzada et al. 2007). The pausing is also dependent on Fob1 which have tight DNA binding at RFBs (Kobayashi 2003). The fork pausing role of Tof1 at RFBs is at least partially also attributed to its

recruitment of Topoisomerase 1 to the replication fork (Shyian, Albert et al. 2020), although the exact pausing mechanism remains to be determined.

While Tof1 is necessary for deliberate fork pausing at FRBs, a study in chicken cells showed that replisomes pause and are unable to replicate through G quadruplexes in absence of Tof1 ortholog Timeless (Lerner, Holzer et al. 2020). They suggest that Timeless interacts with Chl1 ortholog DDX11 to promote Chl1 helicase activity (Calì, Bharti et al. 2016) for processive replication through the G quadruplexes. Tof1 is also shown to be necessary for faithful replication through repetitive DNAs such as trinucleotides repeats of CAG or CTG because there is contraction of the repeat length in their absence (Razidlo and Lahue 2008, Gellon, Kaushal et al. 2019).

Recent advances in mechanisms of replisome disassembly show that Mrc1 at the replisome promotes ubiquitination of Mcm7 in the CMG helicase that is a key step in replisome disassembly (Deegan, Mukherjee et al. 2020). Interestingly, this role is not conserved in *C. elegans* where instead orthologs of Tof1 and Csm3 are necessary for Mcm7 ubiquitination (Xia, Fujisawa et al. 2021).

Finally, as already mentioned, Tof1, Csm3 and Mrc1 are cohesion establishment factors (Xu, Boone et al. 2007). Their mechanism for contribution to sister chromatid cohesion remain unknown and that has been the main focus of my PhD project. The myriad roles of TCM at the replication fork is incredible considering that cells are able to maintain viability in absence of these proteins.

Available literature on contacts between replisome and cohesin complexes

Interaction between cohesin and replisome components including cohesion establishment factors have been previously investigated multiple times in various organisms, either in targeted studies or in broader systematic interaction studies. TCM-cohesin interaction have both been reported and found lacking. As the second half of my thesis focuses on the unbiased identification of direct protein protein interactions between Cohesin and TCM, I have provided a summary of all available literature on contacts between replisome and cohesin subunits.

In *C. elegans*, peptides corresponding to TIM-1, an ortholog of Tof1, was identified among the immunoprecipitation fraction of SMC-1 through mass spectrometry (Chan, Chan et al. 2003). This was further investigated by immunoprecipitating SMC-1 and western blotting against TIM-1 which confirmed association. This interaction was found to be salt sensitive unlike interaction between cohesin subunits. Reciprocal co-immunoprecipitation was performed through IP of TIM-1 which also immunoprecipitated cohesin subunits SMC-1, SMC-3 and SCC-3.

In a coimmunoprecipitation study with *Xenopus* egg extracts using a very covetous set of antibodies against many replisome members, Smc3 seems to coimmunoprecipitate with Claspin (Mrc1 ortholog) although their data is not very clear (Tanaka, Kubota et al. 2009). However, Smc3 was not observed to immunoprecipitate with Tim1 (Tof1 ortholog) and Tipin (Csm3 ortholog).

Similarly, in human embryonic kidney cells, cohesin subunits coimmunoprecipitated with Timeless (Tof1 ortholog) (Leman, Noguchi et al. 2010). Confusingly after DNAse treatment of the extract used in coimmunoprecipitation, Timeless continued to immunoprecipitated Smc1 and SA1 (Scc3 ortholog) but not Smc3. Interaction between Tipin (Csm3 ortholog) and cohesin subunits was not observed after DNAse treatment.

Meanwhile, studies in HeLa cells have observed that AND-1 (Ctf4 ortholog) immunoprecipitates Smc1, Smc3 and Rad21 (Scc1 ortholog) (Yoshizawa-Sugata and Masai 2009). This provides an example of yet another cohesion establishment factor at the replisome, albeit not studied in my project, that could interact with cohesin. A study using budding yeast S phase cell extracts has clarified that Ctf4 interaction with cohesin is mediated by another cohesion establishment factor Chl1 (Samora, Saksouk et al. 2016).

All of these studies have been done in vivo therefore it is not possible to separate direct interactions from co-immunoprecipitation mediated by other proteins especially considering the crowded nature of the replisome. Meanwhile, there are also examples of large-scale systematic studies which failed to identify interactions between replisome components and cohesin core and accessory subunits. In Hela cells, 55 different replication and sister chromatid cohesion proteins were separately tagged to perform mass spectrometry on the immunoprecipitates (Ivanov, Ladurner et al. 2018). However, they did identify Eco1 interaction with MCMs which has also been reported in budding yeast (Yoshimura, Sutani et al. 2021).

Approach

In the study, I first asked whether any of the replication functions of Tof1, Csm3 and Mrc1 are also contributing to cohesion establishment (Chapter 4). By systematically disrupting these replication pathways independently of Tof1, Csm3 and Mrc1 or by using separation of function mutants, I asked whether any of their replication roles explained their contribution to cohesion establishment. Next, I also tested for presence of direct physical interactions between the cohesion establishment factors and cohesin (Chapter 5). I have mapped some interaction sites using protein crosslinking mass spectrometry.

All of the experiments in Chapter 4 are conducted *in vivo* in *Saccharomyces cerevisiae*, also called budding yeast. Chapter 5 consists of biochemistry using purified *Saccharomyces cerevisiae* proteins. *Saccharomyces cerevisiae* is a model eukaryotic organism where many of the fundamental processes of chromosome biology (as well as other cellular processes) have been studied over the years. Budding yeast is favourable for study because of their ease of genetic manipulation as well as the many methods available for synchronising them at various stages throughout the cell cycle (Nguyen, Co et al. 2001).

Chapter 3: Results (TCM contribute to cohesion)

3.1 Cohesion defects in absence of Tof1, Csm3 or Mrc1

Tof1, Csm3 and Mrc1 (TCM) have been implicated in cohesion establishment because they demonstrate sister chromatid cohesion defects (Xu, Boone et al. 2007, Borges, Smith et al. 2013). Here, I have reproduced the results that lead to this conclusion.

To assess cohesion establishment, I have used two independent assays in budding yeast cells. The first is called the GFP dot assay that was first designed in the mid-1990s in which cells are constitutively expressing GFP that targets a specific locus in the genome (Straight, Belmont et al. 1996) (see Materials and Methods for more information). After replication, when the cells are arrested in metaphase, if sister chromatid cohesion is intact, the GFP cannot be resolved and is observed as one dot under the microscope. However, if sister chromatid cohesion is compromised, GFP signal is separated and two GFP dots are observed (figure 3.1A). In a WT cell, there is always a background of some GFP separation, but this is significantly increased in *tof1Δ*, *csm3Δ* and *mrc1Δ* (figure 3.1B). This was reproducible from previously published results. Going forward in my research, I have continued to probe for sister chromatid cohesion status of only one locus in the genome situated 35kB away from the centromere of chromosome 5. However, the original study that identified Tof1 and Csm3 as cohesion establishment factors have also probed for sister chromatid cohesion status at loci closer and further away from the centromeres of different chromosomes. Specifically, they looked at 12kB away from centromere of chromosome 4 and 1.8kB away from centromere of chromosome 15 and found comparable GFP dot separation at all three loci (Mayer, Pot et al. 2004). Therefore, I find for my purposes that assessing sister chromatid cohesion status at one genomic locus is sufficient.

In *Saccharomyces cerevisiae*, which has a relatively small genome size of approximately 12Mb, the chromosome arms are not well resolved in metaphase and cannot be distinguished by DNA staining. When cohesion defects are scored in larger eukaryotes like *Xenopus* or in human cells, where the chromosomes are bigger and arms are resolved during metaphase, the status of sister chromatids can be assayed by directly observing chromosomes through DNA staining. Such studies have shown that when TCM orthologs

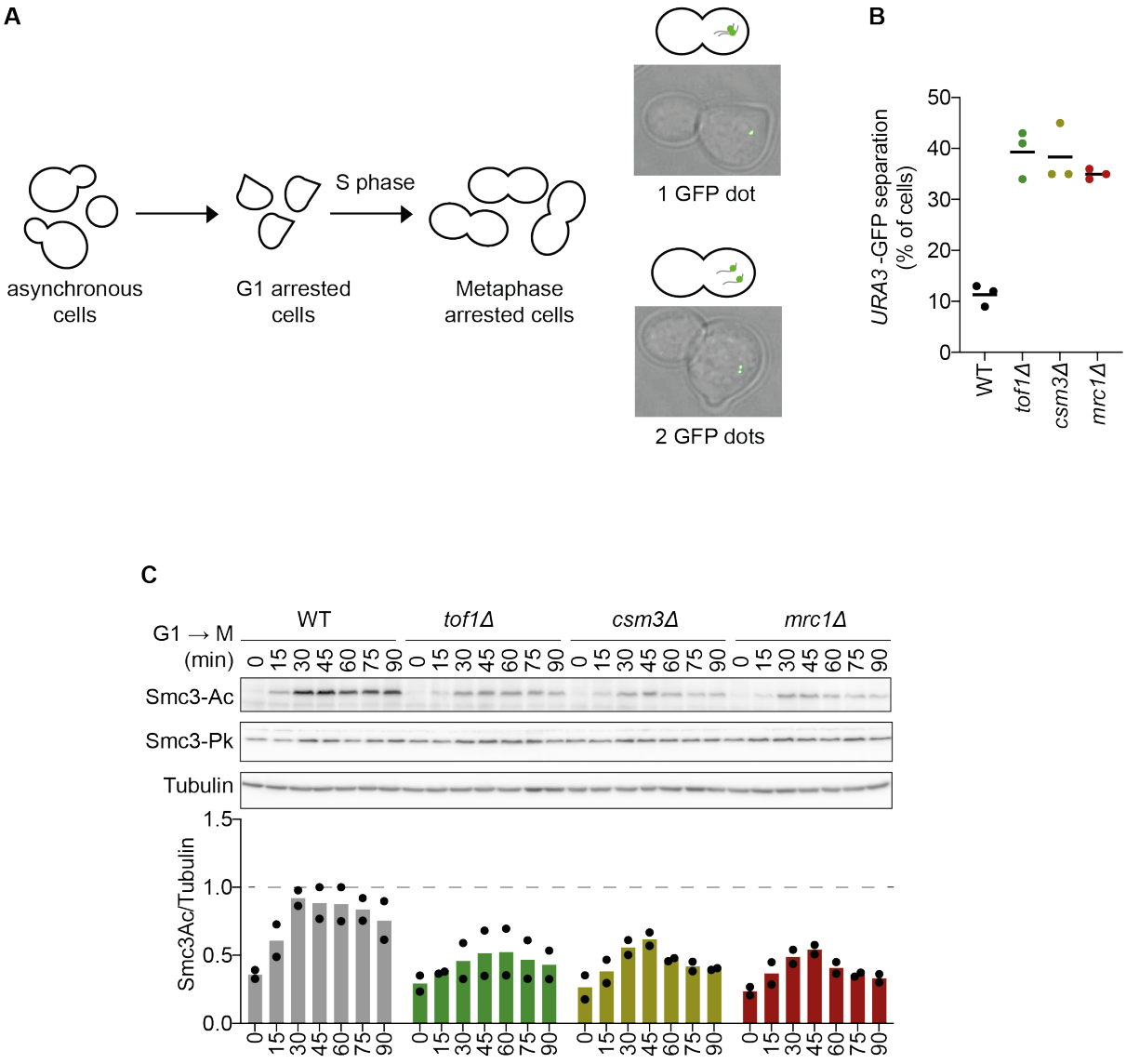

Figure 3.1 Cohesion defects in absence of Tof1, Csm3 and Mrc1

A. Schematic showing experimental procedure for GFP dot assay. Cells are synchronized in G1 and released into S phase in a medium containing nocodazole for 2 hours to arrest in metaphase. Cells are fixed and imaged. Representative images of one GFP dot (top right) indicating intact sister chromatid cohesion and 2 GFP dots (bottom right) indicating cohesion defects.
B. GFP dot assay of indicated genotypes in metaphase as described in A. Mean and individual values of three independent experiments are shown.
B. WB samples of cells of indicated genotypes were taken at indicated time points as cells were released from G1 arrest (0min) into S phase into a medium containing nocodazole to arrest in metaphase. Samples are blotted with anti-Smc3Ac. Smc3 levels are also monitored as Smc3 is tagged with Pk epitope and samples are also blotted with anti-Pk. Tubulin is used as loading control. The Smc3Ac/Tubulin ratio were normalized to highest signal of WT cells. Means and individual values from two individual experiments are shown.

are depleted, cohesion defects are spread across many chromosomes (Leman, Noguchi et al. 2010).

Another independent means of assessing whether cohesion establishment was successful is through monitoring the acetylation status of Smc3. Smc3 is acetylated by Eco1 during cohesion establishment in S phase and S phase Smc3 acetylation status is frequently used as an independent measure of cohesion status. I synchronized cells in G1 using alpha factor, released them into S phase and arrested them in metaphase using spindle poison nocodazole. In WT cells, G1 arrested cells have little to no Smc3 acetylation based on western blotting with an antibody that recognizes only Smc3 acetylated at residues K112 and K113 (figure 3.1C). As replication progresses, the Smc3 acetylation increases. This is expected as cohesion establishment occurs during replication. In contrast, the signal detected on the Pk-tagged Smc3 blot is constant. In *tof1Δ*, *csm3Δ* and *mrc1Δ* cells, the Smc3Ac levels during S phase are lower compared to WT cells (figure 3.1C), as has been previously reported (Borges, Smith et al. 2013). At later time points, a slight decrease in Smc3 acetylation can be observed in WT and mutants. This is expected to be because of Hos1 deacetylase activity (Borges, Lehane et al. 2010).

I also reproduced previously reported observations of additive cohesion defects in *tof1Δ mrc1Δ*, and *csm3Δ mrc1Δ* whereas removing both Tof1 and Csm3 had GFP dot separation count similar to single deletions (figure 3.2B) (Xu, Boone et al. 2007). The double deletion strains *tof1Δ mrc1Δ*, and *csm3Δ mrc1Δ* are also generally sicker and have a longer doubling time (data not shown). Their growth defect can also be observed in the spot assay (figure 3.2A). *mrc1Δ* cells are sensitive to HU and I found that further deletion of Tof1 or Csm3 in this strain further increased HU sensitivity. Smc3 acetylation across all three double deletion strains were also reduced compared to WT but I did not probe this rigorously enough to be able to comment on any additive defects (figure 3.2C).

Overall, I have reproduced previous observations of cohesion defects and epistasis between TCM.

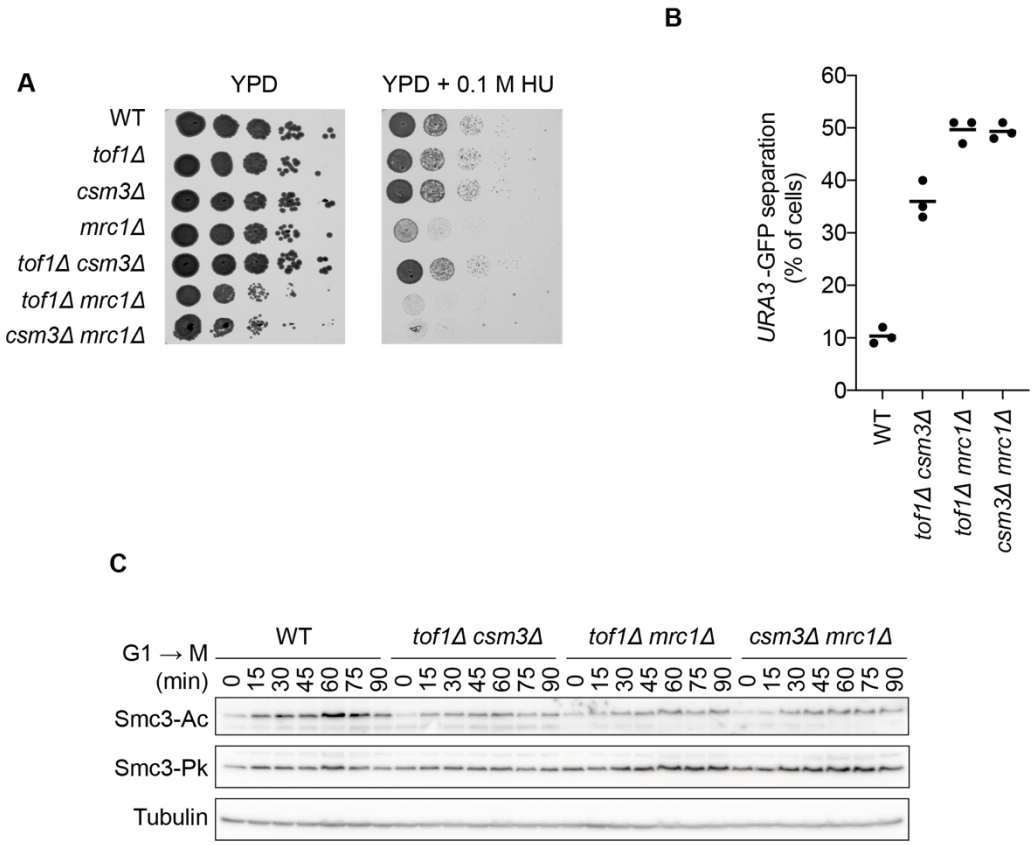

Figure 3.2 Epistasis between Tof1/Csm3 and Mrc1

A. Indicated genotyped were spotted in sequential 10 fold dilutions in YPD agar plates with or without 100 mM HU.
B. GFP dot assay of indicated genotypes in metaphase. Mean and individual values of three independent experiments are shown.
C. WB samples of cells of indicated genotypes were taken at indicated time points as cells were released from G1 arrest (0min) into S phase into a medium containing nocodazole to arrest in metaphase. Samples are blotted with anti-Smc3Ac and anti-Pk. Tubulin is used as loading control.

Chapter 4: Results (TCM Replication roles in cohesion establishment)

The aim of my PhD was to identify the roles of TCM in cohesion establishment. As a first approach to this question, I investigated whether any of the several functions of TCM at the replication fork is the mechanism through which they contribute to cohesion establishment. To address this, I disrupted the replication processes independently of TCM or through use of separation of function TCM mutants to ask what then happens to cohesion establishment.

4.1 Intra S phase checkpoint and cohesion establishment

I considered the possibility that when replisomes during S phase encounter cohesins on DNA, there is temporary replication fork stalling which transiently activates the intra S phase checkpoint. This hypothesis seemed plausible because in single molecule studies of replisome-cohesin encounter, in one-fourth occasions replication stalls upon reaching cohesin (Kanke, Tahara et al. 2016). Recent studies have also shown that the intra S phase checkpoint is active during WT unperturbed replication for upregulation of dNTP pools required in new DNA synthesis (Forey, Poveda et al. 2020). I considered whether this background level of intra S checkpoint activity is also facilitating cohesion establishment, and whether TCM contribution to cohesion is through the intra S checkpoint pathway.

To this end, I performed cohesion assays in the absence of a fully functional intra S phase checkpoint. Integral to the Intra S phase checkpoint is Rad53 protein which acts downstream as the main effector in the checkpoint signalling pathway (Pardo, Crabbé et al. 2017). Cells that instead express a non-conditional mutant *rad53-11* progress through the cell cycle despite being exposed to high doses of HU which normally activate the checkpoint and arrest cells in S phase (Shimada, Pasero et al. 2002, Forey, Poveda et al. 2020). In *rad53-11 cells,* Rad53 is also less stable compared to WT cells (figure 4.1B) and the sparsely expressed protein is not phosphorylated upon exposure to HU (data not shown).

As demonstrated before, in absence of Mrc1, increased GFP separation indicates cohesion defects. However, *rad53-11* cells only demonstrated a background level of GFP dot

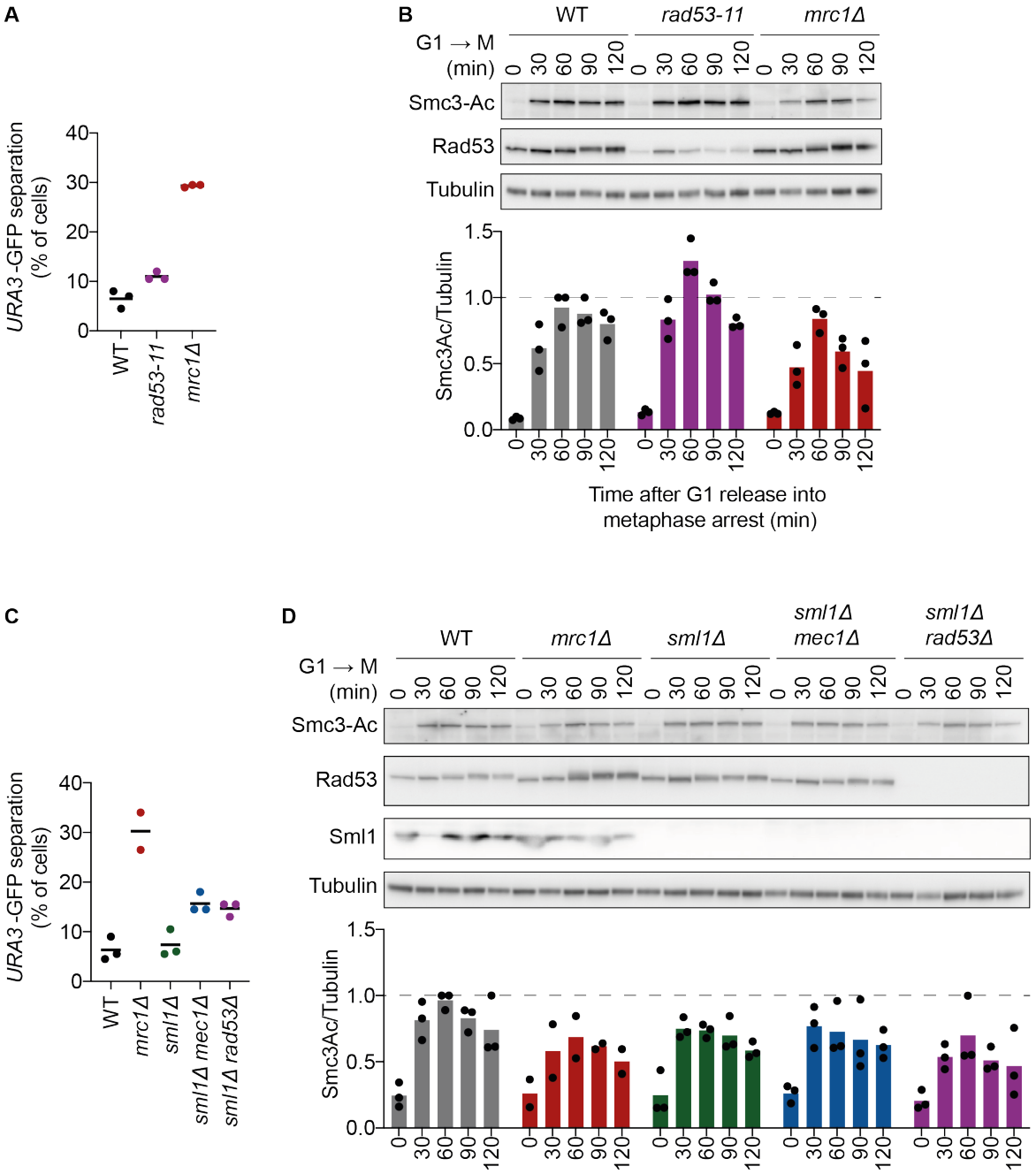

Figure 4.1 Intra S checkpoint and cohesion establishment

A. GFP dot assay of indicated genotypes in metaphase. Mean and individual values of three independent experiments are shown.

B. WB samples of cells of indicated genotypes were taken at indicated time points as cells were released from G1 arrest (0min) into S phase into a medium containing nocodazole to arrest in metaphase. Samples are blotted with anti-Smc3Ac and anti-Rad53. Tubulin is used as loading control. The Smc3Ac/Tubulin ratio were normalized to highest signal of WT cells. Means and individual values from three individual experiments are shown.

C. Same as A.

D. Same as A but samples are also blotted for anti-Sml1.

separation only slightly increased from WT control (figure 4.1A). In parallel, I also monitored levels of acetylated Smc3 during S phase. As previously shown, Smc3 acetylation is reduced in *mrc1Δ* cells. In contrast, Smc3 acetylation is instead slightly higher than WT in *rad53-11* cells. Together, these data suggest that a checkpoint defective Rad53 can still support sister chromatid cohesion.
I also performed cohesion assays in absence of Rad53 as well as the main upstream sensor of intra S phase checkpoint, Mec1. They are essential genes and their essential function is in regulation of dNTP synthesis but both genes can be deleted in *sml1Δ* background (figure 4.1D) (Zhao, Muller et al. 1998, Zhao and Rothstein 2002). Sml1 is the cellular inhibitor for the dNTP synthesis pathway and *sml1Δ* cells was included as a control which did not demonstrate cohesion defects based on GFP dot separation. In both *sml1Δ mec1Δ and sml1Δ rad53Δ* cells, I observed an increase in GFP separation compared to WT although they did not reach the GFP separation levels seen in *mrc1Δ* cells (figure 4.1C). A reduction in Smc3 acetylation was also observed (figure 4.1D). Based on these data, slight cohesion defects are observable in absence of integral checkpoint proteins Mec1 and Rad53.

For thoroughness, I also performed cohesion assays with separation of function mutants of Mrc1 (figure 4.2A). Mr1AQ is a mutant version of Mrc1 in which all 17 SQ or TQ phosphosites of Mec1 are mutated, disabling it from mediating checkpoint activation signal from Mec1 to Rad53 (Osborn and Elledge 2003). Mrc1-ΔC is missing the C terminal region of Mrc1 where is clustered the majority of phosphosites of Rad53 (McClure and Diffley 2021). Interestingly, the GFP dot assay has been reported with *mrc1AQ* cells in two separate conflicting publications in the past, one reporting it similar to WT levels (Xu, Boone et al. 2004) and one reporting cohesion defects similar to *mrc1Δ* cells (Tsai, Vijayraghavan et al. 2015). In our study, there was slightly increased GFP dot separation in both *mrc1AQ* and *mrc1-ΔC* cells compared to WT, but they did not reach the high levels observed in absence of Mrc1 (figure 4.2B). On the other hand, Smc3 acetylation levels for *mrc1AQ* cells slightly surpassed WT and for *mrc1-ΔC* cells were comparable to WT (figure 4.2C).

Although the exact relationship between Intra S checkpoint and cohesion establishment is something that could be investigated further, I have encountered at least one example (*rad53-11* cells) where sister chromatid cohesion was intact even in the absence of a fully functional checkpoint. Further, deletion of integral checkpoint members and Mrc1 checkpoint defective mutants did not lead to the same level of cohesion defects in cells seen in absence of Tof1, Csm3 and Mrc1. Therefore, I do not think that the main mechanism through which

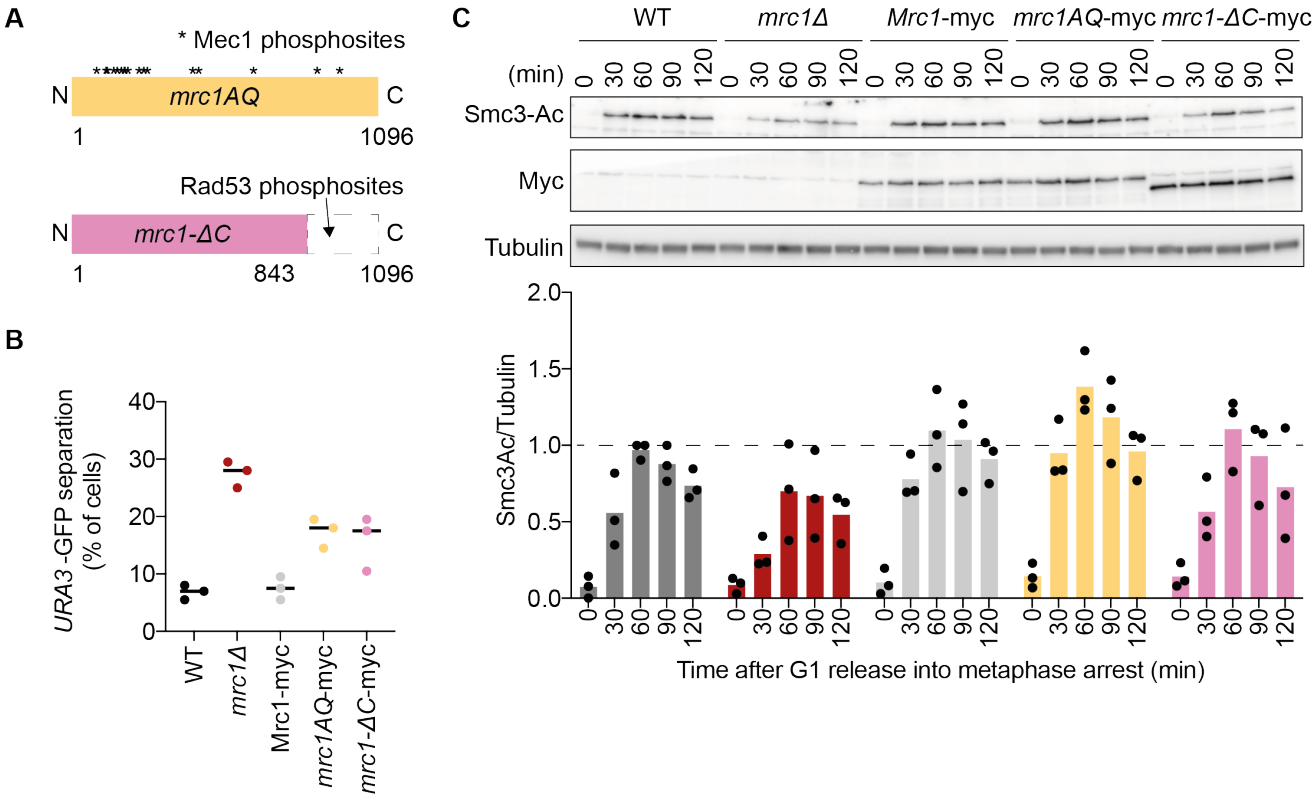

Figure 4.2 Intra S checkpoint mutants of Mrc1 and cohesion establishment

A. Schematic showing alleles *mrc1AQ* and *mrc1-ΔC* of Mrc1 gene. In *mrc1AQ*, the indicated 17 Mec1 phosphosites having SQ or TQ motif were mutated to AQ. In *mrc1-ΔC*, the C terminal (844 - 1096) where are clustered the Rad53 phosphosites is truncated.

B. GFP dot assay of indicated genotypes in metaphase. Mean and individual values of three independent experiments are shown.

C. WB samples of cells of indicated genotypes were taken at indicated time points as cells were released from G1 arrest (0min) into S phase into a medium containing nocodazole to arrest in metaphase. Samples are blotted with anti-Smc3Ac and anti-Myc. Tubulin is used as loading control. The Smc3Ac/Tubulin ratio were normalized to highest signal of WT cells. Means and individual values from three individual experiments are shown.

Tof1, Csm3 and Mrc1 contribute to cohesion establishment is through their role in Intra S checkpoint.

4.2 Replication speed regulation

This next role of Tof1, Csm3 and Mrc1 in replication is a very striking role. When any of these proteins are deleted in cells or omitted from the reconstituted replisome, replication speed becomes slower (Yeeles, Janska et al. 2017, Theulot, Lacroix et al. 2022). This leads us to the hypothesis that the replisome may need to possess a certain speed when it encounters cohesin in order to possess the momentum for any molecular acrobatics involved during cohesion establishment. To test this hypothesis, I modulated speed independently of Tof1, Csm3 and Mrc1. I have slowed down the replication rate when all three proteins are still present in cells. And I have also rescued replication speed when any one of them is absent.

At the replisome there are two main components that can affect the overall replisome speed - the polymerases that add dNTPs to synthesise new DNA at a certain rate and helicase that unwind DNA at a certain rate. In figure 4.3, I have highlighted the methods used to modulate helicase and polymerase to test my hypothesis.

DNA polymerase speed and cohesion establishment

First, I manipulated replisome speed independently of Mrc1 and Tof1/Csm3 by changing the dNTP pools available to the polymerases (figure 4.3A). Low concentrations of hydroxyurea were titrated into WT cells upon their synchronized entry into S phase. Hydroxyurea is a drug that inhibits the RNR enzyme complex which provides dNTP substrates used for DNA replication. 100-200 mM HU is often used to perform S phase arrest as replication is unable to proceed in the absence of dNTPs. I found that 10-fold lower concentrations of HU were appropriate for slowing down replisome progression. Measure of replication fork speed using NanoForkSpeed has also shown that *mrc1Δ* cells and 20 mM HU decrease replisome speed to similar levels (each approx. 1100bp/min compared to WT speed of 2200bp/min) (Theulot, Lacroix et al. 2022). In my experiments, I have monitored progression of S phase by reading DNA content with flow cytometry at 5-minute intervals (figure 4.4B). While in absence of Mrc1, DNA replication is slower, *mrc1Δ* cells also enter S phase faster and have early firing of late origins (Koren, Soifer et al. 2010). This explains the discrepancy in S phase

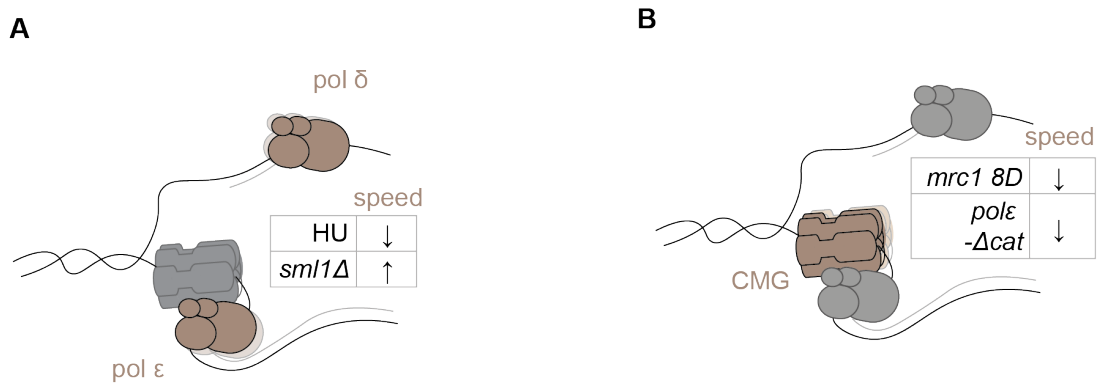

Figure 4.3 Modulation of replisome speed through manipulating helicase and polymerase speed

A. Schematic showing replication fork with CMG helicase in grey, DNA polymerases in brown and the methods utlilized in this study to increase and decrease DNA polymerase speed.
B. Same as A but CMG helicase is in brown, DNA polymerases are in grey and the methods used to decreases helicase speed directly have been listed.

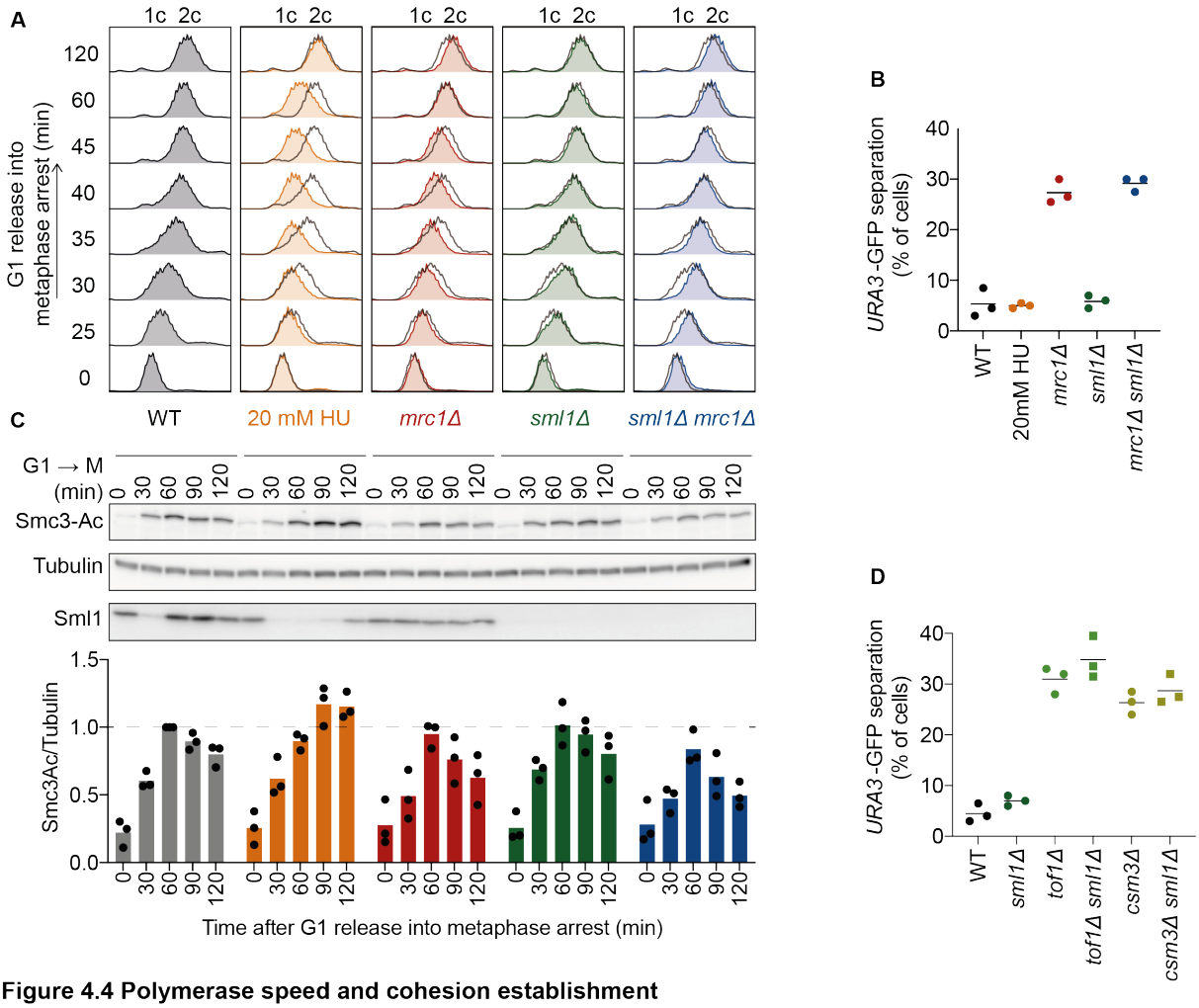

Figure 4.4 Polymerase speed and cohesion establishment

A. Flow cytometry profiles of indicated genotypes at indicated timepoints after release from G1 (0 min) into S phase in a medium containing nocodazole to arrest in metaphase. 20 mM HU refers to WT cells that have been released from G1 into medium containing 20 mM HU and nocodazole. Flow cytometry profiles of WT is overlaid on top of others with a grey outline.

B. GFP dot assay of indicated genotypes in metaphase. Mean and individual values of three independent experiments are shown.

C. WB samples of cells of indicated genotypes were taken at indicated time points as described in B. Samples are blotted with anti-Smc3Ac and anti-Sml1. Tubulin is used as loading control. The Smc3Ac/Tubulin ratio were normalized to highest signal of WT cells. Mean and individual values from three individual experiments are shown.

D. Same as C.

E. Same as D. but samples only taken at 120 min.

progression delay between 20 mM HU and *mrc1Δ* seen in my flow cytometry profiles, even though based on FORK-seq v2 individual fork speeds are more similar between them.

I then asked whether slowdown in replication speed in cells treated with 20 mM HU affected sister chromatid cohesion. Unlike the cohesion defect in *mrc1Δ*, cells treated with 20 mM HU showed only background level GFP dot separation (figure 4.4B). Smc3 acetylation levels of cells treated with 20 mM HU were also in fact slightly/somewhat higher than WT levels, an observation that I will return to in the discussion (figure 4.4C).

Acting on the same enzyme as hydroxyurea, Sml1 is the cellular inhibitor of RNR enzyme. Sml1 is degraded at the start of S phase by intra S checkpoint as detailed earlier to provide the cell with the necessary dNTP pool for new DNA synthesis (figure 4.4C)n(Zhao, Muller et al. 1998, Zhao and Rothstein 2002). As expected, Sml1 protein is also depleted when cells are exposed to HU (figure 4.4C). Interestingly, Sml1 levels were constant during S-phase in *mrc1Δ* cells. Meanwhile, in *sml1Δ*, there is overall more available dNTP leading to increase in replication speed as observed via DNA fibre combing studies (Poli, Tsaponina et al. 2012). Despite increase in replication speed, *sml1Δ* does not demonstrate more cohesion defects (figure 4.4B, C). So far, neither slower nor faster replication speed impedes cohesion establishment.

I also removed Sml1 to rescue replication speed in *mrc1Δ*. DNA flow cytometry showed that the increase of DNA content over S phase in *mrc1Δ sml1Δ* followed a pattern more like WT compared to the S phase progression delay in *mrc1Δ* (figure 4.4A). However, cohesion defects were not rescued for *mrc1Δ sml1Δ* as it demonstrated high GFP dot separation and low Smc3 acetylation levels (figure 4.4B, C). This further suggests that replication speed and cohesion establishment are independent of each other.

I also attempted to rescue replication speed in *tof1Δ* cells and *csm3Δ* cells by removing Sml1. Cohesion defects observed through GFP dot separation and Smc3 acetylation were not rescued to WT in cells with double deletions *tof1Δ sml1Δ* and *csm3Δ sml1Δ* (figure 4.4D,E). The decrease is replication speed in *tof1Δ* cells and *csm3Δ* cells is more modest compared to *mrc1Δ* cells (Theulot, Lacroix et al. 2022). Cells treated with lower levels of hydroxyurea (5mM and 10mM shown in figure 4.5A) also did not demonstrate any cohesion defects (figure 4.5B). However, this did illuminate a trend of increasing Smc3 acetylation levels with increasing hydroxyurea treatment (figure 4.5C). Superficially, I asked whether supplying *tof1Δ*, *csm3Δ,* and *mrc1Δ* cells with 20 mM HU could increase their Smc3 acetylation and whether increased Smc3 acetylation was sufficient to rescue sister chromatid cohesion observed via GFP dot assay. Indeed, I observed that exposure to

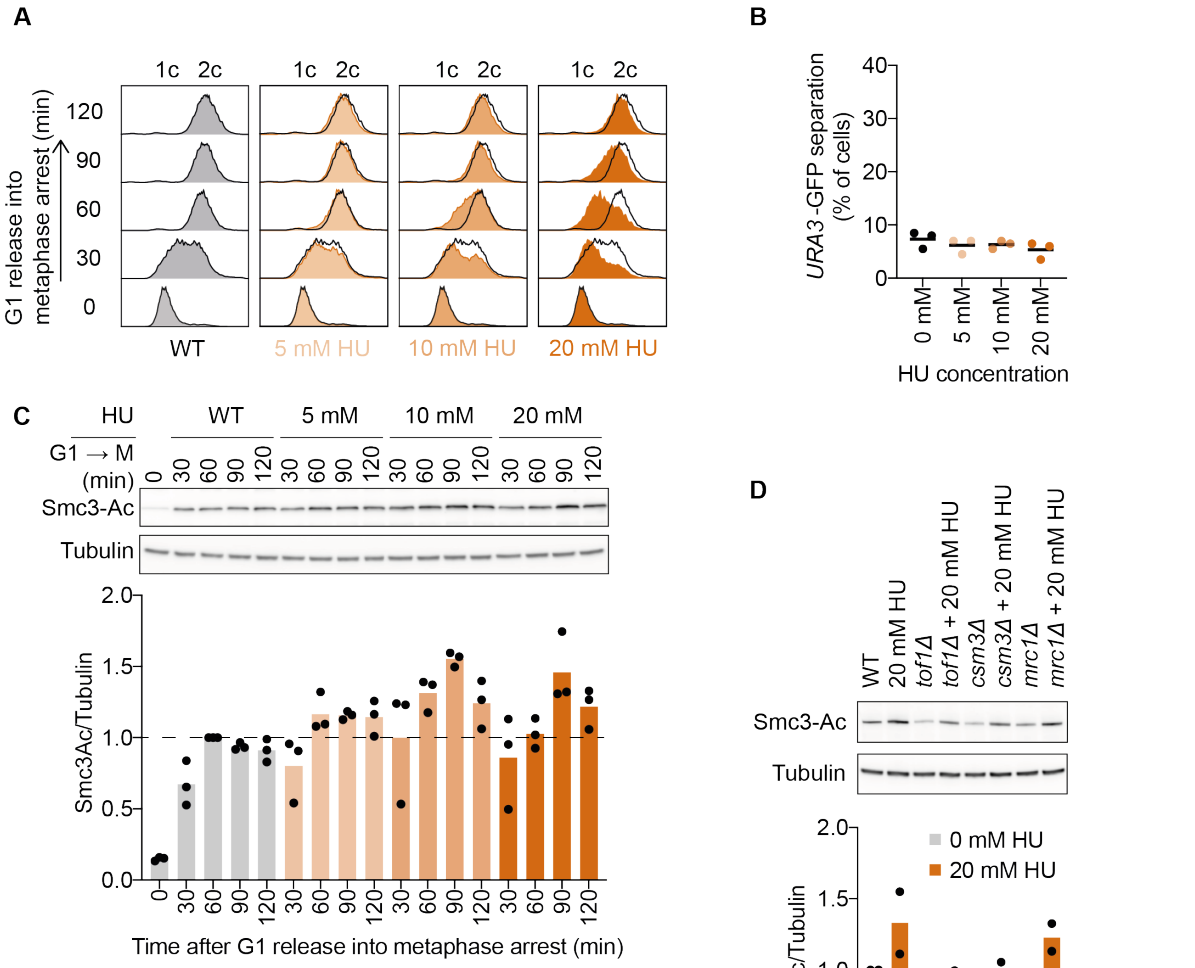

Figure 4.5 Hydroxyurea induced slowdown of replication and cohesion establishment

A. Flow cytometery profiles at indicated timepoints of WT cells arrested in G1 and split into four to bereleased into medium containing nocodazole and indicated concentration of Hydroxyurea (HU). Flow cytometry profiles of WT cells not treated with HU is overlaid on others in grey.

B. GFP dot assay of metaphase arrested WT cells that were treated with indicated concentrations of HU upon S phase entry. Mean and individual values of three independent experiments are shown.

C. WB samples of cells described in A. Samples are blotted with anti-Smc3Ac. Tubulin is used as loading control. The Smc3Ac/Tubulin ratio were normalized to highest signal of WT cells. Mean and individual values from three individual experiments are shown.

D. Same as C but including cells of indicated genotypes with or without treatment of 20 mM HU only at 120 min timepoint. Mean and individual values from two individual experiments are shown.

E. Same as B. but including cells of indicated genotypes with or without treatment of 20 mM HU. Mean and individual values from two individual experiments are shown.

20 mM HU rescued Smc3 acetylation to WT levels in *tof1Δ*, *csm3Δ,* and *mrc1Δ* cells (figure 4.5D). However, this increase in Smc3 acetylation was not sufficient to rescue cohesion defects (figure 4.5E).

Modulation of DNA replication speed by altering the dNTP pool used by polymerases so far suggest that polymerase DNA synthesis rate does not affect cohesion establishment.

DNA helicase speed and cohesion establishment

So far, I have altered replisome speed by increasing or decreasing the dNTP pool used by DNA polymerases. However, Mrc1 has been shown to be able to directly increase helicase unwinding rate based on an in vitro assay that measures helicase unwinding rate in the absence of dNTPs and DNA synthesis (McClure and Diffley 2021). Hence, I also decreased replisome speed by using an Mrc1 mutant Mrc1-8D that directly slows down the helicase.

In *mrc1-8D* cells, 8 potential Rad53 phosphosites of Mrc1 are mutated to the phospho-mimicking aspartic acid which slows helicase and replication speed *in vitro* and *in vivo* (McClure and Diffley 2021) (figure 4.6A). The slowdown of replication in *mrc1-8D* cells has been reported to be very mild and I could not observe it by flow cytometry (figure 4.6B). *mrc1-8D* cells did not demonstrate GFP dot separation or reduction in Smc3 acetylation (figure 4.6C,D) corroborating all our other results to suggest that Mrc1 is not contributing to cohesion establishment through regulation of replisome speed. It seems that cohesion establishment is successful at a range of replication speeds.

Finally, leading strand DNA polymerase epsilon has also been studied to be important for maximal rates of helicase unwinding. Cells can survive in the absence of the catalytic domain of polymerase epsilon, in which case polymerase delta takes over leading strand synthesis, albeit with slower helicase unwinding and therefore slower replication speed (Yeeles, Janska et al. 2017, Devbhandari and Remus 2020) (figure 4.7A). I finally also assessed *polε-Δcat* for sister chromatid cohesion. *polε-Δcat* cells demonstrated higher than WT GFP dot separation and reduced Smc3 acetylation (figure 4.7B,C). This was inconsistent with all our other results demonstrating that replication speed and cohesion establishment are separable entities. I think that instead the cohesion defect in *polε-Δcat* cells could be due to a potential role of polymerase epsilon in cohesion establishment (Edwards, Li et al. 2003), which remains to be rigorously studied. Polymerase epsilon physically interacts with another cohesion establishment factor Ctf18-RFC but a previous study from our lab has shown that this interaction is dispensable for sister chromatid cohesion (Liu, Bouchoux et al. 2020).

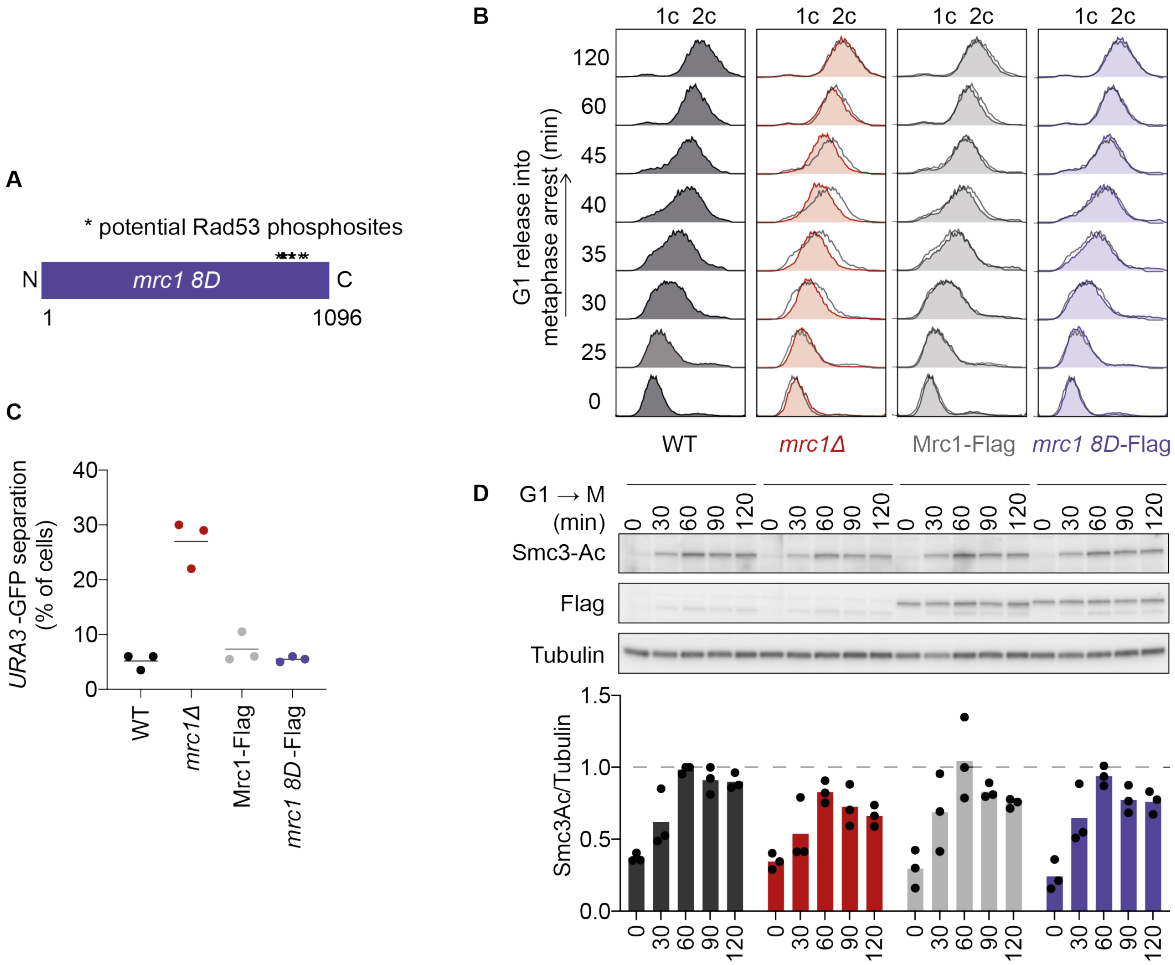

Figure 4.6 Helicase speed and cohesion establishment

A. Schematic showing alleles *mrc1 8D* of Mrc1 gene where indicated 8 potential Rad53 phosphosites are mutated to phospho-mimicking aspartic acid.
B. Flow cytometry profiles of indicated genotypes at indicated timepoints after release from G1 (0 min) into S phase in a medium containing nocodazole to arrest in metaphase. Flow cytometry profiles of WT is overlaid on top of others with a grey outline.
C. GFP dot assay of indicated genotypes in metaphase. Mean and individual values of three independent experiments are shown.
D. WB samples of cells of indicated genotypes were taken at indicated time points as described in B. Samples are blotted with anti-Smc3Ac and anti-Flag. Tubulin is used as loading control. The Smc3Ac/Tubulin ratio were normalized to highest signal of WT cells. Mean and individual values from three individual experiments are shown.

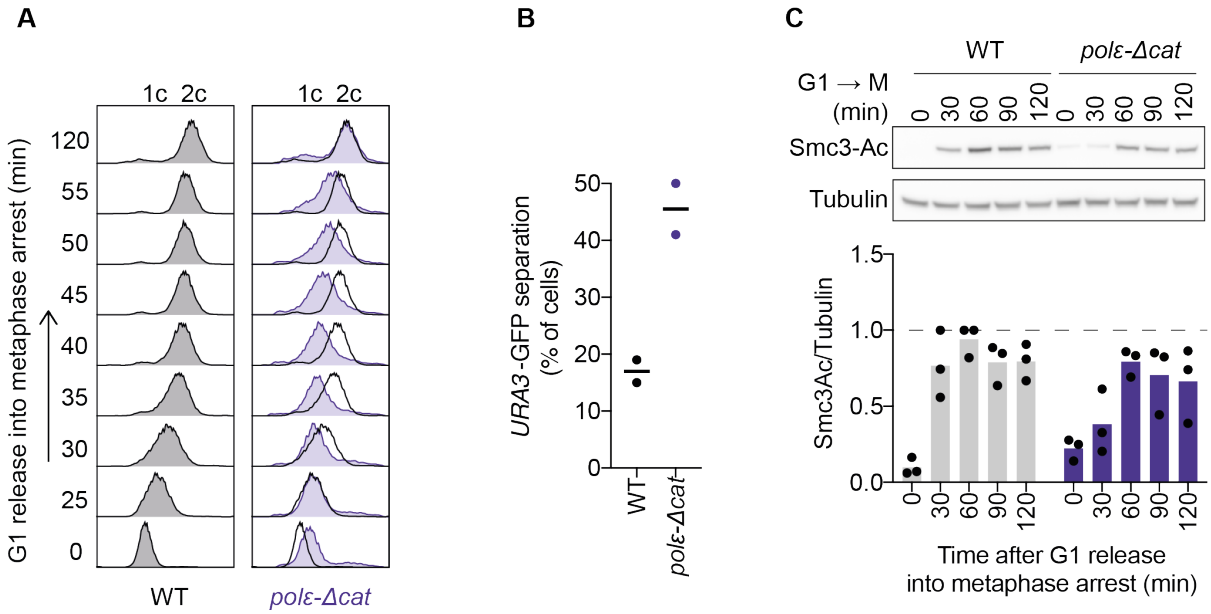

Figure 4.7 Polymerase epsilon and cohesion establishment

A. Flow cytometry profiles of indicated genotypes at indicated timepoints after release from G1 (0 min) into S phase in a medium containing nocodazole to arrest in metaphase. Flow cytometry profiles of WT is overlaid on top of *polε-Δcat* with a grey outline.
B. GFP dot assay of indicated genotypes in metaphase. Mean and individual values of two independent experiments are shown.
C. WB samples of cells of indicated genotypes were taken at indicated time points as cells were released from G1 arrest (0min) into S phase into a medium containing nocodazole to arrest in metaphase. Samples are blotted with anti-Smc3Ac. Tubulin is used as loading control. The Smc3Ac/Tubulin ratio were normalized to highest signal of WT cells. Means and individual values from three individual experiments are shown.

ssDNA capture by cohesin

As mentioned earlier, the CMG helicase as well as the leading strand and lagging strand DNA polymerase epsilon and delta respectively can influence replisome speed. How helicase speed and polymerase speed are coupled remains an open question in the DNA replication field. Instances of decoupling between the helicases and polymerases have been observed in cells in absence of TCM. I speculated on a scenario where cohesion establishment is dependent on the relative speeds of DNA helicase and lagging strand polymerase delta (figure 4.8A). I predicted that in absence of Mrc1, CMG helicase is slower, but the relative speed of DNA polymerase delta that is catching up is not slowed down.

Biochemical reconstitution of cohesin loading on DNA has shown that cohesin loads onto two copies of DNA in a sequential manner and that this is most effective when it first loads onto dsDNA and then captures a second ssDNA (Murayama, Samora et al. 2018). Based on this, cohesin is predicted to first load at the leading strand before capturing a ssDNA from the lagging strand. As shown in figure 4.8A, I speculated that the ssDNA available at the lagging strand is dependent on the relative helicase and polymerase speed. My hypothesis is that with slower helicase speed in absence of Tof1, Csm3 or Mrc1, cohesin at the leading strand has a very short length of ssDNA available for capture at the lagging strand, making second ssDNA capture by cohesin difficult.

To test this hypothesis, I first directly tested whether there is less ssDNA available at the lagging strand in absence of Tof1, Csm3 or Mrc1 using BrdU-IP strand specific sequencing (BrdU-IP ssSeq). WT, *tof1Δ*, *csm3Δ* and *mrc1Δ* cells were released from a G1 arrest into BrdU containing medium and collected at an early S phase timepoint. Newly synthesized DNA is hence labelled with BrdU and BrdU IP of denatured DNA from the cell extracts was sequenced. Sequencing reads were then mapped to Watson and Crick strands of the reference genome for budding yeast. The Watson/Crick log ratio sequencing read count of multiple origins can be collapsed to obtain information about the presence of ssDNA at the replication fork (Yu, Gan et al. 2014). Figure 4.8B shows a schematic of expected Watson/Crick log ratio demonstrating no bias, leading strand bias and lagging strand bias. More ssDNA at the lagging strand would show a profile of leading strand bias in BrdU IP.

As has been previously reported, in WT cells, there is a small bias towards the leading strand indicating as nomenclature suggests that the lagging strand synthesis is slightly slower (figure 4.8C) (Gan, Yu et al. 2017). If, as my hypothesis predicts, there is a decrease in ssDNA at the lagging strand, I expected that the bias toward leading strand would decrease in *tof1Δ*, *csm3Δ* and *mrc1Δ* cells. However, I did not observe a decrease in

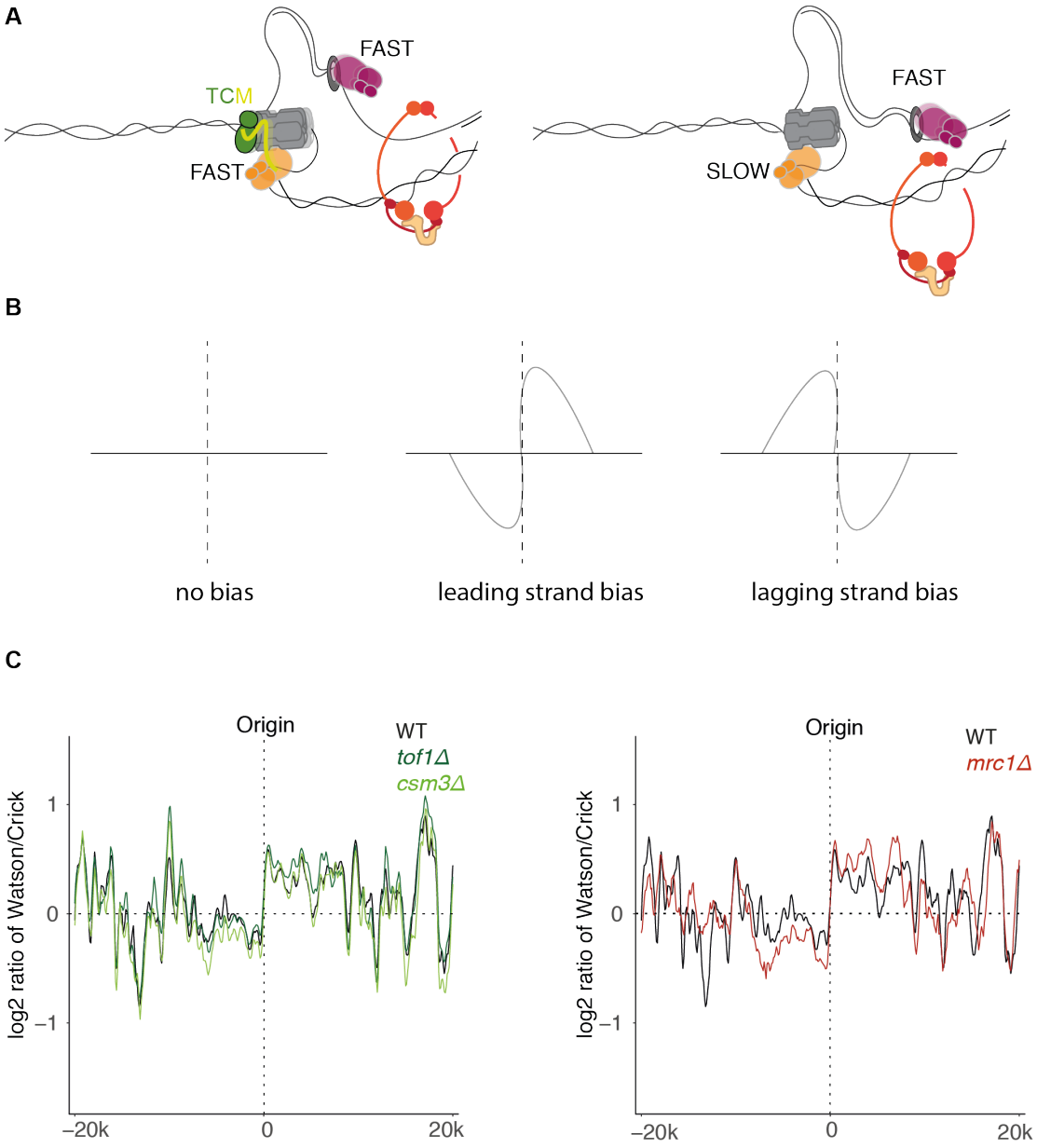

Figure 4.8. An alternative hypothesis for how TCM regulation of speed could contribute to cohesion establishment

A. A model schematic showing the hypothesis that absence of Tof1, Csm3 and Mrc1 could have an effect on the relative speed of helicase and polymerase delta at the replisome, which may make second ssDNA capture by cohesin more difficult.

B. Schematic showing expected profiles for no bias, leading strand bias and lagging strand bias in BrdU IP ssSeq.

B. BrdU IP ssSeq of indicated genotypes in early S phase. Cells of indicated genotypes were arrested in G1 and released into S phase. Cell and DNA extract from early S phase timepoint was denatured before performing BrdU IP. DNA libraries were prepared and sequenced. The graph shows the normalized sequencing count of log2 ratio of Watson/Crick strands.

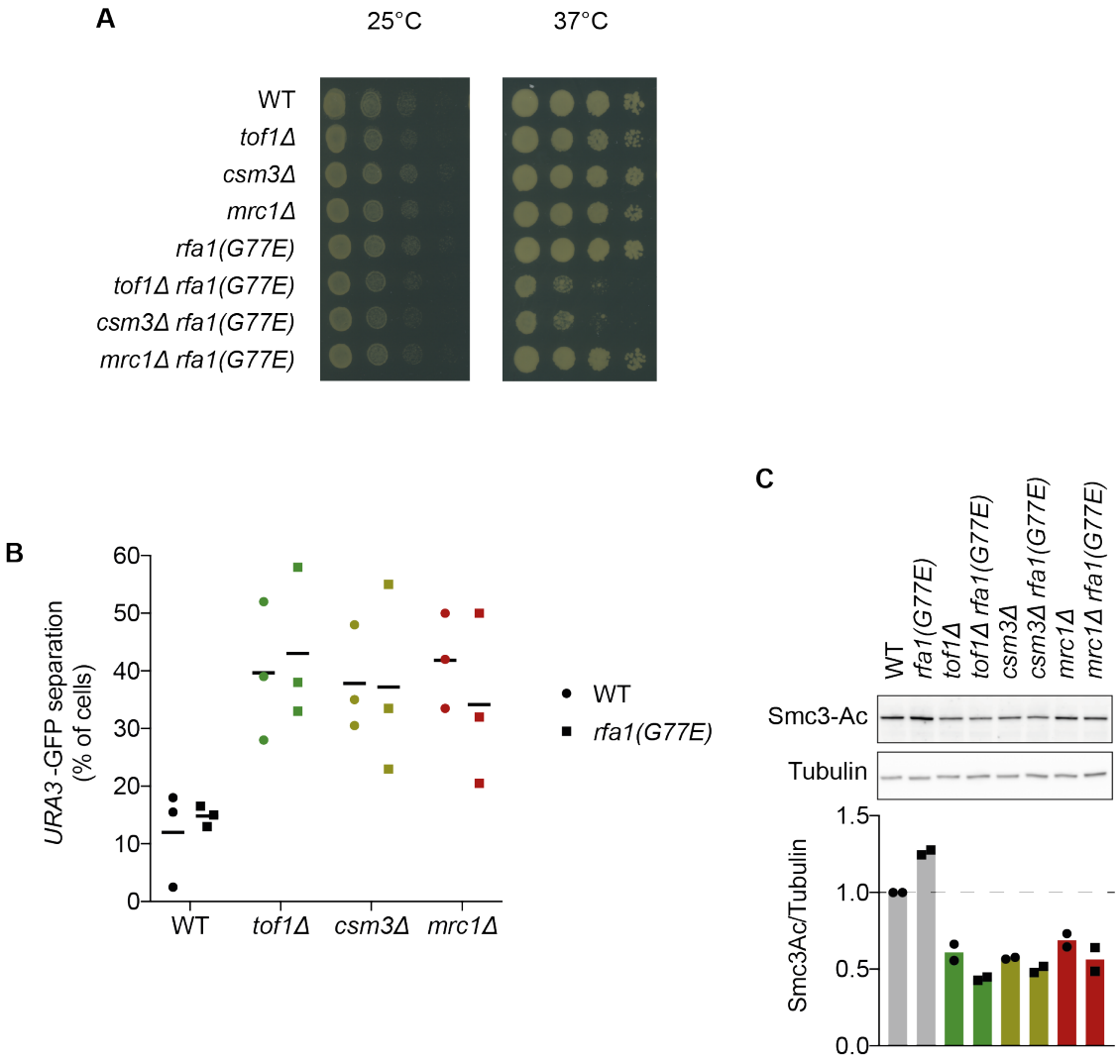

Figure 4.9 Tof1, Csm3 and Mrc1 do not directly facilitate second ssDNA capture by cohesin

A. Indicated genotypes were plated on YPD plates with subsequent 10 fold dilutions at 25°C or 37°C as indicated. 25°C was imaged 1-2 days after plating and 37°C was imaged 3 days after plating

B. GFP dot assay of indicated genotypes in metaphase. Cells were released from G1 arrest into S phase and metaphase arrest at restrictive temperature of 37°C. Mean and individual values of three independent experiments are shown.

D. WB samples of cells of indicated genotypes were taken for metaphase arrested cells, 120 min after release from G1 arrest into 37°C YPD + nocodazole. Samples are blotted with anti-Smc3Ac. Tubulin is used as loading control. The Smc3Ac/Tubulin ratio were normalized to that of WT cells. Mean and individual values from two individual experiments are shown.

leading strand bias, if anything there is a slight increase in leading strand bias in *mrc1Δ* cells, suggesting that ssDNA does not decrease in the lagging strand in absence of TCM. This was also corroborated by recently published NanoForkSpeed that found no difference in leading and lagging strand synthesis rate in absence of TCM (Theulot, Lacroix et al. 2022).

To be thorough I also directly tested the model in figure 4.8A through another method. Second ssDNA capture by cohesin has been shown to be less efficient when it is bound by ssDNA binding protein RPA (Murayama, Samora et al. 2018). If absence of TCM makes second ssDNA capture difficult, reducing RPA at ssDNA should rescue cohesion defects to some extent. To this end, I mutated Rfa1 subunit to ts mutant *rfa1(G77E)* which demonstrates reduced ssDNA binding (Akai, Kurokawa et al. 2011, Samora, Saksouk et al. 2016).

First I performed spot assays of *rfa1(G77E)* strains at restrictive temperature of 37°C. Double mutants *tof1Δ rfa1(G77E)* and *csm3Δ rfa1(G77E)* demonstrated synthetic growth defects at restrictive temperature but *mrc1Δ rfa1(G77E)* did not (figure 4.9A).

For GFP dot assay and monitoring Smc3 acetylation levels, cells were released from G1 into S phase at 37°C and subsequently arrested in metaphase. When assaying cohesion defects in these double mutants, *rfa1(G77E)* was unable to reduce GFP separation and it was unable to rescue Smc3 acetylation in *tof1Δ*, *csm3Δ* and *mrc1Δ* cells (figure 4.9B,C). Taken together all of these experiments clarify that the specific hypothesis of slow helicase speed in absence of TCM affecting second ssDNA capture by cohesin is incorrect. I believe I have exhausted all conceivable relationships between TCM regulation of replisome speed and cohesion establishment, and all the data suggests that replisome speed and cohesion establishment are independent of each other.

4.3 Tof1 recruitment of Topoisomerase 1 and FACT, and cohesion establishment

Given that Tof1/Csm3 and Mrc1 are part of two separate cohesion establishment pathways (Xu, Boone et al. 2007), we next considered replication roles of Tof1 that are independent of Mrc1. The C terminus of Tof1 (amino acid residues 782 - 1238) is predicted to be a flexible tail as it could not be resolved in cryo-EM of Tof1/Csm3 in complex with the CMG helicase (Baretić, Jenkyn-Bedford et al. 2020). The second half of this C terminal region (amino acid

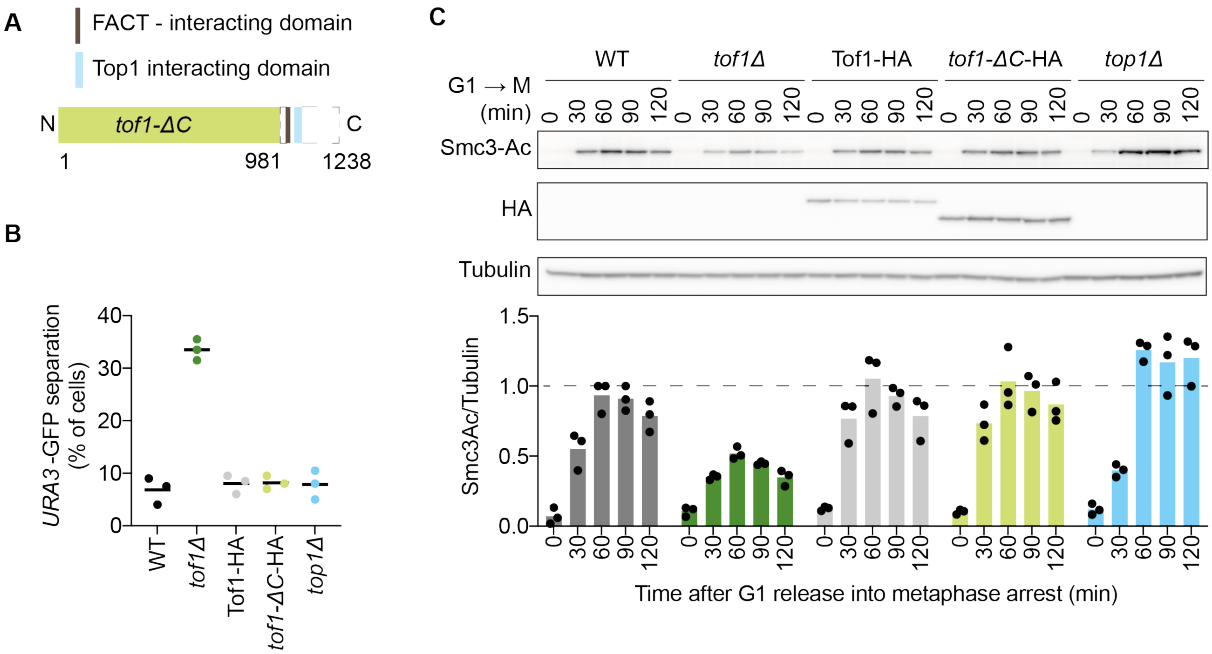

Figure 4.10 Topoisomerase recruitment to the replication fork and cohesion establishment

A. Schematic showing truncation *tof1-ΔC* of Tof1 gene. In *tof1-ΔC*, the C terminal (982 - 1096) containing the Topoisomerase 1 and FACT interacting sites are removed.
B. GFP dot assay of indicated genotypes in metaphase. Mean and individual values of three independent experiments are shown.
C. WB samples of cells of indicated genotypes were taken at indicated time points as cells were released from G1 arrest (0min) into S phase into a medium containing nocodazole to arrest in metaphase. Samples are blotted with anti-Smc3Ac and anti-HA. Tubulin is used as loading control. The Smc3Ac/Tubulin ratio were normalized to highest signal of WT cells. Means and individual values from three individual experiments are shown.

residues 982-1238) has been implicated in the local recruitment to the replication fork of both Topoisomerase I (Park and Sternglanz 1999, Shyian, Albert et al. 2020, Westhorpe, Keszthelyi et al. 2020) and the essential histone chaperone FACT (Safaric, Chacin et al. 2022) (figure 4.10A). Recruitment of topoisomerase I also participates in the fork protection role of Tof1 (Larcher and Pasero 2020, Shyian, Albert et al. 2020), and recruitment of FACT enhances nucleosome disassembly by FACT ahead of the fork (Safaric, Chacin et al. 2022). Both of these pathways affect DNA topology ahead of the replication fork.

In absence of Topoisomerase I recruitment by Tof1, the supercoiling ahead of the fork is less effectively removed by Topoisomerase II in absence of Topoisomerase I and this might affect the DNA topology ahead of the fork for when replisome meets cohesin. In absence of local FACT recruitment by Tof1, inefficiently disassembled nucleosomes may impede encounter with cohesin. To determine whether any of these replication roles of Tof1 contribute to cohesion establishment, I performed cohesion assays in *tof1ΔC* (Δ 982-1238) cells.

The C terminal truncation of Tof1 is tagged and Tof1-ΔC protein is well expressed in S phase (figure 4.10C). Consistent with previous observations, levels of Smc3ac during S phase is lower in *tof1Δ* cells compared to WT cells. Meanwhile, *tof1ΔC* cells did not demonstrate lower Smc3ac than cells expressing tagged or untagged Tof1(figure 4.10C). *tof1ΔC* cells also did not demonstrate cohesion defects with only background level of separated GFP dots, compared to the high GFP dot separation observed in *tof1Δ* (figure 4.10B). Meanwhile, cohesion defects were also not observed when topoisomerase I was directly removed from cells. A higher level of the Smc3ac compared to WT was observed in *top1Δ* (figure 4.10C), and this provides another example of increase in Smc3ac that is not necessarily tied to cohesion establishment process.

Based on these experiments, I am able to conclude that the replication roles associated with Tof1, namely fork protection, relieving of topological stress and efficient nucleosome disassembly are not the mechanism of Tof1 contribution to cohesion establishment.

Chapter 5: Results (Protein - Protein Interactions)

So far, all the well-known replication roles of Tof1/Csm3 and Mrc1 that we have studied are independent of cohesion establishment. I began to entertain the hypothesis that perhaps Tof1/Csm3 and Mrc1 have a novel and unique role for cohesion establishment.

A clue to the role of Tof1, Csm3 and Mrc1 in this encounter can be provided by structural studies on the replisome which places Tof1, Csm3 and the N-terminal of Mrc1 at a prime location to encounter anything sitting on DNA ahead of the replication fork (Baretić, Jenkyn-Bedford et al. 2020), which would include cohesin complexes loaded onto DNA in G1. I investigated whether a novel role might involve direct protein-protein interaction of TCM with cohesin subunits.

5.1 Direct protein-protein interactions between Cohesin and cohesion establishment factors

The hypothesis is that Tof1, Csm3 and Mrc1 come into direct and meaningful contact with cohesin molecules on DNA for their role in cohesion establishment. A few studies in diverse eukaryotes have reported interaction between replisome components and cohesin subunits based on co-immunoprecipitations (Chan, Chan et al. 2003, Leman, Noguchi et al. 2010). Since these studies were conducted *in vivo*, they are unable to differentiate between direct protein protein interactions or interactions mediated by other proteins especially those present in the crowded replisome. On the other hand, a systematic unbiased large scale probe of interactions failed to find any interaction between cohesion establishment factors and cohesin/cohesin loader (Ivanov, Ladurner et al. 2018). It remains unclear whether cohesin subunits make direct contact with Tof1, Csm3 and Mrc1 at the replication fork.

I have used co immunoprecipitation assays with purified proteins to test whether there exists direct protein protein interactions between Tof1, Csm3, Mrc1 and the cohesin tetramer. Use of purified proteins ensures that any interaction observed is direct. Importantly, the interaction was assayed at buffer conditions of 100mM Potassium Glutamate salt which is the buffer used in biochemically reconstituted replication assays, and is expected to mimic physiological conditions.

To this end, I used previously established methods to purify cohesin tetramer that include subunits Smc1, Smc3, Scc1 and Scc3 (Minamino, Higashi et al. 2018) and Tof1/Csm3 and Mrc1 (Yeeles, Janska et al. 2017) and performed coimmunoprecipitation assays. Tof1 and

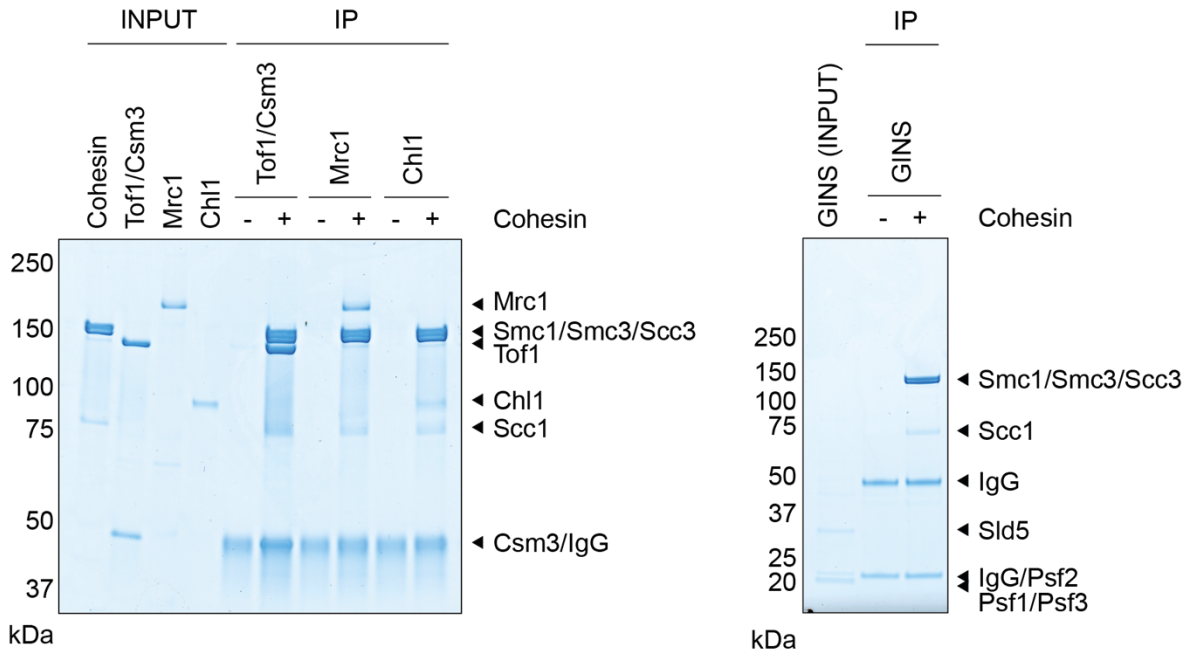

Figure 5.1 Direct protein-protein interactions between cohesion establishment factors and cohesin

Interaction screen with purified proteins. 10% of proteins are loaded as input. Dynabeads coated with anti-Pk are incubated ± cohesin tetramer with Smc1 subunit tagged with Pk and subsequently incubated with 200nM Tof1/Csm3, Mrc1, Chl1 or GINS complex. The bead retained fraction after wash is loaded on protein gel and stained with Commassie Brilliant Blue.

Csm3 form a tight heterodimer and therefore they are purified together. Purified Chl1 was also included as it is expected to have an interaction with cohesin (Samora, Saksouk et al. 2016). Budding yeast Chl1 purification protocol has been established by Masashi Minamino in our lab and will be published for the first time with this study.

Cohesin with Pk-tagged Smc1 are on dynabeads coated with antibody against Pk epitope are co-incubated with Chl1, Tof1-Csm3 or Mrc1. As a control, I used dynabeads coated with anti-Pk (antibody against Pk epitope) that are not exposed to cohesin. After coincubation, the beads bound fraction was washed and loaded on a protein gel. As expected, I observed Chl1 in the beads bound fraction in a cohesin dependent manner, confirming the interaction between Chl1 and Cohesin (figure 5.1) (Samora, Saksouk et al. 2016). Along with Chl1, cohesin was also found to directly interact with Tof1-Csm3 and Mrc1 as both complexes were retained in the bead bound fraction in a cohesin dependent manner (figure 5.1). When we also incubated cohesin on beads with GINS, a complex that forms part of the CMG helicase, GINS did not coimmunoprecipitate with cohesin (figure 5.1). The GINS subunits are smaller sizes compared to all other proteins used in the interaction assay which make them less visible in a Coomassie stained gel. We added 4X more GINS to the interaction assay and still did not observe an interaction. We therefore believe that the pairwise interactions observed between Tof1/Csm3 and Mrc1 with cohesin is specific. Similarly, the interaction was also corroborated when the assay was performed with Tof1-Csm3 or Mrc1 on beads and incubated with cohesin (figure 5.2A,C).

Since I observed pairwise interactions of cohesin with Tof1-Csm3, Mrc1 and Chl1, which are all at the replisome, I wondered whether cohesin and the above cohesion establishment factors together form a large complex and perhaps any one's interaction with cohesin is enhanced when more cohesion establishment factors are present. For this purpose, Mrc1 on beads were incubated with ± Tof1-Csm3 before further incubation with cohesin. As expected, interaction between Tof1-Csm3 and Mrc1 can be observed. However, the presence of a heterotrimeric TCM complex did not further enhance interaction with cohesin (figure 5.2A). Meanwhile, Mrc1 alone or with Tof1-Csm3 did not interact with GINS consistent with their structural allocations at the replisome (figure 5.2B) (Baretić, Jenkyn-Bedford et al. 2020).

To test for complex formation between cohesin and cohesion establishment factors further, I prepared Tof1-Csm3 on beads incubated first with Mrc1 followed by Chl1 before incubation with Cohesin (figure 5.3C). No increase was observed in cohesin retained in the bead bound fraction with Tof1-Csm3 when Mrc1 and Chl1 were also present. This may suggest that the

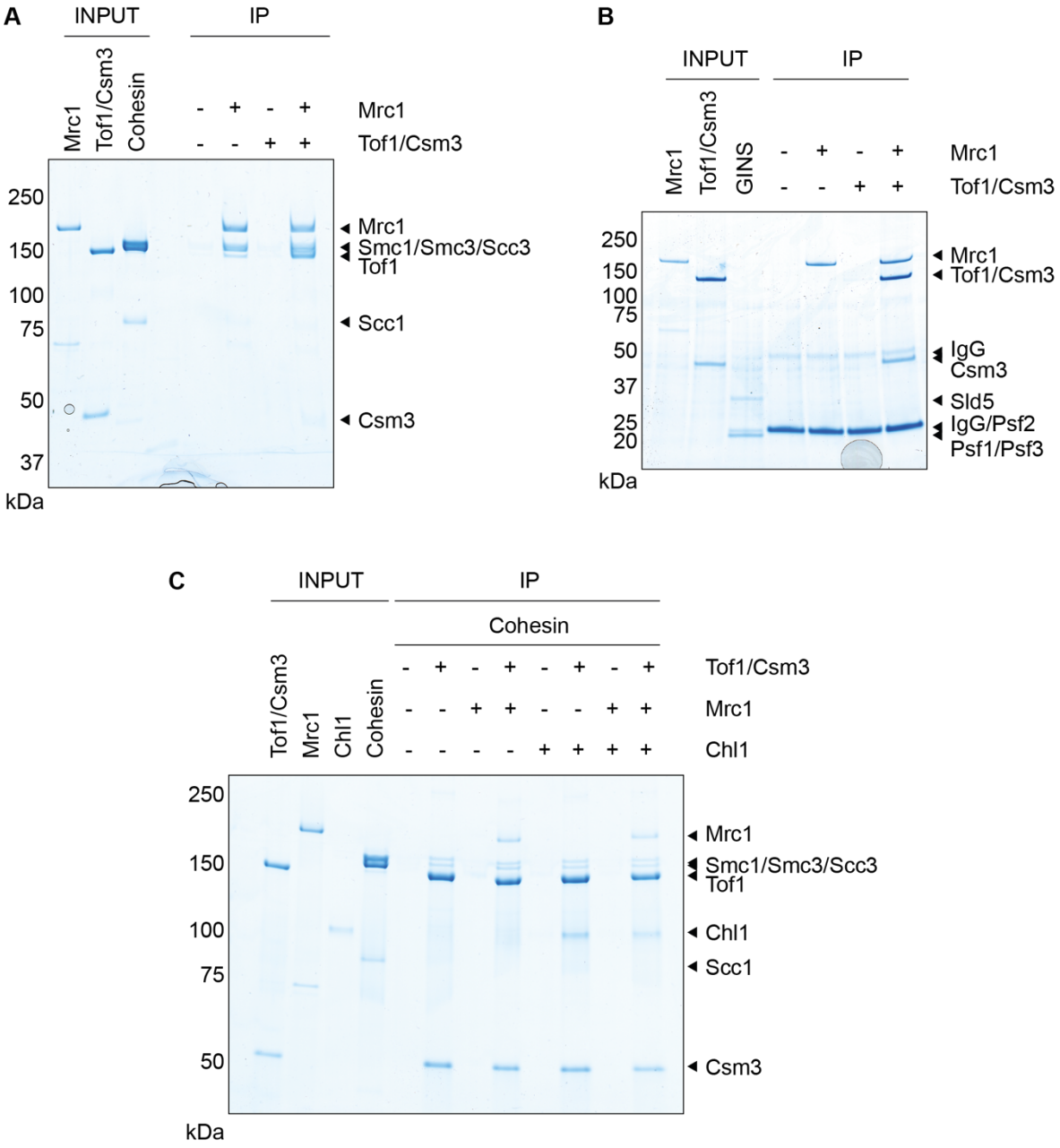

Figure 5.2 Interaction between cohesion establishment factors and cohesin.

A. Interaction screen with purified proteins. 10% of input is loaded onto gel. Anti-Flag M2 beads ±Mrc1 were first incubated with ± Tof1/Csm3 and then incubated with cohesin. Bead bound fraction is eluted with Flag peptide and loaded onto gel and stained with Commassie Brilliant Blue.
B. Same as A but final incubation with GINS instead of cohesin. Bead bound fraction is eluted by boiling.
C. Calmoudulin beads ± Tof1/Csm3 were first incubated with ± Mrc1, followed by ± Chl1 and then incubated with cohesin. Bead bound fraction is loaded onto gel and stained with Commassie Brilliant Blue.

interactions are pairwise and independent of each other but would require further structural investigation to affirm.

Since identification of direct protein-protein interaction between Tof1-Csm3 and cohesin and Mrc1 and cohesin, I did further controls to confirm that the interactions are not mediated by DNA by adding benzonase during the coincubation step (figure 5.3A,B). The proteins still coimmunoprecipitated together. This was an important control because Cohesin and Tof1-Csm3 interact with DNA. I also found that the interaction is not dependent on ATP binding or hydrolysis (figure 5.3C,D). This was of interest to test because cohesin has an ATPase where Smc1 and Smc3 meet at its head domain.

I also performed the coincubation step of the interaction assay by replacing the salt in the buffer with increasing concentrations of NaCl. Interaction of cohesin with both Tof1-Csm3 and Mrc1 complexes is already weakened at 150mM NaCl and barely detectable at 250mM NaCl (figure 5.4 A,B). The sensitivity to increasing salt suggests that the interactions are electrostatic. Lower salt concentrations used in the assay are also more representative of physiological conditions in cells.

Finally, I also attempted to perform size exclusion chromatography to observe if the interactions identified above are strong enough for complex formation. I incubated the proteins together or separately before loading them into a micro gel filtration column. Western blotting of protein tags on the eluted fractions showed that Tof1-Csm3 and Cohesin eluted at their expected fractions when incubated separately or together (figure 5.5A). It is possible that the interactions between them are transient in nature and do not support stable complex formation. However, size exclusion chromatography of Mrc1 and Cohesin were eluted in the same fraction (figure 5.5B). Mrc1 alone has two populations in fractions 16-25 and fractions 2-5 which is expected to be aggregations of this famously unstable protein. When incubated with cohesin, majority of Mrc1 was instead eluted with cohesin fractions. This suggests that Mrc1 and Cohesin may be capable of forming a stable complex.

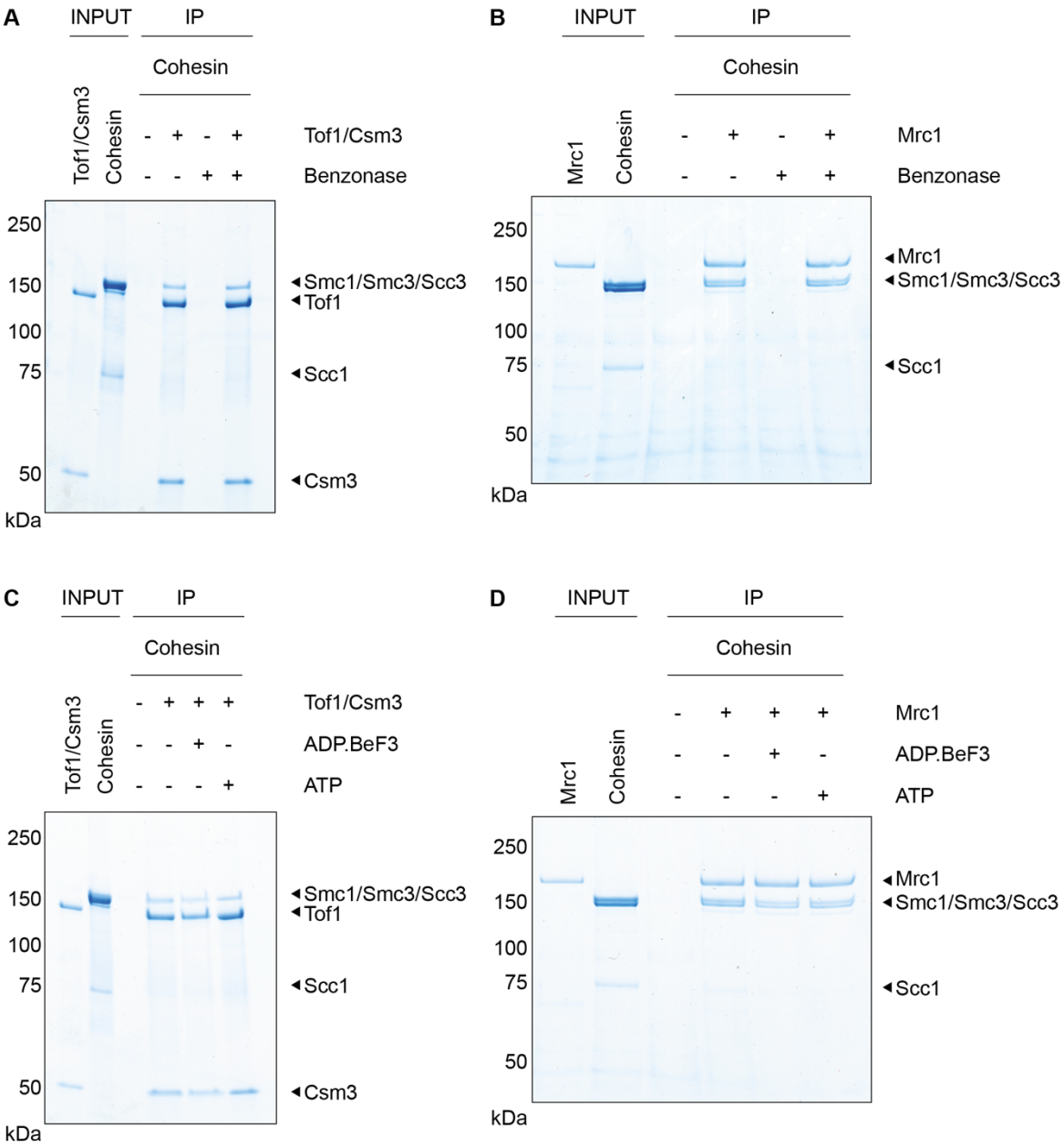

Figure 5.3 Cohesin interaction with Tof1/Csm3 and Mrc1 is DNA-independent and ATP-independent

A. Interaction screen with purified proteins. 10% of input is loaded onto gel. Calmoudulin beads ±Tof1/Csm3 were incubated with cohesin in the presence or absence of Benzonase. Bead bound fraction is loaded onto gel and stained with Commassie Brilliant Blue.
B. Same as A but with anti-Flag M2 beads ±Mrc1.
C. Calmoudulin beads ±Tof1/Csm3 were incubated with cohesin in the presence of ADP.BeF3, ATP or no ATP. Bead bound fraction is loaded onto gel and stained with Commassie Brilliant Blue.
B. Same as A but with anti-Flag M2 beads ±Mrc1.

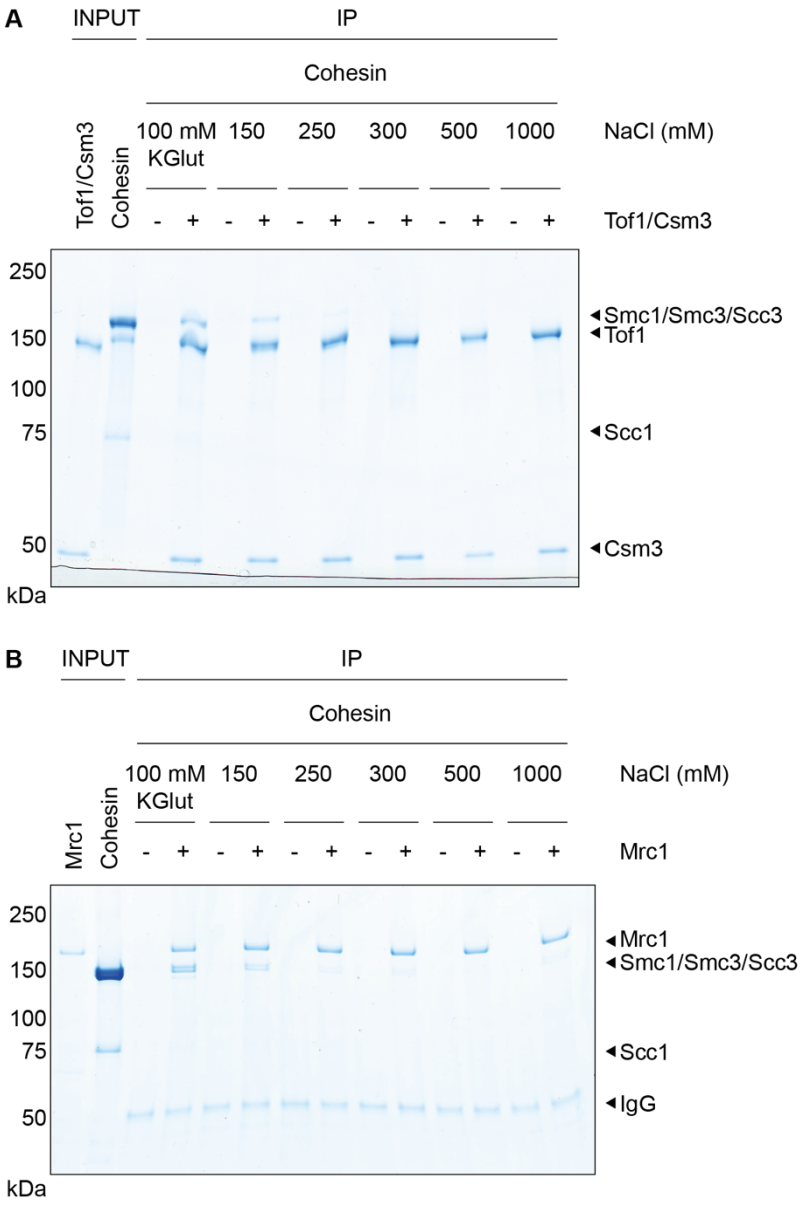

Figure 5.4 Cohesin interaction with Tof1/Csm3 and Mrc1 is salt sensitive

A. Interaction screen with purified proteins. 10% of input is loaded onto gel. Calmoudulin beads ±Tof1/Csm3 were incubated with cohesin in the presence of indicated salt concentrations. Bead bound fraction is loaded onto gel and stained with Commassie Brilliant Blue.
B. Same as A but with anti-Flag M2 beads ±Mrc1.

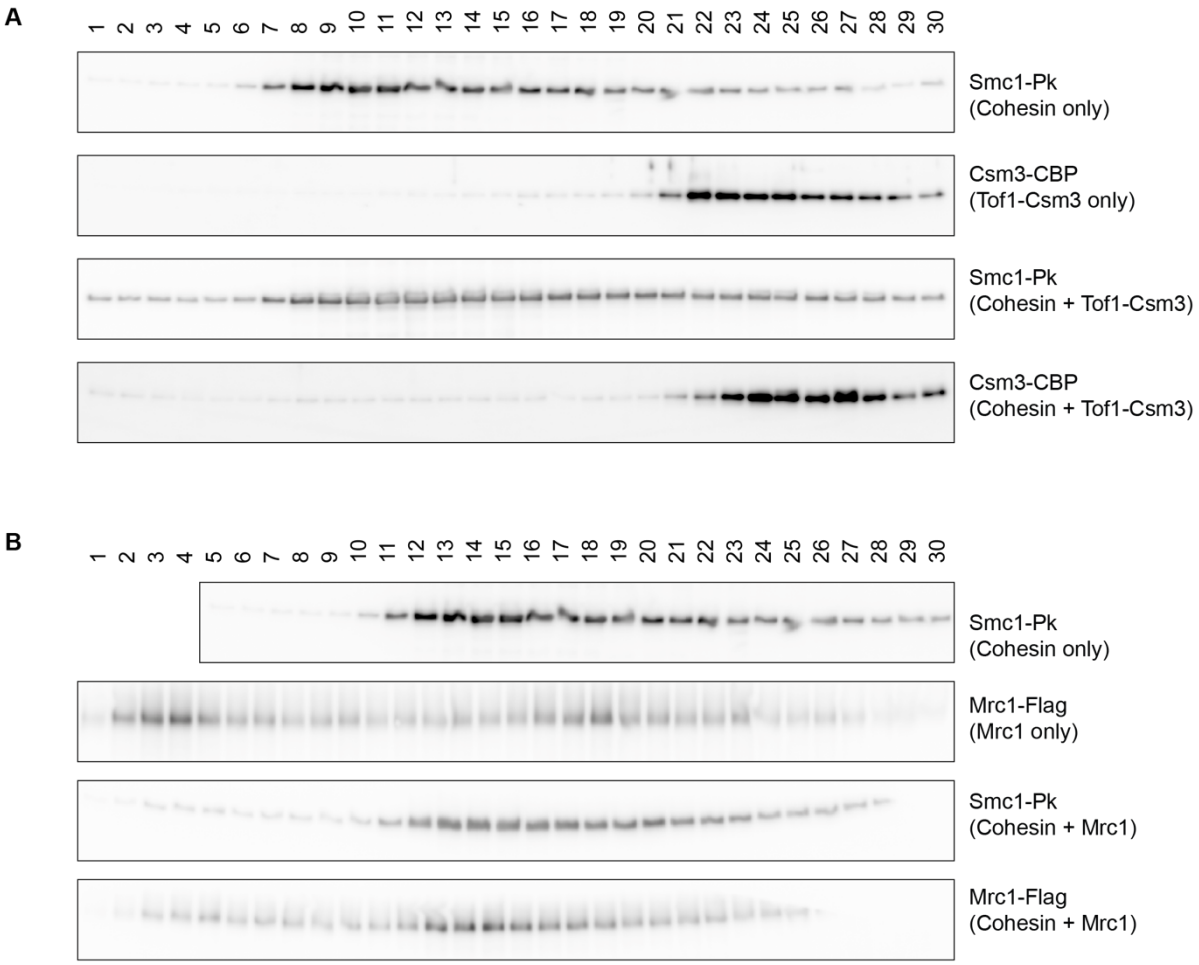

Figure 5.5 Size Exclusion Chromatography of Cohesin with Tof1/Csm3 and Mrc1

A. Purified cohesin tetramer and Tof1/Csm3 were co-incubated together or separately and then loaded onto Superose 6 gel filtration column. The fractions were loaded onto a gel and western blotting was performed with anti-Pk against Smc1 subunit of Cohesin tagged with Pk and anti-CBP against Csm3 tagged with CBP.

B. Same as A but Cohesin with Mrc1. Anti-Flag was used to blot against Mrc1 tagged with Flag.

5.2 CLMS to identify crosslinking sites

Next, we performed protein crosslinking mass spectrometry (CLMS) to identify sites of interaction between these proteins. To this end, we collaborated with Zhuo Chen in Juri Rappsilber's lab to perform protein cross linking mass spectrometry (CLMS) with sulfo-SDA crosslinker. The theoretical SDA crosslinking limit is 25 Angstroms. For reference, the distance between a turn in an alpha helix structure is 5.4 Angstroms so sulfo-SDA crosslinker catches very little background which is important in the case of a flexible protein like cohesin. The crosslinking is a two-step process where the NHS-ester in the crosslinker first reacts with K, Y, S and T amino acids of proteins and in the second step, UV-A activation of diazarine part of the crosslinker interacts with any nearby amino acid residue. Intially crosslinking efficiency was tested at a range of protein to crosslinker weight ratio. Based on crosslinking efficiency (figure 5.6A), we chose to use proceed with the protein to crosslinker weight ratio of 1:0.75 for the main experiment. Next, mass spectrometry analysis of digested peptides after crosslinking identified interaction sites.

The crosslinking mass spectrometry was able to recapitulate previously identified crosslinks between cohesin subunits (Higashi, Eickhoff et al. 2020), as well as crosslinks between Tof1 and Csm3 (Baretić, Jenkyn-Bedford et al. 2020) suggesting that the CLMS overall worked well . The CLMS was unable to identify any interaction between Tof1-Csm3 and Mrc1. The heterotrimeric complex has been well established and a different CLMS has also previously identified interactions between them in the context of CMG helicase.

CLMS identified a few interactions of cohesin with Tof1 and Mrc1 that were clustered at the Smc1 and Smc3. One more interaction between Mrc1 and Scc3 was identified at a flexible region of Scc3. These interactions have been mapped in an available model of cohesin tetramer (figure 5.6B). Since cohesin is a very flexible protein, a comprehensively resolved structure is not yet available. I have mapped the crosslinking sites to homologous amino acids in a fission yeast model of Cohesin modelled based on incorporating structures of subunit domains from *Saccharomyces cerevisiae* and *Chaetomium thermophilum* (Higashi, Eickhoff et al. 2020).

The crosslinking data suggests that both Mrc1 and Tof1 are mostly interacting with SMC subunits of cohesin. To further test this, I also performed interaction assays using purified SMC dimer (consisting of Smc1 and Smc3 subunits that form the coiled coils), purified cohesin trimer (consisting of Smc1, Smc3 and Scc1 which are the necessary bare components for ring topology of cohesin) along with the purified cohesin tetramer (consisting

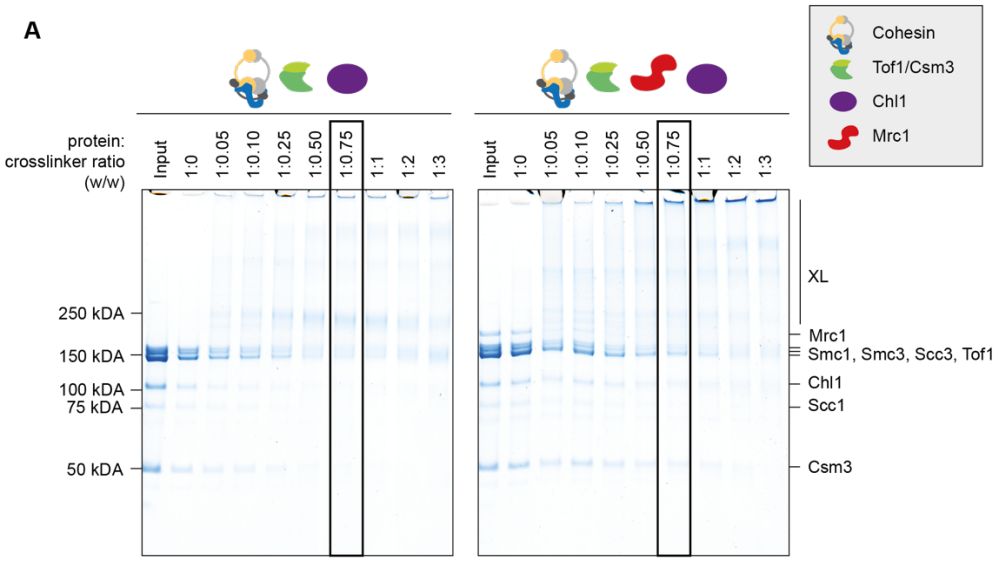
A
Cohesin
Tof1/Csm3
Chl1
Mrc1
protein:
crosslinker ratio
(w/w)
Input
1:0
1:0.05
1:0.10
1:0.25
1:0.50
1:0.75
1:1
1:2
1:3
250 kDA
150 kDA
100 kDA
75 kDA
50 kDA
XL
Mrc1
Smc1, Smc3, Scc3, Tof1
Chl1
Scc1
Csm3

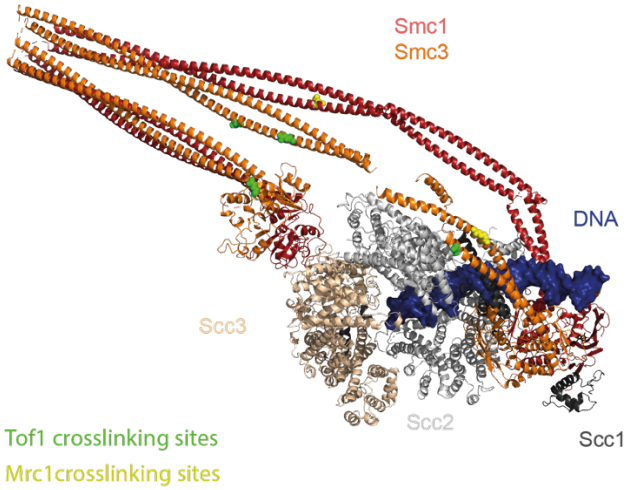
B
Smc1
Smc3
DNA
Scc3
Scc2
Scc1
Tof1 crosslinking sites
Mrc1crosslinking sites

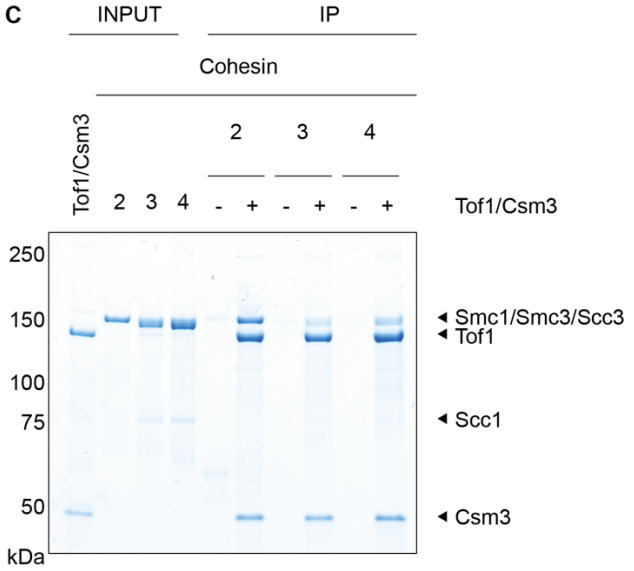
C
INPUT
IP
Cohesin
Tof1/Csm3
2
3
4
- + - + - +
Tof1/Csm3
250
150
100
75
50
kDa
Smc1/Smc3/Scc3
Tof1
Scc1
Csm3

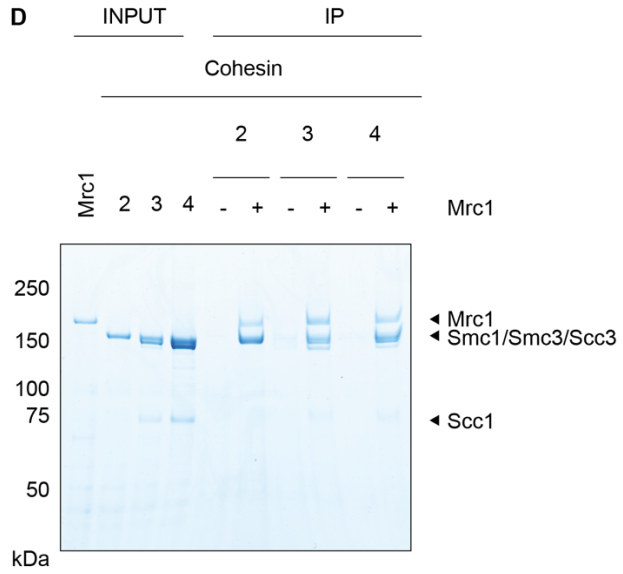
D
INPUT
IP
Cohesin
Mrc1
2
3
4
- + - + - +
Mrc1
250
150
100
75
50
kDa
Mrc1
Smc1/Smc3/Scc3
Scc1

Figure 5.6 Tof1/Csm3 and Mrc1 interact with Cohesin dimer

A. Sulfo-SDA crosslinker titration. Cohesin and the indicated cohesion establishment factors were incubatedwith the indicated Sulfo-SDA concentrations. Crosslinked samples were analyzed by SDS-polyacrylamide gel electrophoresis followed by Coomassie Blue staining. Based on this analysis, a protein : crosslinker ratio of 1 : 0.75 was selected to prepare the samples for mass spectrometry analysis.

B. Protein crosslinking mass spectrometry was performed after incubating Tof1, Csm3, Mrc1, Chl1 and Cohesin together. The amino acids in Cohesin that crosslinked with Tof1 and Mrc1 are highlighted in Cohesin structure in green and yellow respectively.

C. Interaction screen with purified proteins. 10% of input is loaded onto gel. Calmoudulin beads ±Tof1/Csm3 were incubated with cohesin dimer (Smc1 and Smc3 indicated as 2), trimer (Smc1, Smc3 and Scc1 indicated as 3) and tetramer (Smc1, Smc3, Scc1 and Scc3 indicated as 4). Bead bound fraction is loaded onto gel and stained with Commassie Brilliant Blue.

D. Same as A but with anti-Flag M2 beads ±Mrc1.

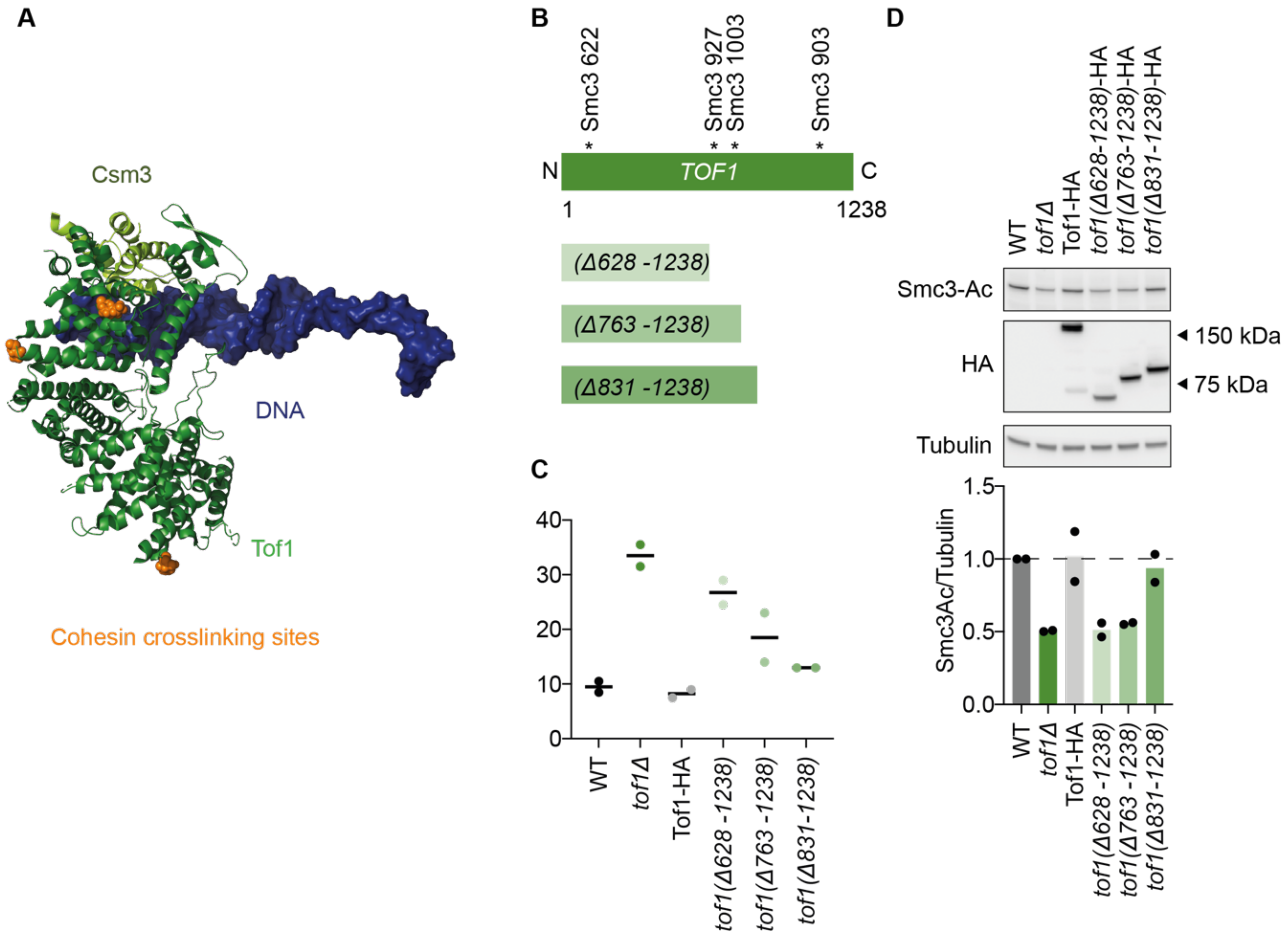

Figure 5.7 Tof1 domains important for sister chromatid cohesion

A. Structure of Tof1 and Csm3 where amino acids in Tof1 that were identified to be in close proximi-tiy with Cohesin subunits were identified by Protein Crosslinking Mass Spectrometry
B. Schematic of Tof1 gene showing the locations along the length of the gene where crosslinks were identified with Cohesin subunits. The cohesin subunit and amino acid that was identified to be crosslinked are indicated. The schematic also shows three C terminal truncations of Tof1 protein that are used furhter in cohesion assays
C. GFP dot assay of indicated genotypes in metaphase. Mean and individual values of three inde-pendent experiments are shown.
C. WB samples of cells of indicated genotypes were taken at metaphase, 120 minutes after G1 release into nocodazole arrest. Samples are blotted with anti-Smc3Ac and anti-HA. Tubulin is used as loading control. The Smc3Ac/Tubulin ratio were normalized to highest signal of WT cells. Means and individual values from three individual experiments are shown.

of Smc1, Smc3, Scc1 and Scc3 which is the cohesin complex I have been using so far). Both Tof1-Csm3 and Mrc1 were able to interact with just the cohesin dimer on this interaction assay and if anything, the co-immunoprecipitation of cohesin dimer was stronger than for cohesin trimer or tetramer (figure 5.6C,D). Consider that at 140kDa, cohesin has three subunits in tetramer and only 2 subunits in dimer and trimer as observed in the 10% input fraction. Despite this, cohesin dimer is more abundant compared to cohesin tetramer in the Tof1-Csm3 or Mrc1 dependent bead bound fractions. This interaction assay corroborates the CLMS results that Tof1 and Mrc1 are interacting with Smc1 and Smc3 subunits of cohesin.

Four crosslinks in Tof1 were identified across the length of the protein (figure 5.7A,B). To test the relevance of these sites, I further truncated Tof1 protein at the C terminal based on truncations that have been previously published (figure 5.7B) (Westhorpe, Keszthelyi et al. 2020). There seems to be a slight decrease in the expression of these proteins with increasing truncations, also has been previously observed (figure 5.7D). When testing these truncations for cohesion defects, I observed that *tof1(Δ763-1238)* begins to demonstrate an increase in GFP separation and this is further increased in *tof1(Δ628-1238)* although it does not fully reach the levels observed in *tof1Δ*. The two shortest truncations also demonstrated lowered Smc3Ac levels even while *tof1(Δ831-1238*) demonstrated WT Smc3Ac levels (figure 5.7D). This suggests that the central domain of Tof1 around where two interaction sites were observed for Cohesin may be biologically relevant for cohesion establishment. Interestingly, Mrc1 interaction with Tof1 has also been published to occur around this region.

In conclusion, I have identified potential interaction between Cohesin and cohesion establishment factors Tof1 and Mrc1 and that preliminary data suggests that the cohesion establishment factors are engaging with the Smc1 and Smc3 dimer of Cohesin.

5.3 Direct protein-protein interactions between cohesion establishment factors

Cohesion establishment factors associate with and travel with the replisome, therefore it is not surprising that there exist physical interactions between them. Tof1, Csm3 and Mrc1 form a complex. Chl1 and Ctf4 form a complex. Human orthologs of Tof1 (Timeless) and Chl1 (DDX11) have been found to interact and this interaction has been reported to be important for sister chromatid cohesion (Cortone, Zheng et al. 2018)). However, based on weak conservation of the interaction motif in DDX11, the same study predicted that budding yeast Tof1 and Chl1 do not interact.

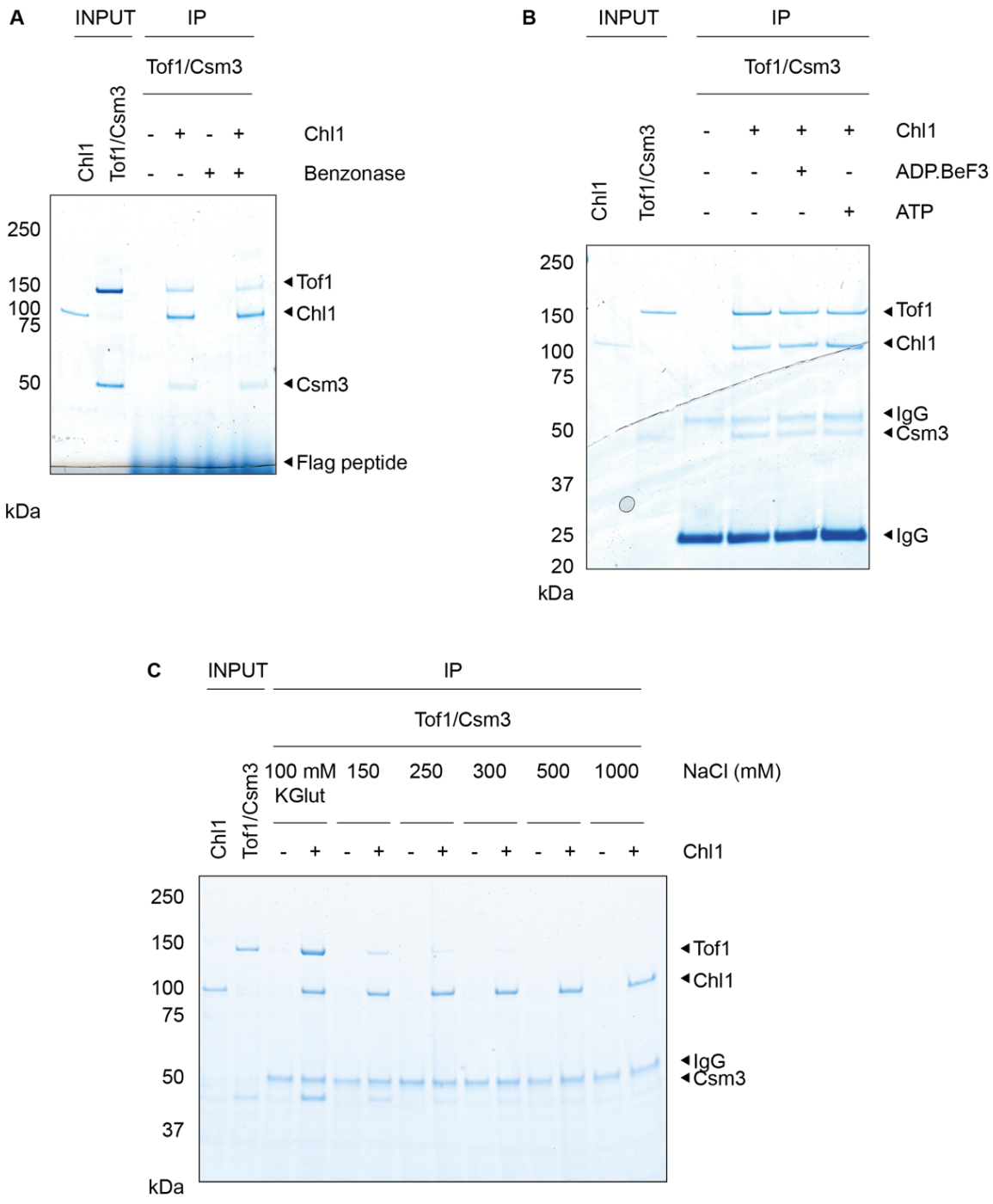

Figure 5.8 Tof1-Csm3 interacts with Chl1
A. Interaction screen with purified proteins. 10% of input is loaded onto gel. M2 anti-flag beads ± Chl1-Flag were incubated with Tof1-Csm3 in the presence or absence of benzonase. Bead bound fraction is loaded onto gel and stained with Commassie Brilliant Blue.
B. Same as A but incubation occured in the presence or absence of ATP or ADP.BeF3
C. Same as A but incubation occured at indicated salt concentratins of NaCl or KGlut in the buffer

I performed an interaction assay using purified budding yeast Tof1-Csm3 and Chl1 to test whether there exists direct interaction between these proteins. Beads prepared with or without Chl1 were incubated with Tof1-Csm3. Contrary to prediction, I found an interaction between Tof1 and Chl1 because Tof1-Csm3 was retained on the beads in a Chl1 dependent manner (figure 5.8A). This interaction is also DNA-independent and salt sensitive (figure 5.8A,B). This interaction is not dependent on ATP and do not change in presence of non-hydrolysable ADP.BeF3 (data not shown). I also performed far western to see whether Chl1 was binding to Tof1 or Csm3, and identified that Chl1 recognizes interaction motifs in Tof1 (data not shown).

Therefore, I have identified that similar to humans, budding yeast Tof1 and Chl1 also engage in direct protein protein interactions. This incentivizes further investigation into the role of this interaction in cohesion establishment.

Chapter 6: Discussion

Despite being non-essential proteins, Tof1, Csm3 and Mrc1 participate in myriad roles during replication. Their role in cohesion establishment has been known for almost two decades but the basis of their contribution has remained elusive. In this study, I have systematically ruled out four of their replication roles for contribution to cohesion establishment. Instead, I have identified direct protein protein interactions between cohesin and Tof1-Csm3 as well as cohesin and Mrc1. These findings open the possibility that a series of direct physical interactions between replication fork components and the cohesin complex facilitate successful establishment of sister chromatid cohesion during DNA replication.

6.1 Physical interactions between replisome components and cohesin

The interactions I have identified are interesting to consider in the context of available structural knowledge of Tof1, Csm3, Mrc1 and Chl1 with the CMG helicase. Tof1 and Csm3 form a complex at the head of the helicase and are therefore positioned at the perfect vantage point to interact with any DNA binding protein complex ahead of the replication fork (Baretić, Jenkyn-Bedford et al. 2020, Jones, Baris et al. 2021). The structure for Mrc1 has not been resolved, but it has multiple contacts spanning from Tof1, multiple MCMs, Ctf4 (Baretić, Jenkyn-Bedford et al. 2020) and polymerase epsilon (Lou, Komata et al. 2008) and is expected to have unstructured domains that may engage in interactions. Chl1 interacts with Ctf4 which is also associated closely with the CMG (Samora, Saksouk et al. 2016). Given that cohesin molecules are loaded onto DNA in late G1, the replisome inevitably encounters cohesin on DNA. It is possible that specific proteins of the replisome engage in a choreographed series of interactions with cohesin that lead to cohesion establishment (figure 6.1). Especially since, unlike the cohesion establishment factors we studied, another integral part of the replisome - GINS - did not interact with cohesin.

In the interaction assays, purified Tof1 and Csm3 are always in the form of a complex so it is not possible to delineate whether one among them or both are involved in interaction with cohesin. CLMS in this study identified contacts between Tof1 and Cohesin but not between

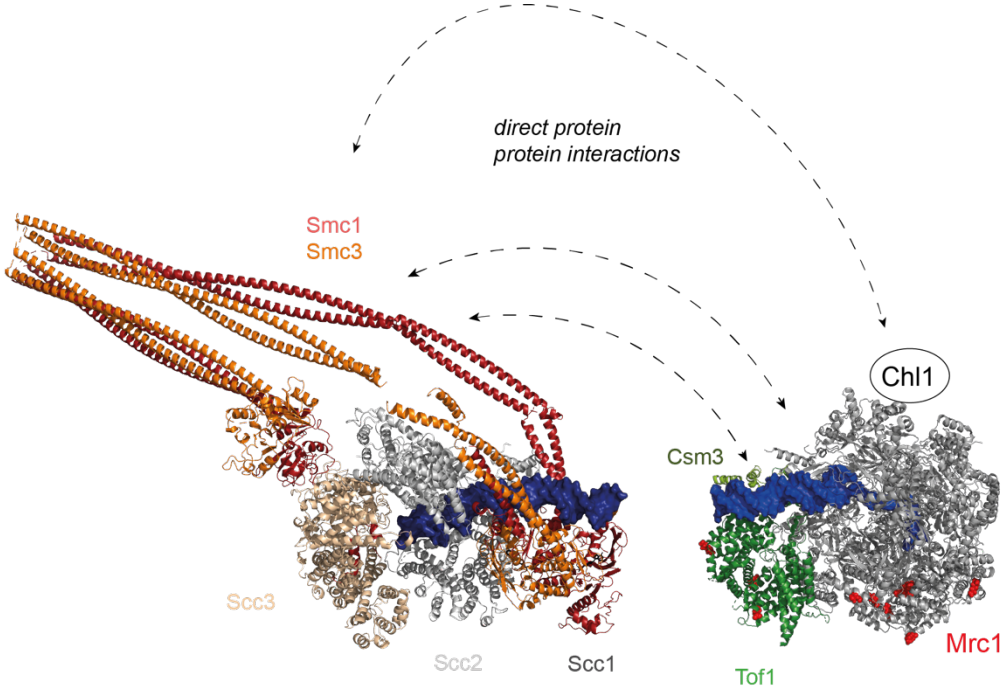

Figure 6.1 Model suggesting cohesin interaction with cohesion establishment factors upon encounter with replisome

Juxtaposed are structures of cohesin loading on DNA and Tof1/Csm3 at replication fork
Modelled prediction of *Schizosaccharomyces pombe* Cohesin structure in the process of DNA loading as described in Higashi et al. 2018.
Strcuture of Tof1 and Csm3 associated with the MCM subunits of the CMG helicase.Highlighted in red, expected localization of Mrc1 based on amino acids in Tof1 and MCMs that was shown to crosslink with Mrc1 (PDB: 6SKL and Baretić, Jenkyn-Bedford et al. 2020)

Csm3 and Cohesin. It is possible that the interaction with cohesin is entirely mediated by Tof1. *In vivo*, Tof1 and Csm3 form a tight complex before they can associate with the replisome and that if one is absent, the other is not recruited to the replisome, making it impossible to separate phenotypes of *tof1Δ* and *csm3Δ* (Bando, Katou et al. 2009). It is possible that Csm3 contribution to cohesion establishment could be to simply stabilise Tof1 at the replisome. However, this would need to be directly tested.

Crosslinks with Tof1 and Mrc1 were not identified close to the ATPase heads and co-immunoprecipitation experiments showed that the interaction is ATP independent. This suggests that the role of Tof1 and Mrc1 on cohesion establishment is not likely to act through its ATPase which is necessary for its DNA loading and unloading (Murayama and Uhlmann 2015). Instead, Tof1 and Csm3 contact with cohesin may directly alter the quaternary structure of cohesin.

CLMS and coimmunoprecipitation of purified Cohesin dimer suggest that Tof1 and Mrc1 contact Cohesin at the Smc1 and Smc3 dimer. It is difficult not to speculate on the biological significance of this interaction. When cohesin is in the process of loading onto DNA, structural studies have shown that it sits in a closed conformation where the coiled coils of its SMC subunits are together and folded at the elbow (Higashi, Eickhoff et al. 2020). Are Tof1 and Mrc1 perhaps able to unravel this to facilitate the open conformation of the Cohesin ring? Does Chl1 interaction with Cohesin also play a similar role? Although a structure of the replisome which includes Chl1 is not available, negative stains of Chl1 and Ctf4 complex can be used to predict Chl1 position at two different positions at the replisome (Samora, Saksouk et al. 2016). One of these positions places Tof1 and Chl1 at opposite ends of the replisome heads, at a distance of 24 nm; are they perhaps each responsible for unravelling one coiled coil of cohesin? Such opening of the coiled coils may facilitate passage of replisome through the cohesin ring. Consistent with this, Tof1, Csm3, Chl1 and Ctf4 have been identified through two separate assays to form part of the same genetic pathway, and specifically to be part of the “conversion pathway” where pre-loaded cohesin is converted into cohesive cohesion (Srinivasan, Fumasoni et al. 2020). One way to test this hypothesis would be to use folding markers on Cohesin in presence or absence of Tof1 and Chl1.

Genetic studies show that Tof1 and Mrc1 belong to two separate cohesion establishment pathways (Xu, Boone et al. 2007, Srinivasan, Fumasoni et al. 2020), yet they both interact with cohesin. It is of interest to consider whether the pairwise interactions (Tof1 and Cohesin, Mrc1 and Cohesin) contribute separately to two different modes of cohesion

establishment. Perhaps both pathways require interaction of some form between replisome and Cohesin, but the functional consequence of the interaction is different.

Single molecule studies of TCM at the replication fork have suggested that Mrc1 association with the replisome is dynamic (Lewis, Spenkelink et al. 2017). Even when a saturation of TCM is available during replication, a single trajectory of DNA replication rapidly switched between short and fast replication rate. In their study, they have opened a question about the biological reason for dynamic association of Mrc1 with the replisome. Is it possible that the dynamic nature of Mrc1 allows it to come off CMG and interact with the cohesion ring to facilitate cohesion establishment? A competitive interaction assay of TCM with Cohesin and CMG helicase might be of interest in addressing this question.

It is likely that TCM interaction with cohesion is transient in nature. A transient contact may be working in a conveyor belt like model as has been suggested with nucleosome reassembly behind the fork which is mediated through multiple contacts of histones and histone chaperone FACT with replisome components (unpublished work from Christopher Smith, Diffley lab) (Safaric, Chacin et al. 2022). It is of great interest to perform pairwise interactions screens between different replisome components, comprehensively including almost 30 protein complexes, and Cohesin core and accessory subunits with include cohesin loader Scc2/Scc4, Pds5 and Wpl1. In this study, I have also identified cohesion defects when the catalytic domain of polymerase epsilon is absent (figure 4.7). This highlights that while the original genetic screens caught the non-essential replisome components for their role in cohesion establishment (Mayer, Pot et al. 2004), there are essential replisome components that may perform specific roles in cohesion establishment. They have not been systematically investigated.

I recognize that it is also important to be guarded in my speculations and that these preliminary findings about interactions between Cohesin and cohesion establishment factors provide a window into further research that is necessary to understand the longstanding mystery of cohesion establishment. Three different models of cohesion establishment have been proposed, including cohesin conversion through fork passage or reloading behind the fork, de novo loading of cohesin behind the fork or cohesion establishment at replication termination. The interactions we have identified are consistent with the likelihood of each model and cannot currently exclude any of them.

While the CLMS study provides interesting preliminary data, it is of great interest to identify the interaction surfaces between these proteins either through optimization of CLMS or through structural studies. After this, future work will need to address directly whether the

interactions between replisome components and Cohesin is necessary for the process of cohesion establishment. This can be done through mutations of key amino acids in TCM involved in interaction to disrupt interactions and assaying their sister chromatid cohesion phenotype *in vivo*.

This is at least a second example of replication associated phenomenon where the majority of the job is mediated through interactions. Histone recycling behind the replication fork is also largely mediated by direct contacts of histones and histone chaperones across the replisome components. The results presented in this thesis suggest that cohesion establishment too may be mediated through contacts with Tof1 and Mrc1. This really informs our understanding of the replisome, which has evolved not just to participate directly in the molecular process of DNA replication but to facilitate processes surrounding DNA replication through direct protein protein interactions.

6.2 Separable roles of TCM in replication and cohesion establishment

In this study, I have shown that the four roles of Tof1, Csm3 and Mrc1 that I have studied are separable from cohesion establishment namely, their role in intra S checkpoint signalling, regulation of replisome speed, and Tof1 role in recruitment of topoisomerase 1 and FACT locally to the replisome. To demonstrate this, I have sometimes utilised separation of function mutants. Further separation of function mutants, especially mutations at the interaction surfaces between cohesin and Tof1, Csm3 and Mrc1, will also be useful to fully confirm separation of function with general replication roles.

TCM has further roles at the replication fork that I have not addressed in my study. Most notably, is the role in Mcm7 ubiquitination. This role became clear with advances in replisome disassembly studies. Tof1 and Csm3 orthologs Timeless and Tipin are necessary Mcm7 ubiquitination in *C. elegans* but Claspin and DDX11, orthologs of Mrc1 and Chl1 were not found to be important for this process (Xia, Fujisawa et al. 2021). However, this role is not conserved in budding yeast. Instead, in a biochemical assay in budding yeast, Mrc1 and to a lesser extent, Chl1 were shown to be necessary for Mcm7 ubiquitination (Deegan, Mukherjee et al. 2020). The lack of conservation of Mcm7 ubiquitination roles of these proteins suggests that their role in Mcm7 ubiquitination may not be the mechanism through which they contribute to cohesion establishment which is expected to be a highly conserved

process. Disrupting Mcm7 ubiquitination *in vivo* prior to performing cohesion assays can be used to address this question.

However, I have not directly resolved this question in my study. It remains an important question to study because one of the models that has been proposed for cohesion establishment is that upon encounter with cohesin, replisome pushes cohesin and cohesion is established at termination sites. An attempt to address this model had been undertaken by studies in the mid-2000s by performing cohesin ChIP at intervals as cells go through S phase. Cohesin localization in the genome did not change between these timepoints although a confounding factor that was not directly addressed is the quick action of transcription which pushes cohesin rapidly may mask cohesin pushing by the replisome (Lengronne, Katou et al. 2004).

TCM also has roles in replication through G quadruplexes and repetitive regions, specifically islands of CAG repeats were found to increase in instability in absence of TCM (Razidlo and Lahue 2008). However, given that repetitive elements do not form the majority of budding yeast DNA and anyways cohesion loading sites and cohesion occupancy sites do not necessarily coincide with repetitive regions. Instead, cohesin loading is found to be at loader sites and occupancy including during S phase is mostly located at transcription convergent sites (Lengronne, Katou et al. 2004, Ocampo-Hafalla, Muñoz et al. 2016).

6.3 Smc3 acetylation during S phase

Smc3Ac has been used as an independent and complementary way of assessing status of sister chromatid cohesion.

However, published studies have also already recognized that Smc3Ac does not directly correlate with sister chromatid cohesion status. Cohesion defect of *eco1-1* cells at permissive temperature is similar to *chl1Δ* and *ctf4Δ* cells even while Smc3Ac levels in *eco1-1* cells are much lower (Borges, Smith et al. 2013). In my study I encountered examples where despite having WT Smc3Ac levels, the cells demonstrated cohesion defects. The Smc3Ac levels of *tof1Δ*, *csm3Δ* and *mrc1Δ* cells were elevated to WT levels when they underwent replication in presence of low concentrations of HU drug (figure 4.5 D). However, this did not lead to rescue of cohesion defects in these cells as determined by the GFP dot assay (figure 4.5 E). This observation challenges the use of S phase Smc3Ac levels as a

blanket indicator for sister chromatid cohesion and reveals the complex relationship between Smc3Ac and cohesion establishment.

In S phase, exposed ssDNA at HU stalled replication forks have been found to recruit more cohesin in a cohesin loader and Chl1 dependent manner (Delamarre, Barthe et al. 2020). Based on my observation of increasing Smc3 acetylation with increasing concentrations of HU, I speculate whether cohesins that get recruited to stalled replication forks in S phase also get acetylated at Smc3. If so, this leads to the question why WT levels of Smc3 acetylated cohesin is unable to contribute to sister chromatid cohesion in some genotypes. Does this have to do with where in the chromosome the acetylated cohesin are situated? Is the cohesin acetylated upon HU exposure cohesive?

Along with an increase in Smc3 acetylation upon HU exposure, I also observed such an increase in *rad53-11*, *mrc1AQ* and *top1Δ* cells (figure 4.1B, 4.2C, 4.10C). This further demonstrates the fluctuation of Smc3 acetylation across genotypes. It also hints at the possibility that in some scenarios, acetylation of Smc3 may be independent of cohesion establishment.

6.4 Mrc1 roles in replication

Although my study focused on the roles of replication proteins in cohesion establishment, it is perhaps unsurprising that I stumbled across interesting observations related to TCM during replication.

Mec1 and Rad53 are essential proteins of the replication checkpoint, and their essential role has been attributed to the depletion of Sml1 at the start of DNA replication since they can only be deleted in the absence of Sml1. Sml1 is the cellular inhibitor of RNR enzyme that synthesizes dNTPs that are utilized in DNA synthesis (Zhao, Muller et al. 1998). A recent paper found that when cells begin DNA replication, the early origins exhaust the cell's dNTP pool which leads to activation of Mec1 and depletion of Sml1 protein, ultimately resulting in replenishing of dNTPs required for DNA synthesis (Forey, Poveda et al. 2020).

Surprisingly, I found the levels of Sml1 remain constant in *mrc1Δ* cells as enter the S phase (figure 4.4C). I have also followed Sml1 levels in *mrc1Δ* cells at shorter time intervals corresponding to S phase entry of cells and did not observe the strong depletion of Sml1 visible in WT cells (data not shown). As I have described previously, Mrc1 mediates one

branch of the Mec1-Rad53 checkpoint pathway. Could Mrc1 also contribute to the replication checkpoint regulation of Sml1 levels in the normal unperturbed cell cycle in WT cells?

A previous study has found no difference in the dNTP pool between WT and *mrc1Δ* cells in G1 arrested cells and cells arrested with hydroxyurea (Poli, Tsaponina et al. 2012). It would be of interest to monitor dNTP levels as cells enter S phase in *mrc1Δ* cells and compare them to WT cells.

It is surprising that *mrc1Δ* cells are viable despite their lack of cell-cycle regulation of Sml1. Perhaps this is possible due to the overall levels of Sml1 in *mrc1Δ* being lower than WT cells. Based on studies performed with reconstituted DNA replication, Mrc1 directly increases efficiency of helicase unwinding and when Mrc1 is omitted, helicase unwinding rate is slower (McClure and Diffley 2021). Perhaps in cells slower moving replication forks are also less affected by scarce dNTPs compared to WT forks. Furthermore, I also wonder whether the slow replication observed *in vivo* in *mrc1Δ* cells can be explained by both direct regulation of helicase unwinding speed and as well a reduced dNTP pool due to continued presence of Sml1 upon S phase entry.

Chapter 7: Concluding Remarks

Conceptually, the basis of life and role of the genomic code in perpetuating it is very simple. There is semiconservative replication of DNA followed by distribution of the genome into two cells. While the concept is simple, the molecular details surrounding the process are very complex. As such, replication proteins have not only evolved for their roles in DNA replication but also for their roles in processes that surround DNA replication. This research provides preliminary data suggesting that Tof1, Csm3 and Mrc1 at the replication fork make key contributions to numerous processes by making connections between the replisome and the outside world.

Chapter 8: Materials and Methods

8.1 Yeast genetics and *in vivo* studies

Yeast strain construction

All budding yeast strains are of W303 background and have been listed in Table I. Strains were constructed either by lithium acetate transformation or genetic crossing followed by tetrad dissection using auxotrophic or antibiotic markers. Colonies were tested using PCR for gene deletions. For tagging, the strain was also determined using western blot probing for the relevant tag. For mutations, the genotype was confirmed using sanger sequencing.

Yeast cell cycle and synchronization

All cultures are grown in YPD medium at 25°C in shaking incubators at 180rpm unless otherwise stated

Cells of MAT **a** of relevant genotypes are grown overnight in YPD and back diluted in the morning. 4 µg/mL alpha factor is added at OD 0.2 and subsequently twice more after 55 min each to arrest cells in G1. After 2 hours 45 minutes since first alpha factor addition, cells are released from G1 arrest by washing in a filtration tank with 10X volume of YP. The cells are then resuspended in YPD + 6µg/mL nocodazole culture to allow them to progress through S phase and arrest in metaphase. Samples for FACS analysis, Western Blotting and GFP dot assay are taken at relevant timepoints after release from G1 arrest.

For hydroxyurea induction, after G1 arrest, cells are released into YPD + 6 µg/ml nocodazole + hydroxyurea at the relevant concentration. The delay in S phase is followed through FACS analysis at relevant timepoints.

Flow Cytometry

Approximately 1mL culture of cells (OD_{660} 0.2 – 0.7) are fixed overnight in cold 70% ethanol. The RNA in cells are digested with 0.1 mg/mL ribonuclease (RNAse) for 4 hours to overnight at 37°C in 50 mM tris-HCl pH 7.5 buffer. To stain the DNA, the cells are resuspended in 200 mM tris-HCl pH 7.5, 210 mM NaCl, 78 mM MgCl2 buffer containing 0.025 mg/mL Propidium Iodide. The cells are sonicated and diluted in 50 mM tris-HCl pH 7.5. before being run in the

FACSCalibur cell analyzer (BD Biosciences). For each sample, 10,000 cells are counted and then analyzed using FlowJo v10 software.

Western Blotting

Cells at indicated timepoints during synchronized cell cycle are collected in cold 20% TCA and fixed for at least 1 hr. Cells are resuspended in sample buffer containing 100 mM tris-HCl pH 6.8, 4% SDS, 20% glycerol and 4% β-mercaptoethanol. After bead beating to break cells open and removal of cell debris, Bradford test is conducted with the protein extracts to determine protein concentration. Approximately 15 µg of each protein sample are separated by SDS-polyacrylamide gel electrophoresis and then transferred to nitrocellulose membranes. Antibodies utilized for western blot detection are α-Smc3Ac (gift from Shirahige lab), α-Tubulin (Crick Cell services, clone TAT-1), α-Rad53 (Abcam, ab104232 and ab166859), α-Sml1 (Antibodies-online GmbH, ABIN3197499), α-Myc (Santa Cruz Biotechnology, clone 9E10), α-Flag (Merck, M2), and α-HA (Merck, clone 12CA5). ECL or ECL Prime was used to visualize the western blots using Amersham Imager 600 (GE Healthcare) or ChemiDoc MP Imaging System (Bio-Rad). Over-exposure of western blots was avoided. Smc3Ac signal was quantified using FIJI software and normalized against the loading control of tubulin.

GFP dot assay

Strains containing tetO repeats at the URA locus (35 kbp away from centromere of chromosome 5) and constitutively expressing tetR-GFP fusion proteins are arrested in metaphase by waiting 2 hours after G1 release into nocodazole containing media. 2mL culture are taken and fixed in 70% cold ethanol overnight. For imaging, thin agarose patches are prepared on glass slides using 2% agar. A drop of sonicated cells resuspended in PBSA are added to the agarose patches and GFP signals are imaged using DeltaVision wide-field fluorescence microscope using FITC filter (475/28 excitation and 525/50 emission) and polychroic option. z-stacks with 35 images at 0.2 µm intervals were captured, deconvolved and merged by maximum intensity projection. The number of GFP dots in each cell are later manually counted. Between 100-200 cells are scored for each sample for each individual experiment.

The Smc3 acetylation levels of the WT strain used for GFP dot assay is comparable to a WT W303 strain, a control that was conducted by another PhD student Kimberly Quillian in our laboratory.

Spot assay

Asynchronous cells at 0.3 OD_{660} are diluted by 10-fold 5 times and plated on YPD plates at 25°C for control, YPD + HU plates at 25°C or YPD plates at 37°C for assaying temperature sensitivity. The plates were imaged between days 1-3 after growth.

BrdU-IP ssSeq

BrdU-IP ssSeq was performed as described as part of eSPAN protocol in (Yu, Gan et al. 2014). This protocol was originally established by Hon Lui, a previous PhD student in our lab and the full details can be obtained here (Liu, Bouchoux et al. 2020) (Liu 2019). The protocol was performed with assistance from Hon Lui and a brief description of it is described below.

Cells were arrested in G1 using alpha factor as describe above. The cells were then released into YPD medium containing 400 µg/mL BrdU at 25°C. To catch cells at an early S phase timepoint, at 25 minutes after G1 release, cells were fixed with 1% w/v paraformaldehyde for 20 minutes at 25°C at 180 rpm. 150mM final concentration of glycine was added to quench the fixation reaction.

After quenching, cells were washed 3 times with cold TBS +1 mM PMSF. Again, cells were washed with lysis buffer (50 mM HEPES/KOH pH 7.5, 140 mM NaCl, 1mM EDTA, 1% Tx-100, 0.1% Na-deoxycholate) + PI (1 mM PMSF, 1mM Pefabloc, 1mM Benzamide, 1mg/mL Bacitracin, 10 µg/mL Leupeptin) and resuspended in 100 µL lysis buffer + PI. After bead breaking to break cells open and removal of cell debris, cell extract was collected. After centrifugation to collect cell pellet, supernatant was discarded and 250 µL lysis buffer + PI was again added to the cell pellet. Diagenode Bioruptor Sonication Device was used for sonication (30s on, 30s off) X 25. After sonication, samples were further centrifuged twice and supernatant was collected each time and pooled. BrdU-IP was performed on the extract.

Before BrdU-IP, DNA was denatured at 95°C for 3 min and then added to 1.2 mL BrdU IP Buffer (1X PBSA, 0.0625% w/v Triton X-100) which was initially mixed with 1 µL MRE600 E. coli tRNA (10 mg/mL), 150 µL PBSA (10x) and 0.5 µL anti-BrdU and placed in cold wheel 4 C for 2 hours. After this, it was further incubated in cold wheel for 1 hour with 20 µL Protein G Sepharose beads previously washed with BrdU-IP buffer. Then, the Sepharose bead

mixture was taken and washed 3X with cold BrdU-IP buffer followed by 1X wash with room temperature TE Buffer. BrdU labelled DNA from the beads was eluted by incubating with 100 µL 1X TE/ 1% SDS at 65°C for 5 minutes. The supernatant was taken and the beads were again incubated with 50 µL 1X TE/ 1% SDS. 150 µL of BrdU-IP thus obtained was purified using Qiagen Minelute Gel Extraction Kit.

DNA library was prepared using Accel-NGS 1S Plus DNA Library Kit (Swift Biosciences). Illumina HiSeq 2500 or 4000 was performed by Advanced Sequencing Facility at The Francis Crick Institute. Data analysis was performed by Harshil Patel using pipeline described in (Liu, Bouchoux et al. 2020). The sequences were aligned to budding yeast reference genome sacCer3 and visualized in IGV software after normalization. I manually selected Brdu-IP-sSeq peaks at expected early active yeast origins. Collapsing this set of early replicating origins, log ratio of Watson/Crick was calculated and mapped.

8.2 Biochemistry

Protein purification

Cohesin (tetramer) purification

S. cerevisiae cohesin tetramer complex was purified as previously published (Minamino, Higashi et al. 2018). Second copy genes of cohesin subunits Smc1, Smc3, Scc1 and Scc3 under the GAL promoter were overexpressed in a budding yeast strain 5226 by galactose induction for 2 hours at 30°C in a 100L YP + 2% Raffinose culture using the fermentation service at the Francis Crick Institute. Cells were harvested using CEPA centrifuge, washed with distilled water and then resuspended in buffer (50mM Hepes pH7.5, 300mM NaCl, 2mM MgCl2, 0.5mM TCEP, 20% Glycerol, 0.5mM PEFABLOC+ Complete). These cells suspended in buffer was made into popcorn and pulverized in the freezer mill. Powder obtained in this manner was thawed in lysis buffer (50mM Hepes pH 7.5, 20% Glycerol, 300mM NaCl, 0.5mM TCEP, 0.5mM PefaBloc, 1X complete tablet –EDTA).

Cell debris was removed after Ti45 centrifugation at 40krpm for 1 hr and in the supernatant thus obtained, rabbit/human IgG agarose bead, benzonase and RNAse were added and incubated with stirring at 4C for 2 hrs. The beads were then washed, ATP washed, and then incubated overnight with 3C protease in the same buffer. The eluate of the beads was loaded onto a preequilibrated heparin column with 50mM Hepes pH 7.5, 300mM NaCl, 20% Glycerol, 0.5 mM TCEP. It was eluted with a 20mL gradient in the Heparin column from 300mM to 1M NaCl. The fractions based on gel were pooled, concentrated with 100kDa vivaspin concentrator and loaded onto Superose 6 Increase column with a 0.5mL loop. It was eluted in 20mM Tris pH 7.5, 150mM NaCl, 10% Glycerol, 0.5mM TCEP and concentrated with 100kDa vivaspin concentrator.

Cohesin (trimer) purification

Purification protocol is identical as for Cohesin (tetramer) except budding yeast strain ___ is used in which second copy genes of cohesin subunits Smc1, Smc3 and Scc1 are overexpressed under the GAL promoter.

Cohesin (dimer) purification

Purification protocol is identical as for Cohesin (tetramer) except budding yeast strain ___ is used in which second copy genes of cohesin subunits Smc1 and Smc3 are overexpressed under the GAL promoter.

Tof1-Csm3 purification

A complex of *S. cerevisiae* Tof1 and Csm3 was purified as published (Yeeles, Janska et al. 2017). Second copy genes of Tof1 and Csm3 under the GAL promoter were expressed in budding yeast strain yAE48 by galactose induction for 2 hours at 30°C in a 100L YP + 2% Raffinose culture using the fermentation service at the Francis Crick Institute. Cells were harvested using CEPA centrifuge, washed with distilled water and resuspended in generic replication lysis buffer (25mM Tris-HCl, 1mM DTT, Protease Inhibitor cocktail). Cells were frozen dropwise in liquid nitrogen to make 'popcorn' and pulverized in the freezer mill.

Powder obtained in this manner was thawed in equal volume of lysis buffer (25 mM Tris-HCl, 400 mM NaCl, 20% Glycerol, 0.5 mM TCEP, 0.5 mM PefaBloc, 1X complete tablet –EDTA). Cell debris was removed after Ti45 centrifugation at 40krpm for 1 hr and in the supernatant thus obtained, calmoudulin beads, 2mM final volume $CaCl_2$, benzonase and RNAse were added and incubated with stirring at 4C for 2 hrs. The beads were then washed and ATP washed in buffer containing $CaCl_2$, and then eluted with 2mM EGTA in Buffer (25 mM Tris-HCl, 200 mM NaCl, 10% Glycerol, 0.5 mM TCEP). The eluate of the beads was loaded onto a Superdex 200 10/300 GL Increase column preequilibrated with 25 mM Tris-HCl, 150 mM NaCl, 10% Glycerol, 0.02% NP40, 1 mM EDTA, 0.5 mM TCEP and eluted in the same buffer. The fractions based on gel were pooled, concentrated with 100kDa vivaspin concentrator if necessary.

Mrc1 purification

S. cerevisiae Mrc1 was purified as published (Yeeles, Janska et al. 2017). Second copy Mrc1 under the GAL promoter were expressed in budding yeast strain yJY32 by galactose induction for 2 hours at 30°C in a 100L YP + 2% Raffinose culture using the fermentation service at the Francis Crick Institute. Cells were harvested using CEPA centrifuge, washed with distilled water and resuspended in generic replication lysis buffer (25mM Tris-HCl, 1mM DTT, Protease Inhibitor cocktail). Cells were frozen dropwise in liquid nitrogen to make 'popcorn' and pulverized in the freezer mill.

Powder obtained in this manner was thawed in equal volume of lysis buffer (25 mM Tris-HCl pH 7.2, 0.02% NP40, 800 mM NaCl, 20% Glycerol, 2 mM EDTA, 0.5 mM TCEP, 0.5 mM

PefaBloc, 1X complete tablet –EDTA). Cell debris was removed after Ti45 centrifugation at 40krpm for 1 hr and in the supernatant thus obtained, M2 Flag agarose beads, benzonase and RNAse were added and incubated with stirring at 4C for 2 hrs. The beads were then washed and ATP washed, and then eluted with 0.5 mg/mL Flag peptide in Buffer (25 mM Tris-HCl pH 7.2, 0.02% NP40, 400 mM NaCl, 10% Glycerol, 1 mM EDTA, 0.5 mM TCEP). The eluate of the beads was diluted to bring final salt concentration to 150 mM NaCl. The diluted eluate was then laoded to a MonoQ 1mL column at preequilibrated with 25 mM Tris-HCl pH 7.2, 150 mM NaCl, 10% Glycerol, 0.02% NP40, 1 mM EDTA, 0.5 mM TCEP and eluted in a 10mL gradient from 150 mM NaCl to 1M NaCl. The fractions based on gel were pooled and dialysed with 25 mM Tris-HCl pH 7.2, 150 mM NaCl, 40% Glycerol, 0.02% NP40, 1 mM EDTA, 0.5 mM TCEP wbich reduced the volume by approximately half.

Chl1 purification

This protocol was developed by Masashi Minamino in our lab.

Second copy gene of codon optimized Chl1 under the GAL promoter was overexpressed in a budding yeast strain y5226 by galactose induction for 2 hours at 30°C in a 100L YP + 2% Raffinose culture of 1.0 OD_{660} using the fermentation service at the Francis Crick Institute. Cells were harvested using CEPA centrifuge, washed with distilled water and then resuspended in lysis buffer (50 mM Tris-HCl pH7.0, 500 mM NaCl, 10% Glycerol, 2 mM MgCl2, 0.1% Triton X-100, 0.5 mM TCEP, 0.5 mM PEFABLOC+ Complete). Cells were frozen dropwise in liquid nitrogen to make ‘popcorn’ and pulverized in the freezer mill.

Powder obtained in this manner was thawed in lysis buffer as above. Cell debris was removed after Ti45 centrifugation at 40krpm for 1 hr and in the supernatant thus obtained, rabbit/human IgG agarose bead, benzonase and RNAse were added and incubated with stirring at 4°C for 2 hrs. The beads were then washed, ATP washed, and then incubated overnight with 3C protease in the same buffer. The eluate of the beads was loaded onto a preequilibrated heparin column with 50 mM Tris-HCl pH 7.0, 160 mM NaCl, 10% Glycerol, 2 mM MgCl2, 0.5 mM TCEP. It was eluted with a 15 mL gradient in the Heparin column from 160 mM to 1M NaCl. The fractions chosen after observation of purity on SDS-PAGE gel were pooled, concentrated with 30 kDa Vivaspin concentrator and loaded onto Superdex 200 Increase column with a 0.5mL loop. It was eluted in 20 mM Tris pH 7.5, 150 mM NaCl, 10% Glycerol, 0.5 mM TCEP and concentrated with 30 kDa vivaspin concentrator.

Repurification in alternate buffers

Cohesin tetramer and Tof1/Csm3 were repurified in 25 mM Hepes-KOH, 150 mM NaOAc, 0.5 mM TCEP, 2 mM EDTA to make them compatible with protein crosslinking mass spectrometry and size exclusion chromatography. For the same purpose, Chl1 protein was repurified in 25 mM Hepes-KOH, 100 mM NaCl, 0.5 mM TCEP, 2 mM EDTA and Mrc1 was repurified in 25 mM Hepes-KOH, 150 mM NaCl, 0.5 mM TCEP, 2 mM EDTA.

Purified protein coimmunoprecipitation

Coimmunoprecipitation with purified proteins was performed based on a protocol adapted from Christopher Smith from John Diffley's lab that he has optimized for interrogating interaction between replisome components.

Briefly, for each individual interaction test, 5 µL Protein A dynabeads were washed and incubated with interaction buffer (25 mM Hepes-KOH, pH 7.6, 100 mM K-Glut, 10 mM MgOAc, 0.12% NP- 40) containing anti-Pk antibody in a cold wheel for at least 2 hours. The beads were washed and incubated in interaction buffer containing 200 nM – 600 nM purified cohesin tetramer (with Pk-tagged Smc1) at 30°C for 10 minutes at 1000 rpm. The beads were washed prior to the coincubation step where beads were incubated with 200 nM proteins of interest in interaction buffer at 30°C for 5 min at 1000rpm. The beads were washed again, and bead-bound proteins were eluted with sample buffer (100 mM tris-HCl pH 6.8, 4% SDS, 20% glycerol and 4% β-mercaptoethanol) at 95°C for 5 minutes and loaded onto an SDS-PAGE gel to separate by size, along with 10% Input. The Input and bead-bound proteins were visualized by Coomassie Brilliant Blue.

The interaction screen was also performed the other way around with Tof1/CBP-Csm3 or Mrc1-Flag on beads first and later incubated with proteins being tested for interaction. In this case, 3 µL Calmodulin (CAM) MagneZoom (Paramagnetic beads) or 4 µL Anti-FLAG M2 Magnetic Beads were used respectively. The first incubation step with antibody was not necessary in these cases as the antibodies are already coated on the beads. For elution step with Anti-FLAG M2 Magnetic Beads, in some cases 0.5 mg/mL Flag peptide was used for elution for 10 min, 30°C, 1000rpm.

For checking whether the interactions were dependent on DNA, benzonase was added in the co-incubation step, for checking dependence on ATP binding and hydrolysis, ADP.BeF_3

and ATP were added in the co-incubation step. For checking for salt sensitivity, the salt composition of the buffer was changed as indicated (from 100 mM K-Glut to 150 mM – 1M NaCl) during the coincubation step.

Size Exclusion Chromatography

Superose 6 Increase 3.2/300 was preequilibrated with cold buffer (25 mM Hepes-KOH pH 7.6, 100 mM NaOAc, 0.5 mM TCEP, 2 mM EDTA). 10 µg of proteins at the same molarity (>1 mM) were incubated together in above buffer at 30°C for 5 minutes at 1000 rpm before loading onto Superose 6 Increase column with a 50 µL loop. It was eluted with buffer into 25 µL fractions. The fractions were loaded onto SDS-PAGE gel and transferred to nitrocellulose membrane for western blotting. The proteins at relevant sizes were probed with the antibodies against their respective tags. Smc3-Pk in Cohesin was probed with anti-Pk, Csm3-CBP in Tof1-Csm3 was probed with α-CBP (Merck, 07-482 and Merck, clone C16T) and Mrc1-Flag was probed with α-Flag (Merck, M2).

Protein crosslinking mass spectrometry

A total of 100 µg of Cohesin, Tof1/Csm3 and Chl1 with or without Mrc1 at 300 - 350 nM are co-incubated at 30°C for 5 minutes at 1000 rpm. Sulfo-SDA crosslinker is added at protein to crosslinker weight ratio of 1:0.75 and the mixtures were left in the dark at 4°C for 2 hours. The diazirine group in SDA was then photoactivated by UV irradiation at 365 nm from an CL-1000 Ultraviolet Crosslinker (Spectrum). For photoactivation, the samples are spread thinly in droplets on opened lids of Eppendorf tubes and placed on ice at a distance of 5 cm from the UV-A lamp and irradiated for 20 minutes. The unreacted NHS-ester in sulfo-SDA is then quenched with 20 mM Ammonium bicarbonate at room temperature for 20 minutes. The proteins are precipitated with 4X volume of acetone overnight at -20°C and protein pellet is used for mass spectrometry analysis.

The mass spectrometry analysis was performed by Zhuo Chen of Juri Rappsilber lab. The below detailed protocol has been provided by her.

Precipitated protein samples were resolubilized in digestion buffer (8M urea in 100 mM ammonium bicarbonate) to an estimated protein concentration of 1 mg/ml. Dissolved protein sample was reduced by addition of 1M Dithiothreitol (DTT) to a final concentration of 5 mM. The reaction was incubated at room temperature for 30 minutes. The free sulfhydryl groups in the sample were then alkylated by adding 500 mM iodoacetamide (final concentration of 15mM) and incubation at room temperature for 20 minutes in dark. After alkylation,

additional 1M DTT was added (total concentration 10 mM) to quench excess of iodoacetamide. Next, protein samples were digested with LysC (at a 50:1 (m/m) protein to protease ratio) at room temperature for four hours. The sample was then diluted with 100 mM ammonium bicarbonate to reach a urea concentration of 1.5 M. Trypsin was added at a 50:1 (m/m) protein to protease ratio to further digest proteins overnight (~15 hours) at room temperature. Resulting peptides were desalted using C18 StageTips (Rappsilber et al., 2007).

For each sample, resulting peptides were fractionated using size exclusion chromatography in order to enrich for crosslinked peptides (Leitner et al., 2013). Peptides were separated using a Superdex™ 30 Increase 3.2/300 column (GE Healthcare) at a flow rate of 10 ml/minute. The mobile phase consisted of 30% (v/v) acetonitrile and 0.1% trifluoroacetic acid. The earliest six peptide-containing fractions (50 µl each) were collected. Solvent was removed using a vacuum concentrator. The fractions were then analysed by LC-MS/MS.

LC-MS/MS analysis was performed using an Orbitrap Fusion Lumos Tribrid mass spectrometer (Thermo Fisher Scientific), connected to an Ultimate 3000 RSLCnano system (Dionex, Thermo Fisher Scientific). Each size exclusion chromatography (SEC) fraction was resuspended in 1.6% v/v acetonitrile 0.1% v/v formic acid and analysed with LC-MS/MS acquisitions. Each SEC fraction was analyzed with duplicated LC-MS/MS acquisitions. Peptides were injected onto a 50-centimetre EASY-Spray C18 LC column (Thermo Scientific) that is operated at 50 °C column temperature. Mobile phase A consists of water, 0.1% v/v formic acid and mobile phase B consists of 80% v/v acetonitrile and 0.1% v/v formic acid. Peptides were loaded and separated at a flowrate of 0.3 µl/min. Peptides were separated by applying a gradient ranging from 2% to 45% B over 90 minutes. The gradient was optimized for each fraction. Following the separating gradient, the content of B was ramped to 55% and 95% within 2.5 minutes each. Eluted peptides were ionized by an EASY-Spray source (Thermo Scientific) and introduced directly into the mass spectrometer.

The MS data is acquired in the data-dependent mode with the top-speed option. For each three-second acquisition cycle, the full scan mass spectrum was recorded in the Orbitrap with a resolution of 120,000. The ions with a charge state from 3+ to 7+ were isolated and fragmented using higher-energy collisional dissociation (HCD). For each isolated precursor, stepped collision energy (26%, 28% or 30%) was applied. The fragmentation spectra were then recorded in the Orbitrap with a resolution of 50,000. Dynamic exclusion was enabled with single repeat count and 60 second exclusion duration.

MS2 peak lists were generated from the raw mass spectrometric data files using the MSConvert module in ProteoWizard (version 3.0.11729). Precursor and fragment m/z values

were recalibrated. Identification of crosslinked peptides was carried out using xiSEARCH software (https://www.rappsilberlab.org/software/xisearch) (version 1.7.6.4) (PMID 31556486). The peak lists were searched against the sequences and the reversed sequences of x cohesion subunits and Mrc1. The following parameters were applied for the search:

MS accuracy = 3 ppm; MS2 accuracy = 5 ppm

enzyme = trypsin (with full tryptic specificity);

allowed number of missed cleavages = 3

missing monoisotopic peak = 2

cross-linker = SDA (the reaction specificity for SDA was assumed to be for lysine, serine, threonine, tyrosine and protein N termini on the NHS ester end and any amino acids for the diazirine end)

fixed modifications = carbamidomethylation on cysteine

variable modifications = oxidation on methionine

SDA loop link

hydrolyzed SDA on the diazirine end

acetylation on lysine

deamidation on asparagine

phosphorylation on serine

acetone modification on lysine and histidine

maximum variable modification per peptide=2

Identified crosslinked peptide candidates that has at least three matched fragment ions (at least two contains crosslinked residue) in each crosslinked peptide were filtered using xiFDR (ref. PMID: 29256016). A false discovery rate of 1% on residue-pair level was applied with “boost between” option selected.

Table I: Strain List

All strains generated in this study are under W303 background and share the common genotype *ade2-1, can1-100, leu2-3,112, his3-11,15, ura3, trp1, GAL, psi+*

Masashi Minamino (MM) and Celine Bouchoux (CB) generated a few strains that is first being published in this study and they have been credited by their initials in the following table.

Strain list	**Genotype**	**Source**
Y193	*MAT* a *ura3::3XURA3 tetO$_{112}$, his3::HIS3tetR-GFP*	Lab stock
Y3854	*MAT* a *ura3::3XURA3 tetO$_{112}$, his3::HIS3tetR-GFP, tof1Δ::TRP*	Lab stock
Y3855	*MAT* a *ura3::3XURA3 tetO$_{112}$, his3::HIS3tetR-GFP, csm3Δ::TRP*	Lab stock
Y3857	*MAT* a *ura3::3XURA3 tetO$_{112}$, his3::HIS3tetR-GFP, mrc1Δ::TRP*	Lab stock
Y3914	*MAT* a *Smc3-3Pk::HIS, tof1Δ::TRP*	Lab stock
Y3915	*MAT* a *Smc3-3Pk::HIS, csm3Δ::TRP*	Lab stock
Y3914	*MAT* a *Smc3-3Pk::HIS, mrc1Δ::TRP*	Lab stock
Y5762	*MAT* a *ura3::3XURA3 tetO112, his3::HIS3tetR-GFP, tof1Δ::TRP, csm3Δ::LEU*	This study
Y5764	*MAT* a *ura3::3XURA3 tetO112, his3::HIS3tetR-GFP, tof1Δ::TRP, mrc1Δ::LEU*	This study
Y5766	*MAT* a *ura3::3XURA3 tetO112, his3::HIS3tetR-GFP, mrc1Δ::TRP, csm3Δ::LEU*	This study
Y5767	*MAT* a *Smc3-3Pk::HIS, tof1Δ::TRP, mrc1Δ::URA*	This study
Y5768	*MAT* a *Smc3-3Pk::HIS, csm3Δ::TRP, tof1Δ::URA*	This study
Y5769	*MAT* a *Smc3-3Pk::HIS, mrc1Δ::TRP, csm3Δ::URA*	This study
Y6802	*MAT* a *ura3::3XURA3 tetO$_{112}$, his3::HIS3tetR-GFP, rad53-11*	This study
Y6644	*MAT* a *ura3::3XURA3 tetO$_{112}$, his3::HIS3tetR-GFP, mrc1Δ::TRP, mrc1^{AQ}-MYC9::LEU*	This study
Y6805	*MAT* a *ura3::3XURA3 tetO$_{112}$, his3::HIS3tetR-GFP, mrc1ΔC$^{(Δ844-1096)}$-MYC9::TRP*	This study

Y6806	*MAT* a *ura3::3XURA3 tetO$_{112}$, his3::HIS3tetR-GFP, MRC1-MYC$_9$::TRP*	This study
Y5770	*MAT* a *ura3::3XURA3 tetO$_{112}$, his3::HIS3tetR-GFP, sml1Δ::TRP*	This Study
Y1092	*MAT* a *ura3::3XURA3 tetO$_{112}$, his3::HIS3tetR-GFP, sml1Δ::URA3, mec1Δ::TRP*	Lab stock
Y6807	*MAT a ura3::3XURA3 tetO$_{112}$, his3::HIS3tetR-GFP, sml1Δ::TRP, rad53Δ::LEU*	This study
Y5771	*MAT* a *ura3::3XURA3 tetO$_{112}$, his3::HIS3tetR-GFP, tof1Δ::TRP, sml1Δ::LEU*	This study
Y5772	*MAT* a *ura3::3XURA3 tetO$_{112}$, his3::HIS3tetR-GFP, csm3Δ::TRP, sml1Δ::LEU*	This study
Y5773	*MAT* a *ura3::3XURA3 tetO$_{112}$, his3::HIS3tetR-GFP, mrc1Δ::TRP, sml1Δ::LEU*	This study
Y6733	*MAT* a *ura3::3XURA3 tetO$_{112}$, his3::HIS3tetR-GFP, MRC1-FLAG$_3$::NAT*	This study
Y6734	*MAT* a *ura3::3XURA3 tetO$_{112}$, his3::HIS3tetR-GFP, MRC1^{8D}-FLAG$_3$::nat*	This study
Y5611	*MAT* a *pADH1-hENT1-TK::TRP1*	Lab Stock
Y6211	*MAT* a *pADH1-hENT1-TK::TRP1, tof1Δ::LEU*	This study
Y6210	*MAT* a *pADH1-hENT1-TK::TRP1, csm3Δ::LEU*	This study
Y6209	*MAT* a *pADH1-hENT1-TK::TRP1, mrc1Δ::LEU*	This study
Y6104	MAT a *ura3::3XURA3 tetO112, his3::HIS3tetR-GFP, rfa1(G77E)::KAN*	This study
Y6809	MAT a *ura3::3XURA3 tetO112, his3::HIS3tetR-GFP, rfa1(G77E)::KAN*, *tof1Δ::LEU*	This study
Y6810	MAT a *ura3::3XURA3 tetO112, his3::HIS3tetR-GFP, rfa1(G77E)::KAN*, *csm3Δ::LEU*	This study
Y6811	MAT a *ura3::3XURA3 tetO112, his3::HIS3tetR-GFP, rfa1(G77E)::KAN, mrc1Δ::LEU*	This study
Y6808	*MAT* a *ura3::3XURA3 tetO$_{112}$, his3::HIS3tetR-GFP, polε^{Δcat}::TRP*	This study
Y6182	*MAT* a *ura3::3XURA3 tetO$_{112}$, his3::HIS3tetR-GFP, tof1ΔC$^{(Δ982-1238)}$-HA$_3$::TRP*	This study
Y6185	*MAT* a *ura3::3XURA3 tetO$_{112}$, his3::HIS3tetR-GFP, TOF1-HA$_3$::TRP*	This study
Y6732	*MAT* a *ura3::3XURA3 tetO$_{112}$, his3::HIS3tetR-GFP, top1Δ::TRP*	This study
Y6179	*MAT* a *ura3::3XURA3 tetO$_{112}$, his3::HIS3tetR-GFP, tof1$^{(Δ628-1238)}$-HA$_3$::TRP*	This study

Y6180	*MAT* a *ura3::3XURA3 tetO$_{112}$, his3::HIS3tetR-GFP, tof1$^{(\Delta 763\text{-}1238)}$-HA$_3$::TRP*	This study
Y6181	*MAT* a *ura3::3XURA3 tetO$_{112}$, his3::HIS3tetR-GFP, tof1$^{(\Delta 831\text{-}1238)}$-HA$_3$::TRP*	This study
Y5226	*MAT* a *Δpep4::HIS3, Δwpl1::LEU2, Δeco1::KANMX6, GAL4 - SMC1-PK3 + SMC3 + SCC1-3C- ProtA + SCC3-Myc*	Lab Stock
yAE48	MAT a *bar1::Hyg pep4::KanMX ura3::URA3pRS306-CBP-Csm3 + Tof1*	Diffley Lab Stock
yJY32	MAT a *bar1::Hyg pep4::KanMX his3::HIS3pRS303-Mrc1 C-term 2x Flag*	Diffley Lab Stock
Y5562	*MAT* a *Δpep4::HIS3, GAL-Chl1-FLAG-2ProtA,*	This Study (MM)
Y4702	*MAT* a *Δpep4::HIS3, Δwpl1::LEU2, Δeco1::KANMX6, pRSII402-pGAL1 10 Gal4 Smc1-PK-2ProtA Yiplac204-pGAL-SMC3-HA3*	This Study (CB)
Y4702	*MAT* a *Δpep4::HIS3, Δwpl1::LEU2, Δeco1::KANMX6, pRSII402-pGAL1/10-GAL4+Smc1-PK3 Yiplac204-pGAL-SMC3-HA3+SCC1-HIS-HA-3C-2ProtA*	This Study (CB)

Table II: Plasmid List

Plasmids provided by Allison McClure (AM) from Diffley Lab have been credited in Source section.

Plasmid Number	**Genotype**	**Source**
p1395	pBSII-scrfa1(G77E)-KANMX6	This Study
p1942	pRS305-mrc1(AQ)-MYC9	This Study
p2002	pRS40N-Mrc1-3XFlag	Diffley Lab (AM)
p2003	pRS40N-Mrc1(8D)-3XFlag	Diffley Lab (AM)

Table III: Antibody List

Protein detected	**Biological source and clonality**	**Source**	**Dilution**
α-Smc3Ac	mouse monoclonal	gift from Shirahige lab	1 in 500

α-Tubulin	mouse monoclonal	Cell Services Science Technology Platform, The Francis Crick Institute, clone TAT-1	1 in 5000
α-Rad53	rabbit polyclonal	Abcam, ab104232	1 in 2000
α-Rad53	mouse monoclonal	Abcam, ab166859	1 in 2000
α-Myc	mouse monoclonal	Santa Cruz Biotechnology, 9E10	1 in 2000
α-Flag	mouse monolconal	Merck, M2	1 in 2000
α-HA	mouse monoclonal	Merck, 12CA5	1 in 2000
α-HA	rabbit polyclonal	Abcam, ab9110	1 in 2000
α-Sml1	rabbit polyclonal	Antibodies-online GmbH, ABIN3197499	1 in 1000
α-Rfa1	rabbit polyclonal	Antibodies-online GmbH, ABIN4369396	1 in 5000
α-RNR1	rabbit polyclonal	Antibodies-online GmbH, ABIN4966296	1 in 5000
α-CBP	rabbit monoclonal	Merck, clone C16T	1 in 2000
α-CBP	rabbit polyclonal	Merck, 07-482	1 in 2000
α-V5	mouse monoclonal	BioRad, MCA1360, clone Pk	1 in 2000
α-Myc	mouse monoclonal	Santa Cruz Biotechnology, 9B11	1 in 2000

Interesting facts

Here I have compiled a list of qualitatively determined interesting facts that are tangential to my study that I encountered during literature review for this thesis.

- Orthologs of Tof1 in multicellular eukaryotes are called Timeless (*Drosophila melanogaster*), Timeless/ Tim1 (mammals), Tim1 (*Xenopus laevis*), Tim-1 (*Caenorhabditis elegans*). This nomenclature exists because it was first identified in *Caenorhabditis elegans* as a paralog to a protein required for production of circadian rhythms (Myers, Wager-Smith et al. 1996, Chan, Chan et al. 2003).

- *TOF1* is toxic to *Escherichia coli*. (Foss 2001) determined systematically that *Escherichia coli* could not be transformed with a plasmid containing TOF1.

- The ring architecture of Cohesin has led many researchers including this PhD candidate (see page 3) to include references to the rings of power of Lord of the Rings (LoTR) in their publication or review article titles (Peters 2012, Livak and Nussenzweig 2019, Piché, Van Vliet et al. 2019). However, cohesin is not the first ring complex in chromosome biology field with allusions to LoTR. To my knowledge, the first is PCNA (Green 2006) followed by MCM helicase (Deegan and Diffley 2016).

- Mrc1 is considered to be a very flexible non-globular protein that threads through the replisome interacting with many replisome components. Frank (my supervisor) unofficially described Mrc1 as a ribbon that giftwraps the replisome.

- Simian Virus 40 (SV40) T-antigen helicase can directly bind to polymerase alpha for assisting in viral replication in host cells (Smale and Tjian 1986).

- When yeast cells suffer osmotic stress, Mrc1 is phosphorylated by Hog1/MAPK, and this results in decreased Mrc1-Pol2 interaction and Cdc45 loading (Duch, de Nadal et al. 2013)

- Condensin and the SMC 2/4 dimer possess DNA reannealing activity, that is not found in cohesin (Sutani and Yanagida 1997, Sakai, Hizume et al. 2003)

- Several human cancer cell lines overexpress Claspin (Lin, Li et al. 2004)

Science Writing

For my family and friends, whom I do not want to subject to jargon but whom I still want to share my PhD thesis with, I have rewritten my project in metaphors.

Molecular acrobatics

I have been interested in watching Cirque du Soleil for a while now, however, the tickets to the show are just so expensive. I especially want to watch a Contortionist who performs high above the ground on a tightrope. The Contortionist first perches on the tightrope, then she swings hers legs, bends her spine backwards and in a swift motion before she can fall, she grabs her feet with her hands forming a ring around the rope. Her body makes a complete circle and she does not fall off the tightrope. A snapshot of her body contorted in this manner is included in the posters for the performance outside the theatre.

On the poster, I can also see another acrobat skating on the same tightrope. Walking on the tightrope is already so impressive so the Skater must doubtless be talented. In the final act, the Contortionist and Skater perform together. Something phenomenal is performed when the Skater reaches where the Contortionist is encircling the DNA. It is the coolest trick in the Cirque du Soleil show, I can tell because even from outside the theatre where they perform, I can hear the audience cheer. What acrobatic madness must occur! If only I could just see the Contortionist and the Skater perform live on the tightrope!

I prowl the streets outside the theatre gleaning whatever information I can to piece together their performance. I was curious if the Contortionist and the Skater always performed together, or whether they could pull off solo acts. To test this theory, I once tried to kidnap first the Contortionist and then on another day the Skater but they are each such important performers that the entire show got cancelled on both occasions.

On a separate day, I intercepted and stole the food and drink that the Skater consumes before the performance. I wanted to make the Skater tired so that instead of skating speedily on the tightrope, he would be slower. Maybe he needs a certain momentum to perform his tricks? However, even when the Starved Skater was slower on the tightrope, the final act was still just as good. I could tell because the cheer from the audience was not any different on that day.

Then another day I managed to pour wet paint on the Skater's leotard as he was walking into the theatre. I thought if the Skater touches the Contortionist during their performance

some of the paint will also get into the Contortionist's leotard. Illuminatingly, when I watched them leave the theatre after the performance, the Contortionist's leotard had a lot of the wet paint, more so than in the leotard of most other acrobats.

I have been spending all my time sleuthing in this way outside the Cirque du Soleil theatre for the last 4 years. I still don't know exactly what kind of acrobatics is being performed but I am pretty sure now that the Skater and the Contortionist touch during their performance. I have been spilling wet paint on the Skater again and especially paying attention to which parts of Contortionist's body I can see the paint with the hope of reconstructing their acrobatic performance based on these clues.

The above is a dubious metaphor because I have not been prowling the streets of London dedicating all my time on some amateur sleuthing but actually, it is not very far from the truth. This analogy for me really captures the great lengths molecular biologists go to spy into the molecular world. Because the scale at which DNA/proteins and us operate is so different, we do not directly experience the realities of the molecular space.

In my PhD research, I studied what happens to cohesin rings on DNA when the replisome duplicates DNA. Although I took liberties with setting up this scenario in a Cirque du Soleil performance, the main question remains the same. What molecular acrobatics are taking place when the replisome meets cohesin on DNA? Does replisome simply pass inside cohesin's ring? Or does cohesin come off the DNA and back on after replisome's passage? I cannot simply observe replisome and cohesin directly because they are tiny and hidden deep within the pockets of a crowded cell. Like in the Cirque du Soleil metaphor, I have to utilize all sorts of creative clever ways to observe by proxy.

In the case of the acrobats, cheering from the audience was a useful indicator for whether the final act was successful. In my cells, I use the GFP dot assay to determine cohesion of sister chromatids at a specific location of the genome. For the acrobats, the wet paint could help determine where Cohesin was touching Replisome. Not dissimilarly, I am using protein crosslinking mass spectrometry to determine where cohesin and replisome are interacting with each other.

Such are the lengths we go to in lab simply to observe something that is always happening in our cells. The molecular acrobatics of the protein complexes is no less than the acrobatic greatness performed in shows like Cirque du Soleil. Sadly, tickets for molecular acrobatics are just not so readily available.

Intertwining

When dashing cohesin meets the formidable replisome,

their union is inevitably condoned

It is of course an exciting event to witness,

unfortunately hidden away in the microscopic mystery of the nucleus

Tof1, Csm3 and Mrc1 are bridesmaids for this uni-on,

putting them in charge of getting the ring on

And if on the day, topoisomerase1 gets sick and doesn't show,

Tof1 says its fine, we'll still get the sisters intertwined

Mec1 and Rad53 were invited on behalf of the checkpoint

But they're frontline workers fighting crisis, and replied we'll try but don't count on it

Now our replisome is complex, formidable, intricate and incredible

Yet in matters of attraction, she is like any other molecular complex and is easily susceptible

She frets, she stresses, should she run down the aisle or perhaps just walk timidly

Her bridesmaids console her, it's up to you, it's your moment to treasure vividly

How you walk does not matter, just make sure you get the ring on

For it still remains a mystery, what are all the subtle factors that guarantee a uni-on

References

Akai, Y., Y. Kurokawa, N. Nakazawa, Y. Tonami-Murakami, Y. Suzuki, S. H. Yoshimura, H. Iwasaki, Y. Shiroiwa, T. Nakamura and E. Shibata (2011). "Opposing role of condensin hinge against replication protein A in mitosis and interphase through promoting DNA annealing." Open biology **1**(4): 110023.

Alcasabas, A. A., A. J. Osborn, J. Bachant, F. Hu, P. J. Werler, K. Bousset, K. Furuya, J. F. Diffley, A. M. Carr and S. J. Elledge (2001). "Mrc1 transduces signals of DNA replication stress to activate Rad53." Nature cell biology **3**(11): 958-965.

Anderson, D. E., A. Losada, H. P. Erickson and T. Hirano (2002). "Condensin and cohesin display different arm conformations with characteristic hinge angles." The Journal of cell biology **156**(3): 419-424.

Bando, M., Y. Katou, M. Komata, H. Tanaka, T. Itoh, T. Sutani and K. Shirahige (2009). "Csm3, Tof1, and Mrc1 form a heterotrimeric mediator complex that associates with DNA replication forks." Journal of Biological Chemistry **284**(49): 34355-34365.

Barber, T. D., K. McManus, K. W. Yuen, M. Reis, G. Parmigiani, D. Shen, I. Barrett, Y. Nouhi, F. Spencer and S. Markowitz (2008). "Chromatid cohesion defects may underlie chromosome instability in human colorectal cancers." Proceedings of the National Academy of Sciences **105**(9): 3443-3448.

Baretić, D., M. Jenkyn-Bedford, V. Aria, G. Cannone, M. Skehel and J. T. Yeeles (2020). "Cryo-EM structure of the fork protection complex bound to CMG at a replication fork." Molecular cell **78**(5): 926-940. e913.

Baris, Y., M. R. Taylor, V. Aria and J. T. Yeeles (2022). "Fast and efficient DNA replication with purified human proteins." Nature **606**(7912): 204-210.

Barton, R. E., L. F. Massari, D. Robertson and A. L. Marston (2022). "Eco1-dependent cohesin acetylation anchors chromatin loops and cohesion to define functional meiotic chromosome domains." Elife **11**: e74447.

Bastia, D., P. Srivastava, S. Zaman, M. Choudhury, B. K. Mohanty, J. Bacal, L. D. Langston, P. Pasero and M. E. O'Donnell (2016). "Phosphorylation of CMG helicase and Tof1 is required for programmed fork arrest." Proceedings of the National Academy of Sciences **113**(26): E3639-E3648.

Beckouët, F., M. Srinivasan, M. B. Roig, K.-L. Chan, J. C. Scheinost, P. Batty, B. Hu, N. Petela, T. Gligoris and A. C. Smith (2016). "Releasing activity disengages cohesin's Smc3/Scc1 interface in a process blocked by acetylation." Molecular cell **61**(4): 563-574.

Ben-Shahar, T. R., S. Heeger, C. Lehane, P. East, H. Flynn, M. Skehel and F. Uhlmann (2008). "Eco1-dependent cohesin acetylation during establishment of sister chromatid cohesion." Science **321**(5888): 563-566.

Bermejo, R., Y. Doksani, T. Capra, Y.-M. Katou, H. Tanaka, K. Shirahige and M. Foiani (2007). "Top1-and Top2-mediated topological transitions at replication forks ensure fork progression and stability and prevent DNA damage checkpoint activation." Genes & development **21**(15): 1921-1936.

Bernard, P., C. K. Schmidt, S. Vaur, S. Dheur, J. Drogat, S. Genier, K. Ekwall, F. Uhlmann and J. P. Javerzat (2008). "Cell-cycle regulation of cohesin stability along fission yeast chromosomes." The EMBO journal **27**(1): 111-121.

Borges, V., C. Lehane, L. Lopez-Serra, H. Flynn, M. Skehel, T. R. Ben-Shahar and F. Uhlmann (2010). "Hos1 deacetylates Smc3 to close the cohesin acetylation cycle." Molecular cell **39**(5): 677-688.
Borges, V., D. J. Smith, I. Whitehouse and F. Uhlmann (2013). "An Eco1-independent sister chromatid cohesion establishment pathway in S. cerevisiae." Chromosoma **122**(1): 121-134.
Caburet, S., V. A. Arboleda, E. Llano, P. A. Overbeek, J. L. Barbero, K. Oka, W. Harrison, D. Vaiman, Z. Ben-Neriah and I. García-Tuñón (2014). "Mutant cohesin in premature ovarian failure." New England Journal of Medicine **370**(10): 943-949.
Calì, F., S. K. Bharti, R. D. Perna, R. M. Brosh Jr and F. M. Pisani (2016). "Tim/Timeless, a member of the replication fork protection complex, operates with the Warsaw breakage syndrome DNA helicase DDX11 in the same fork recovery pathway." Nucleic acids research **44**(2): 705-717.
Cameron, G., D. Gruszka, S. Xie, K. A. Nasmyth, M. Srinivasan and H. Yardimci (2022). "Sister chromatid cohesion establishment during DNA replication termination." bioRxiv.
Chan, K.-L., M. B. Roig, B. Hu, F. Beckouët, J. Metson and K. Nasmyth (2012). "Cohesin's DNA exit gate is distinct from its entrance gate and is regulated by acetylation." Cell **150**(5): 961-974.
Chan, R. C., A. Chan, M. Jeon, T. F. Wu, D. Pasqualone, A. E. Rougvie and B. J. Meyer (2003). "Chromosome cohesion is regulated by a clock gene paralogue TIM-1." Nature **423**(6943): 1002-1009.
Chao, W. C., Y. Murayama, S. Muñoz, A. W. Jones, B. O. Wade, A. G. Purkiss, X.-W. Hu, A. Borg, A. P. Snijders and F. Uhlmann (2017). "Structure of the cohesin loader Scc2." Nature communications **8**(1): 1-8.
Chao, W. C., B. O. Wade, C. Bouchoux, A. W. Jones, A. G. Purkiss, S. Federico, N. O'Reilly, A. P. Snijders, F. Uhlmann and M. R. Singleton (2017). "Structural basis of Eco1-mediated cohesin acetylation." Scientific reports **7**(1): 1-12.
Chetaille, P., C. Preuss, S. Burkhard, J.-M. Côté, C. Houde, J. Castilloux, J. Piché, N. Gosset, S. Leclerc and F. Wünnemann (2014). "Mutations in SGOL1 cause a novel cohesinopathy affecting heart and gut rhythm." Nature genetics **46**(11): 1245-1249.
Chou, D. M. and S. J. Elledge (2006). "Tipin and Timeless form a mutually protective complex required for genotoxic stress resistance and checkpoint function." Proceedings of the National Academy of Sciences **103**(48): 18143-18147.
Ciosk, R., M. Shirayama, A. Shevchenko, T. Tanaka, A. Toth, A. Shevchenko and K. Nasmyth (2000). "Cohesin's binding to chromosomes depends on a separate complex consisting of Scc2 and Scc4 proteins." Molecular cell **5**(2): 243-254.
Collier, J. E., B.-G. Lee, M. B. Roig, S. Yatskevich, N. J. Petela, J. Metson, M. Voulgaris, A. G. Llamazares, J. Löwe and K. A. Nasmyth (2020). "Transport of DNA within cohesin involves clamping on top of engaged heads by Scc2 and entrapment within the ring by Scc3." Elife **9**: e59560.
Collier, J. E. and K. A. Nasmyth (2022). "DNA passes through cohesin's hinge as well as its Smc3–kleisin interface." Elife **11**: e80310.
Cortone, G., G. Zheng, P. Pensieri, V. Chiappetta, R. Tatè, E. Malacaria, P. Pichierri, H. Yu and F. M. Pisani (2018). "Interaction of the Warsaw breakage syndrome DNA helicase DDX11 with the replication fork-protection factor Timeless promotes sister chromatid cohesion." PLoS genetics **14**(10): e1007622.
Davidson, I. F., B. Bauer, D. Goetz, W. Tang, G. Wutz and J.-M. Peters (2019). "DNA loop extrusion by human cohesin." Science **366**(6471): 1338-1345.

Deegan, T. D. and J. F. Diffley (2016). "MCM: one ring to rule them all." Current opinion in structural biology **37**: 145-151.
Deegan, T. D., P. P. Mukherjee, R. Fujisawa, C. P. Rivera and K. Labib (2020). "CMG helicase disassembly is controlled by replication fork DNA, replisome components and a ubiquitin threshold." Elife **9**: e60371.
Delamarre, A., A. Barthe, C. de la Roche Saint-André, P. Luciano, R. Forey, I. Padioleau, M. Skrzypczak, K. Ginalski, V. Géli and P. Pasero (2020). "MRX increases chromatin accessibility at stalled replication forks to promote nascent DNA resection and cohesin loading." Molecular cell **77**(2): 395-410. e393.
Dequeker, B. J., M. J. Scherr, H. B. Brandão, J. Gassler, S. Powell, I. Gaspar, I. M. Flyamer, A. Lalic, W. Tang and R. Stocsits (2022). "MCM complexes are barriers that restrict cohesin-mediated loop extrusion." Nature **606**(7912): 197-203.
Devbhandari, S. and D. Remus (2020). "Rad53 limits CMG helicase uncoupling from DNA synthesis at replication forks." Nature Structural & Molecular Biology **27**(5): 461-471.
Duch, A., E. de Nadal and F. Posas (2013). "Dealing with transcriptional outbursts during S phase to protect genomic integrity." Journal of molecular biology **425**(23): 4745-4755.
Edwards, S., C. M. Li, D. L. Levy, J. Brown, P. M. Snow and J. L. Campbell (2003). "Saccharomyces cerevisiae DNA polymerase ε and polymerase σ interact physically and functionally, suggesting a role for polymerase ε in sister chromatid cohesion." Molecular and cellular biology **23**(8): 2733-2748.
Errico, A., C. Cosentino, T. Rivera, A. Losada, E. Schwob, T. Hunt and V. Costanzo (2009). "Tipin/Tim1/And1 protein complex promotes Polα chromatin binding and sister chromatid cohesion." The EMBO journal **28**(23): 3681-3692.
Feytout, A., S. Vaur, S. Genier, S. Vazquez and J.-P. Javerzat (2011). "Psm3 acetylation on conserved lysine residues is dispensable for viability in fission yeast but contributes to Eso1-mediated sister chromatid cohesion by antagonizing Wpl1." Molecular and Cellular Biology **31**(8): 1771-1786.
Forey, R., A. Poveda, S. Sharma, A. Barthe, I. Padioleau, C. Renard, R. Lambert, M. Skrzypczak, K. Ginalski and A. Lengronne (2020). "Mec1 is activated at the onset of normal S phase by low-dNTP pools impeding DNA replication." Molecular cell **78**(3): 396-410. e394.
Foss, E. J. (2001). "Tof1p regulates DNA damage responses during S phase in Saccharomyces cerevisiae." Genetics **157**(2): 567-577.
Gambus, A., R. C. Jones, A. Sanchez-Diaz, M. Kanemaki, F. Van Deursen, R. D. Edmondson and K. Labib (2006). "GINS maintains association of Cdc45 with MCM in replisome progression complexes at eukaryotic DNA replication forks." Nature cell biology **8**(4): 358-366.
Gan, H., C. Yu, S. Devbhandari, S. Sharma, J. Han, A. Chabes, D. Remus and Z. Zhang (2017). "Checkpoint kinase Rad53 couples leading-and lagging-strand DNA synthesis under replication stress." Molecular cell **68**(2): 446-455. e443.
Gellon, L., S. Kaushal, J. Cebrián, M. Lahiri, S. M. Mirkin and C. H. Freudenreich (2019). "Mrc1 and Tof1 prevent fragility and instability at long CAG repeats by their fork stabilizing function." Nucleic Acids Research **47**(2): 794-805.
Gerlich, D., B. Koch, F. Dupeux, J.-M. Peters and J. Ellenberg (2006). "Live-cell imaging reveals a stable cohesin-chromatin interaction after but not before DNA replication." Current Biology **16**(15): 1571-1578.
Ghosh, S., J. M. Gardner, C. J. Smoyer, J. M. Friederichs, J. R. Unruh, B. D. Slaughter, R. Alexander, R. D. Chisholm, K. K. Lee and J. L. Workman (2012). "Acetylation of the SUN

protein Mps3 by Eco1 regulates its function in nuclear organization." Molecular biology of the cell **23**(13): 2546-2559.
Gottifredi, V. and C. Prives (2005). The S phase checkpoint: when the crowd meets at the fork. Seminars in cell & developmental biology, Elsevier.
Green, C. M. (2006). "One ring to rule them all? Another cellular responsibility for PCNA." Trends in molecular medicine **12**(10): 455-458.
Gruber, S., P. Arumugam, Y. Katou, D. Kuglitsch, W. Helmhart, K. Shirahige and K. Nasmyth (2006). "Evidence that loading of cohesin onto chromosomes involves opening of its SMC hinge." Cell **127**(3): 523-537.
Guacci, V., E. Hogan and D. Koshland (1994). "Chromosome condensation and sister chromatid pairing in budding yeast." The Journal of cell biology **125**(3): 517-530.
Haering, C. H., J. Löwe, A. Hochwagen and K. Nasmyth (2002). "Molecular architecture of SMC proteins and the yeast cohesin complex." Molecular cell **9**(4): 773-788.
Hamdan, S. M. and C. C. Richardson (2009). "Motors, switches, and contacts in the replisome." Annual review of biochemistry **78**: 205.
Hanna, J. S., E. S. Kroll, V. Lundblad and F. A. Spencer (2001). "Saccharomyces cerevisiae CTF18 and CTF4 are required for sister chromatid cohesion." Molecular and cellular biology **21**(9): 3144-3158.
Hara, K., G. Zheng, Q. Qu, H. Liu, Z. Ouyang, Z. Chen, D. R. Tomchick and H. Yu (2014). "Structure of cohesin subcomplex pinpoints direct shugoshin-Wapl antagonism in centromeric cohesion." Nature structural & molecular biology **21**(10): 864-870.
Heidinger-Pauli, J. M., E. Ünal, V. Guacci and D. Koshland (2008). "The kleisin subunit of cohesin dictates damage-induced cohesion." Molecular cell **31**(1): 47-56.
Higashi, T. L., P. Eickhoff, J. S. Sousa, J. Locke, A. Nans, H. R. Flynn, A. P. Snijders, G. Papageorgiou, N. O'reilly and Z. A. Chen (2020). "A structure-based mechanism for DNA entry into the cohesin ring." Molecular cell **79**(6): 917-933. e919.
Hodgson, B., A. Calzada and K. Labib (2007). "Mrc1 and Tof1 regulate DNA replication forks in different ways during normal S phase." Molecular biology of the cell **18**(10): 3894-3902.
Hou, F. and H. Zou (2005). "Two human orthologues of Eco1/Ctf7 acetyltransferases are both required for proper sister-chromatid cohesion." Molecular biology of the cell **16**(8): 3908-3918.
Hu, B., N. Petela, A. Kurze, K.-L. Chan, C. Chapard and K. Nasmyth (2015). "Biological chromodynamics: a general method for measuring protein occupancy across the genome by calibrating ChIP-seq." Nucleic acids research **43**(20): e132-e132.
Ivanov, D. and K. Nasmyth (2005). "A topological interaction between cohesin rings and a circular minichromosome." Cell **122**(6): 849-860.
Ivanov, D., A. Schleiffer, F. Eisenhaber, K. Mechtler, C. H. Haering and K. Nasmyth (2002). "Eco1 is a novel acetyltransferase that can acetylate proteins involved in cohesion." Current biology **12**(4): 323-328.
Ivanov, M. P., R. Ladurner, I. Poser, R. Beveridge, E. Rampler, O. Hudecz, M. Novatchkova, J. K. Hériché, G. Wutz and P. van der Lelij (2018). "The replicative helicase MCM recruits cohesin acetyltransferase ESCO2 to mediate centromeric sister chromatid cohesion." The EMBO journal **37**(15): e97150.
Jones, M. L., Y. Baris, M. R. Taylor and J. T. Yeeles (2021). "Structure of a human replisome shows the organisation and interactions of a DNA replication machine." The EMBO journal **40**(23): e108819.

Kanke, M., E. Tahara, P. J. Huis in't Veld and T. Nishiyama (2016). "Cohesin acetylation and Wapl-Pds5 oppositely regulate translocation of cohesin along DNA." The EMBO journal **35**(24): 2686-2698.
Katou, Y., Y. Kanoh, M. Bando, H. Noguchi, H. Tanaka, T. Ashikari, K. Sugimoto and K. Shirahige (2003). "S-phase checkpoint proteins Tof1 and Mrc1 form a stable replication-pausing complex." Nature **424**(6952): 1078-1083.
Kikuchi, S., D. M. Borek, Z. Otwinowski, D. R. Tomchick and H. Yu (2016). "Crystal structure of the cohesin loader Scc2 and insight into cohesinopathy." Proceedings of the National Academy of Sciences **113**(44): 12444-12449.
Kline, A. D., I. D. Krantz, A. Sommer, M. Kliewer, L. G. Jackson, D. R. FitzPatrick, A. V. Levin and A. Selicorni (2007). "Cornelia de Lange syndrome: clinical review, diagnostic and scoring systems, and anticipatory guidance." American journal of medical genetics part A **143**(12): 1287-1296.
Kline, A. D., J. F. Moss, A. Selicorni, A.-M. Bisgaard, M. A. Deardorff, P. M. Gillett, S. L. Ishman, L. M. Kerr, A. V. Levin and P. A. Mulder (2018). "Diagnosis and management of Cornelia de Lange syndrome: first international consensus statement." Nature Reviews Genetics **19**(10): 649-666.
Kobayashi, T. (2003). "The replication fork barrier site forms a unique structure with Fob1p and inhibits the replication fork." Molecular and cellular biology **23**(24): 9178-9188.
Koren, A., I. Soifer and N. Barkai (2010). "MRC1-dependent scaling of the budding yeast DNA replication timing program." Genome research **20**(6): 781-790.
Kupiec, M. (2016). "Alternative clamp loaders/unloaders." FEMS yeast research **16**(7).
Lammens, A., A. Schele and K.-P. Hopfner (2004). "Structural biochemistry of ATP-driven dimerization and DNA-stimulated activation of SMC ATPases." Current Biology **14**(19): 1778-1782.
Larcher, M. V. and P. Pasero (2020). "Top1 and Top2 promote replication fork arrest at a programmed pause site." Genes & Development **34**(1-2): 1-3.
Lee, B.-G., M. B. Roig, M. Jansma, N. Petela, J. Metson, K. Nasmyth and J. Löwe (2016). "Crystal structure of the cohesin gatekeeper Pds5 and in complex with kleisin Scc1." Cell reports **14**(9): 2108-2115.
Leman, A. R., C. Noguchi, C. Y. Lee and E. Noguchi (2010). "Human Timeless and Tipin stabilize replication forks and facilitate sister-chromatid cohesion." Journal of cell science **123**(5): 660-670.
Lengronne, A., Y. Katou, S. Mori, S. Yokobayashi, G. P. Kelly, T. Itoh, Y. Watanabe, K. Shirahige and F. Uhlmann (2004). "Cohesin relocation from sites of chromosomal loading to places of convergent transcription." Nature **430**(6999): 573-578.
Lengronne, A., J. McIntyre, Y. Katou, Y. Kanoh, K.-P. Hopfner, K. Shirahige and F. Uhlmann (2006). "Establishment of sister chromatid cohesion at the S. cerevisiae replication fork." Molecular cell **23**(6): 787-799.
Lerner, L. K., S. Holzer, M. L. Kilkenny, S. Šviković, P. Murat, D. Schiavone, C. B. Eldridge, A. Bittleston, J. D. Maman and D. Branzei (2020). "Timeless couples G-quadruplex detection with processing by DDX 11 helicase during DNA replication." The EMBO journal **39**(18): e104185.
Lewis, J. S., L. M. Spenkelink, G. D. Schauer, F. R. Hill, R. E. Georgescu, M. E. O'Donnell and A. M. van Oijen (2017). "Single-molecule visualization of Saccharomyces cerevisiae leading-strand synthesis reveals dynamic interaction between MTC and the replisome." Proceedings of the National Academy of Sciences **114**(40): 10630-10635.

Li, Y., K. W. Muir, M. W. Bowler, J. Metz, C. H. Haering and D. Panne (2018). "Structural basis for Scc3-dependent cohesin recruitment to chromatin." Elife **7**: e38356.
Lin, D. C.-H. and A. D. Grossman (1998). "Identification and characterization of a bacterial chromosome partitioning site." Cell **92**(5): 675-685.
Lin, S.-Y., K. Li, G. S. Stewart and S. J. Elledge (2004). "Human Claspin works with BRCA1 to both positively and negatively regulate cell proliferation." Proceedings of the National Academy of Sciences **101**(17): 6484-6489.
Liu, H. W. (2019). "Cohesion establishment by yeast Replication Factor C (RFC) complexes."
Liu, H. W., C. Bouchoux, M. Panarotto, Y. Kakui, H. Patel and F. Uhlmann (2020). "Division of labor between PCNA loaders in DNA replication and sister chromatid cohesion establishment." Molecular cell **78**(4): 725-738. e724.
Livak, F. and A. Nussenzweig (2019). One ring to rule them all, Nature Publishing Group.
Lopez-Serra, L., G. Kelly, H. Patel, A. Stewart and F. Uhlmann (2014). "The Scc2–Scc4 complex acts in sister chromatid cohesion and transcriptional regulation by maintaining nucleosome-free regions." Nature genetics **46**(10): 1147-1151.
Lopez-Serra, L., A. Lengronne, V. Borges, G. Kelly and F. Uhlmann (2013). "Budding yeast Wapl controls sister chromatid cohesion maintenance and chromosome condensation." Current Biology **23**(1): 64-69.
Losada, A. and T. Hirano (2005). "Dynamic molecular linkers of the genome: the first decade of SMC proteins." Genes & development **19**(11): 1269-1287.
Lou, H., M. Komata, Y. Katou, Z. Guan, C. C. Reis, M. Budd, K. Shirahige and J. L. Campbell (2008). "Mrc1 and DNA polymerase ε function together in linking DNA replication and the S phase checkpoint." Molecular cell **32**(1): 106-117.
Mayer, M. L., S. P. Gygi, R. Aebersold and P. Hieter (2001). "Identification of RFC (Ctf18p, Ctf8p, Dcc1p): an alternative RFC complex required for sister chromatid cohesion in S. cerevisiae." Molecular cell **7**(5): 959-970.
Mayer, M. L., I. Pot, M. Chang, H. Xu, V. Aneliunas, T. Kwok, R. Newitt, R. Aebersold, C. Boone and G. W. Brown (2004). "Identification of protein complexes required for efficient sister chromatid cohesion." Molecular biology of the cell **15**(4): 1736-1745.
McClure, A. W. and J. F. Diffley (2021). "Rad53 checkpoint kinase regulation of DNA replication fork rate via Mrc1 phosphorylation." Elife **10**: e69726.
Melby, T. E., C. N. Ciampaglio, G. Briscoe and H. P. Erickson (1998). "The symmetrical structure of structural maintenance of chromosomes (SMC) and MukB proteins: long, antiparallel coiled coils, folded at a flexible hinge." The Journal of cell biology **142**(6): 1595-1604.
Mfarej, M. G. and R. V. Skibbens (2020). "An ever-changing landscape in Roberts syndrome biology: Implications for macromolecular damage." PLoS Genetics **16**(12): e1009219.
Michaelis, C., R. Ciosk and K. Nasmyth (1997). "Cohesins: chromosomal proteins that prevent premature separation of sister chromatids." Cell **91**(1): 35-45.
Minamino, M., T. L. Higashi, C. Bouchoux and F. Uhlmann (2018). "Topological in vitro loading of the budding yeast cohesin ring onto DNA." Life science alliance **1**(5).
Minamino, M., L. Negishi, M. T. Kanemaki, A. Yoshimura, T. Sutani, M. Bando and K. Shirahige (2018). "Temporal regulation of ESCO2 degradation by the MCM complex, the CUL4-DDB1-VPRBP complex, and the anaphase-promoting complex." Current Biology **28**(16): 2665-2672. e2665.

Mohanty, B. K., N. K. Bairwa and D. Bastia (2006). "The Tof1p–Csm3p protein complex counteracts the Rrm3p helicase to control replication termination of Saccharomyces cerevisiae." Proceedings of the National Academy of Sciences **103**(4): 897-902.
Moldovan, G.-L., B. Pfander and S. Jentsch (2006). "PCNA controls establishment of sister chromatid cohesion during S phase." Molecular cell **23**(5): 723-732.
Moreno, S. P. and A. Gambus (2020). "Mechanisms of eukaryotic replisome disassembly." Biochemical Society Transactions **48**(3): 823-836.
Muñoz, S., M. Minamino, C. S. Casas-Delucchi, H. Patel and F. Uhlmann (2019). "A role for chromatin remodeling in cohesin loading onto chromosomes." Molecular cell **74**(4): 664-673. e665.
Murayama, Y., C. P. Samora, Y. Kurokawa, H. Iwasaki and F. Uhlmann (2018). "Establishment of DNA-DNA interactions by the cohesin ring." Cell **172**(3): 465-477. e415.
Murayama, Y. and F. Uhlmann (2014). "Biochemical reconstitution of topological DNA binding by the cohesin ring." Nature **505**(7483): 367-371.
Murayama, Y. and F. Uhlmann (2015). "DNA entry into and exit out of the cohesin ring by an interlocking gate mechanism." Cell **163**(7): 1628-1640.
Myers, M. P., K. Wager-Smith, A. Rothenfluh-Hilfiker and M. W. Young (1996). "Light-induced degradation of TIMELESS and entrainment of the Drosophila circadian clock." Science **271**(5256): 1736-1740.
Nasmyth, K. and C. H. Haering (2009). "Cohesin: its roles and mechanisms." Annual review of genetics **43**: 525-558.
Nasmyth, K., J.-M. Peters and F. Uhlmann (2000). "Splitting the chromosome: cutting the ties that bind sister chromatids." Science **288**(5470): 1379-1384.
Nedelcheva, M. N., A. Roguev, L. B. Dolapchiev, A. Shevchenko, H. B. Taskov, A. Shevchenko, A. F. Stewart and S. S. Stoynov (2005). "Uncoupling of unwinding from DNA synthesis implies regulation of MCM helicase by Tof1/Mrc1/Csm3 checkpoint complex." Journal of molecular biology **347**(3): 509-521.
Nguyen, V. Q., C. Co and J. J. Li (2001). "Cyclin-dependent kinases prevent DNA re-replication through multiple mechanisms." Nature **411**(6841): 1068-1073.
Nicklas, R. B. (1983). "Measurements of the force produced by the mitotic spindle in anaphase." The Journal of cell biology **97**(2): 542-548.
Ocampo-Hafalla, M., S. Muñoz, C. P. Samora and F. Uhlmann (2016). "Evidence for cohesin sliding along budding yeast chromosomes." Open biology **6**(6): 150178.
Osborn, A. J. and S. J. Elledge (2003). "Mrc1 is a replication fork component whose phosphorylation in response to DNA replication stress activates Rad53." Genes & development **17**(14): 1755-1767.
Pardo, B., L. Crabbé and P. Pasero (2017). "Signaling pathways of replication stress in yeast." FEMS yeast research **17**(2): fow101.
Parenti, I. and F. J. Kaiser (2021). "Cornelia de Lange Syndrome as paradigm of chromatinopathies." Frontiers in Neuroscience **15**: 774950.
Park, H. and R. Sternglanz (1999). "Identification and characterization of the genes for two topoisomerase I-interacting proteins from Saccharomyces cerevisiae." Yeast **15**(1): 35-41.
Pasero, P., A. Bensimon and E. Schwob (2002). "Single-molecule analysis reveals clustering and epigenetic regulation of replication origins at the yeast rDNA locus." Genes & development **16**(19): 2479-2484.

Petela, N. J., T. G. Gligoris, J. Metson, B.-G. Lee, M. Voulgaris, B. Hu, S. Kikuchi, C. Chapard, W. Chen and E. Rajendra (2018). "Scc2 is a potent activator of cohesin's ATPase that promotes loading by binding Scc1 without Pds5." Molecular cell **70**(6): 1134-1148. e1137.
Petermann, E., T. Helleday and K. W. Caldecott (2008). "Claspin promotes normal replication fork rates in human cells." Molecular biology of the cell **19**(6): 2373-2378.
Peters, J. M. (2012). "The many functions of cohesin—different rings to rule them all?" The EMBO journal **31**(9): 2061-2063.
Piché, J., P. P. Van Vliet, M. Pucéat and G. Andelfinger (2019). "The expanding phenotypes of cohesinopathies: one ring to rule them all!" Cell Cycle **18**(21): 2828-2848.
Pisani, F. M. (2019). "Spotlight on Warsaw breakage syndrome." The Application of Clinical Genetics **12**: 239.
Poli, J., O. Tsaponina, L. Crabbé, A. Keszthelyi, V. Pantesco, A. Chabes, A. Lengronne and P. Pasero (2012). "dNTP pools determine fork progression and origin usage under replication stress." The EMBO journal **31**(4): 883-894.
Pradhan, B., R. Barth, E. Kim, I. F. Davidson, B. Bauer, T. van Laar, W. Yang, J.-K. Ryu, J. van der Torre and J.-M. Peters (2022). "SMC complexes can traverse physical roadblocks bigger than their ring size." Cell Reports **41**(3): 111491.
Rao, S. S., S.-C. Huang, B. G. St Hilaire, J. M. Engreitz, E. M. Perez, K.-R. Kieffer-Kwon, A. L. Sanborn, S. E. Johnstone, G. D. Bascom and I. D. Bochkov (2017). "Cohesin loss eliminates all loop domains." Cell **171**(2): 305-320. e324.
Razidlo, D. F. and R. S. Lahue (2008). "Mrc1, Tof1 and Csm3 inhibit CAG· CTG repeat instability by at least two mechanisms." DNA repair **7**(4): 633-640.
Remus, D. and J. F. Diffley (2009). "Eukaryotic DNA replication control: lock and load, then fire." Current opinion in cell biology **21**(6): 771-777.
Rocquain, J., V. Gelsi-Boyer, J. Adélaïde, A. Murati, N. Carbuccia, N. Vey, D. Birnbaum, M.-J. Mozziconacci and M. Chaffanet (2010). "Alteration of cohesin genes in myeloid diseases." American journal of hematology **85**(9): 717-719.
Safaric, B., E. Chacin, M. J. Scherr, L. Rajappa, C. Gebhardt, C. F. Kurat, T. Cordes and K. E. Duderstadt (2022). "The fork protection complex recruits FACT to reorganize nucleosomes during replication." Nucleic acids research **50**(3): 1317-1334.
Sakai, A., K. Hizume, T. Sutani, K. Takeyasu and M. Yanagida (2003). "Condensin but not cohesin SMC heterodimer induces DNA reannealing through protein–protein assembly." The EMBO Journal **22**(11): 2764-2775.
Samora, C. P., J. Saksouk, P. Goswami, B. O. Wade, M. R. Singleton, P. A. Bates, A. Lengronne, A. Costa and F. Uhlmann (2016). "Ctf4 links DNA replication with sister chromatid cohesion establishment by recruiting the Chl1 helicase to the replisome." Molecular cell **63**(3): 371-384.
Schleiffer, A., S. Kaitna, S. Maurer-Stroh, M. Glotzer, K. Nasmyth and F. Eisenhaber (2003). "Kleisins: a superfamily of bacterial and eukaryotic SMC protein partners." Molecular cell **11**(3): 571-575.
Selig, S., K. Okumura, D. Ward and H. Cedar (1992). "Delineation of DNA replication time zones by fluorescence in situ hybridization." The EMBO journal **11**(3): 1217-1225.
Shi, Z., H. Gao, X.-c. Bai and H. Yu (2020). "Cryo-EM structure of the human cohesin-NIPBL-DNA complex." Science **368**(6498): 1454-1459.
Shimada, K., P. Pasero and S. M. Gasser (2002). "ORC and the intra-S-phase checkpoint: a threshold regulates Rad53p activation in S phase." Genes & development **16**(24): 3236-3252.

Shyian, M., B. Albert, A. M. Zupan, V. Ivanitsa, G. Charbonnet, D. Dilg and D. Shore (2020). "Fork pausing complex engages topoisomerases at the replisome." Genes & development **34**(1-2): 87-98.
Simon, A. C., J. C. Zhou, R. L. Perera, F. van Deursen, C. Evrin, M. E. Ivanova, M. L. Kilkenny, L. Renault, S. Kjaer and D. Matak-Vinković (2014). "A Ctf4 trimer couples the CMG helicase to DNA polymerase α in the eukaryotic replisome." Nature **510**(7504): 293-297.
Skibbens, R. V. (2009). "Establishment of sister chromatid cohesion." Current Biology **19**(24): R1126-R1132.
Skibbens, R. V., L. B. Corson, D. Koshland and P. Hieter (1999). "Ctf7p is essential for sister chromatid cohesion and links mitotic chromosome structure to the DNA replication machinery." Genes & development **13**(3): 307-319.
Smale, S. and R. Tjian (1986). "Inhibition of simian virus 40 DNA replication by specific modification of T-antigen with oxidized ATP." Journal of Biological Chemistry **261**(31): 14369-14372.
Solomon, D. A., J.-S. Kim and T. Waldman (2014). "Cohesin gene mutations in tumorigenesis: from discovery to clinical significance." BMB reports **47**(6): 299.
Spencer, F., S. Gerring, C. Connelly and P. Hieter (1990). "Mitotic chromosome transmission fidelity mutants in Saccharomyces cerevisiae." Genetics **124**(2): 237-249.
Srinivasan, M., M. Fumasoni, N. J. Petela, A. Murray and K. A. Nasmyth (2020). "Cohesion is established during DNA replication utilising chromosome associated cohesin rings as well as those loaded de novo onto nascent DNAs." Elife **9**: e56611.
Srinivasan, M., J. C. Scheinost, N. J. Petela, T. G. Gligoris, M. Wissler, S. Ogushi, J. E. Collier, M. Voulgaris, A. Kurze and K.-L. Chan (2018). "The cohesin ring uses its hinge to organize DNA using non-topological as well as topological mechanisms." Cell **173**(6): 1508-1519. e1518.
Stigler, J., G. Ö. Çamdere, D. E. Koshland and E. C. Greene (2016). "Single-molecule imaging reveals a collapsed conformational state for DNA-bound cohesin." Cell reports **15**(5): 988-998.
Straight, A. F., A. S. Belmont, C. C. Robinett and A. W. Murray (1996). "GFP tagging of budding yeast chromosomes reveals that protein–protein interactions can mediate sister chromatid cohesion." Current Biology **6**(12): 1599-1608.
Ström, L., H. B. Lindroos, K. Shirahige and C. Sjögren (2004). "Postreplicative recruitment of cohesin to double-strand breaks is required for DNA repair." Molecular cell **16**(6): 1003-1015.
Sutani, T., T. Kawaguchi, R. Kanno, T. Itoh and K. Shirahige (2009). "Budding yeast Wpl1 (Rad61)-Pds5 complex counteracts sister chromatid cohesion-establishing reaction." Current Biology **19**(6): 492-497.
Sutani, T. and M. Yanagida (1997). "DNA renaturation activity of the SMC complex implicated in chromosome condensation." Nature **388**(6644): 798-801.
Szyjka, S. J., C. J. Viggiani and O. M. Aparicio (2005). "Mrc1 is required for normal progression of replication forks throughout chromatin in S. cerevisiae." Molecular cell **19**(5): 691-697.
Tanaka, H., Y. Kubota, T. Tsujimura, M. Kumano, H. Masai and H. Takisawa (2009). "Replisome progression complex links DNA replication to sister chromatid cohesion in Xenopus egg extracts." Genes to cells **14**(8): 949-963.
Tanaka, K. and P. Russell (2001). "Mrc1 channels the DNA replication arrest signal to checkpoint kinase Cds1." Nature cell biology **3**(11): 966-972.

Theulot, B., L. Lacroix, J.-M. Arbona, G. A. Millot, E. Jean, C. Cruaud, J. Pellet, F. Proux, M. Hennion and S. Engelen (2022). "Genome-wide mapping of individual replication fork velocities using nanopore sequencing." Nature Communications **13**(1): 1-14.
Tóth, A., R. Ciosk, F. Uhlmann, M. Galova, A. Schleiffer and K. Nasmyth (1999). "Yeast cohesin complex requires a conserved protein, Eco1p (Ctf7), to establish cohesion between sister chromatids during DNA replication." Genes & development **13**(3): 320-333.
Tourrière, H., G. Versini, V. Cordón-Preciado, C. Alabert and P. Pasero (2005). "Mrc1 and Tof1 promote replication fork progression and recovery independently of Rad53." Molecular cell **19**(5): 699-706.
Tsai, F.-L., S. Vijayraghavan, J. Prinz, H. K. MacAlpine, D. M. MacAlpine and A. Schwacha (2015). "Mcm2-7 is an active player in the DNA replication checkpoint signaling cascade via proposed modulation of its DNA gate." Molecular and cellular biology **35**(12): 2131-2143.
Uhlmann, F. (2009). "A matter of choice: the establishment of sister chromatid cohesion." EMBO reports **10**(10): 1095-1102.
Uhlmann, F. (2016). "SMC complexes: from DNA to chromosomes." Nature reviews Molecular cell biology **17**(7): 399-412.
Uhlmann, F., F. Lottspeich and K. Nasmyth (1999). "Sister-chromatid separation at anaphase onset is promoted by cleavage of the cohesin subunit Scc1." Nature **400**(6739): 37-42.
Uhlmann, F. and K. Nasmyth (1998). "Cohesion between sister chromatids must be established during DNA replication." Current Biology **8**(20): 1095-1102.
Ünal, E. i., J. M. Heidinger-Pauli, W. Kim, V. Guacci, I. Onn, S. P. Gygi and D. E. Koshland (2008). "A molecular determinant for the establishment of sister chromatid cohesion." Science **321**(5888): 566-569.
van der Lelij, P., K. H. Chrzanowska, B. C. Godthelp, M. A. Rooimans, A. B. Oostra, M. Stumm, M. Z. Zdzienicka, H. Joenje and J. P. de Winter (2010). "Warsaw breakage syndrome, a cohesinopathy associated with mutations in the XPD helicase family member DDX11/ChlR1." The American Journal of Human Genetics **86**(2): 262-266.
Villa, F., A. C. Simon, M. A. O. Bazan, M. L. Kilkenny, D. Wirthensohn, M. Wightman, D. Matak-Vinkovíc, L. Pellegrini and K. Labib (2016). "Ctf4 is a hub in the eukaryotic replisome that links multiple CIP-box proteins to the CMG helicase." Molecular cell **63**(3): 385-396.
Warren, C. D., D. M. Eckley, M. S. Lee, J. S. Hanna, A. Hughes, B. Peyser, C. Jie, R. Irizarry and F. A. Spencer (2004). "S-phase checkpoint genes safeguard high-fidelity sister chromatid cohesion." Molecular biology of the cell **15**(4): 1724-1735.
Westhorpe, R., A. Keszthelyi, N. E. Minchell, D. Jones and J. Baxter (2020). "Separable functions of Tof1/Timeless in intra-S-checkpoint signalling, replisome stability and DNA topological stress." Nucleic acids research **48**(21): 12169-12187.
Xia, Y., R. Fujisawa, T. D. Deegan, R. Sonneville and K. P. Labib (2021). "TIMELESS-TIPIN and UBXN-3 promote replisome disassembly during DNA replication termination in Caenorhabditis elegans." The EMBO journal **40**(17): e108053.
Xu, H., C. Boone and G. W. Brown (2007). "Genetic dissection of parallel sister-chromatid cohesion pathways." Genetics **176**(3): 1417-1429.
Xu, H., C. Boone and H. L. Klein (2004). "Mrc1 is required for sister chromatid cohesion to aid in recombination repair of spontaneous damage." Molecular and cellular biology **24**(16): 7082-7090.
Yao, N., J. Turner, Z. Kelman, P. T. Stukenberg, F. Dean, D. Shechter, Z. Q. Pan, J. Hurwitz and M. O'Donnell (1996). "Clamp loading, unloading and intrinsic stability of the PCNA, β and gp45 sliding clamps of human, E. coli and T4 replicases." Genes to Cells **1**(1): 101-113.

Yeeles, J. T., T. D. Deegan, A. Janska, A. Early and J. F. Diffley (2015). "Regulated eukaryotic DNA replication origin firing with purified proteins." Nature **519**(7544): 431-435.
Yeeles, J. T., A. Janska, A. Early and J. F. Diffley (2017). "How the eukaryotic replisome achieves rapid and efficient DNA replication." Molecular cell **65**(1): 105-116.
Yoshimura, A., T. Sutani and K. Shirahige (2021). "Functional control of Eco1 through the MCM complex in sister chromatid cohesion." Gene **784**: 145584.
Yoshinaga, M. and Y. Inagaki (2021). "Ubiquity and origins of structural maintenance of chromosomes (SMC) proteins in eukaryotes." Genome Biology and Evolution **13**(12): evab256.
Yoshizawa-Sugata, N. and H. Masai (2009). "Roles of human AND-1 in chromosome transactions in S phase." Journal of Biological Chemistry **284**(31): 20718-20728.
Yu, C., H. Gan, J. Han, Z.-X. Zhou, S. Jia, A. Chabes, G. Farrugia, T. Ordog and Z. Zhang (2014). "Strand-specific analysis shows protein binding at replication forks and PCNA unloading from lagging strands when forks stall." Molecular cell **56**(4): 551-563.
Yurieva, O. and M. O'Donnell (2016). "Reconstitution of a eukaryotic replisome reveals the mechanism of asymmetric distribution of DNA polymerases." Nucleus **7**(4): 360-368.
Zhang, J., D. Shi, X. Li, L. Ding, J. Tang, C. Liu, K. Shirahige, Q. Cao and H. Lou (2017). "Rtt101-Mms1-Mms22 coordinates replication-coupled sister chromatid cohesion and nucleosome assembly." EMBO reports **18**(8): 1294-1305.
Zhang, J., X. Shi, Y. Li, B.-J. Kim, J. Jia, Z. Huang, T. Yang, X. Fu, S. Y. Jung and Y. Wang (2008). "Acetylation of Smc3 by Eco1 is required for S phase sister chromatid cohesion in both human and yeast." Molecular cell **31**(1): 143-151.
Zhang, N., S. G. Kuznetsov, S. K. Sharan, K. Li, P. H. Rao and D. Pati (2008). "A handcuff model for the cohesin complex." The Journal of cell biology **183**(6): 1019-1031.
Zhao, X., E. G. Muller and R. Rothstein (1998). "A suppressor of two essential checkpoint genes identifies a novel protein that negatively affects dNTP pools." Molecular cell **2**(3): 329-340.
Zhao, X. and R. Rothstein (2002). "The Dun1 checkpoint kinase phosphorylates and regulates the ribonucleotide reductase inhibitor Sml1." Proceedings of the National Academy of Sciences **99**(6): 3746-3751.